

**DESIGN OF A CONNECTED PIPE TEST FACILITY
FOR RAMJET APPLICATIONS**

**A THESIS SUBMITTED TO
THE GRADUATE SCHOOL OF NATURAL AND APPLIED SCIENCES
OF
MIDDLE EAST TECHNICAL UNIVERSITY**

BY

MUSTAFA NEVZAT SARIŞIN

**IN PARTIAL FULFILLMENT OF THE REQUIREMENTS
FOR
THE DEGREE OF MASTER OF SCIENCE
IN
MECHANICAL ENGINEERING**

APRIL 2005

Approval of the Graduate School of Natural and Applied Sciences

Prof. Dr. Canan ÖZGEN
Director

I certify that this thesis satisfies all the requirements as a thesis for the degree of Master of Science.

Prof. Dr. S. Kemal İDER
Head of Department

This is to certify that we have read this thesis and that in our opinion it is fully adequate in scope and quality, as a thesis for the degree of Master of Science.

Prof. Dr. Kahraman ALBAYRAK
Co-Supervisor

Asst. Prof. Dr. Abdullah ULAŞ
Supervisor

Examining Committee Members:

Prof. Dr. M. Haluk AKSEL (METU, ME)

Asst. Prof. Dr. Abdullah ULAŞ (METU, ME)

Prof. Dr. Kahraman ALBAYRAK (METU, ME)

Prof. Dr. İ. Sinan AKMANDOR (METU, AEE)

Dr. H. Tuğrul TINAZTEPE (ROKETSAN)

I hereby declare that all information in this document has been obtained and presented in accordance with academic rules and ethical conduct. I also declare that, as required by these rules and conduct, I have fully cited and referenced all material and results that are not original to this work.

Name, Last name :

Signature :

ABSTRACT

DESIGN OF A CONNECTED PIPE TEST FACILITY FOR RAMJET APPLICATIONS

SARIŞIN, Mustafa Nevzat

M.S., Department of Mechanical Engineering

Supervisor: Asst. Prof. Dr. Abdullah ULAŞ

Co-Supervisor: Prof. Dr. Kahraman ALBAYRAK

April 2005, 164 pages

Development of the combustor of a ramjet can be achieved by connected pipe testing. Connected pipe testing is selected for combustor testing because pressure, temperature, Mach number, air mass flow rate can be simulated by this type of testing. Real time trajectory conditions and transition from rocket motor (booster) to ramjet operation can also be tested. The biggest advantage of connected pipe testing is the low operation cost and simplicity. Air mass flow rate requirement is less than the others which requires less air storage space and some components like supersonic nozzle and ejector system is not necessary.

In this thesis, design of a connected pipe test facility is implemented. Three main systems are analyzed; air storage system, air heater system and test stand.

Design of air storage system includes the design of pressure vessel and pressure & flow regulation system. Pressure and flow regulation system is needed to obtain the actual flow properties that the combustor is exposed to during missile flight. Alternatives for pressure and air mass flow rate regulation are considered in this study. Air storage system designed in this thesis is 27.8 m^3 at 50 bar which allows a test duration of 200 seconds at an average mass flow rate of 3 kg/s.

Air heater system is utilized to heat the air to simulate the aerodynamic heating of the inlet. Several different combustion chamber configurations with different flame holding mechanisms are studied. The most efficient configuration is selected for this study. Combustion analysis of the air heater is performed by FLUENT CFD Code. Combustion process and air heater designs are validated using experimental data. Designed air heater system is capable of supplying air at a temperature range of 400-1000 K and mass flow rate range of 1.5-8 kg/s at Mach numbers between 0.1-0.5 and pressure between 2-8 bar.

Finally the design of the test stand and ramjet combustor analysis are completed. 3D CAD models of the test stand are generated. Ramjet combustor that will be tested in the test setup is modeled and combustion analysis is performed by FLUENT CFD Code. The ramjet engine cruise altitude is 16 km and cruise Mach number is 3.5.

Key-words: Air Breathing Engines, Ramjet, Connected Pipe, Direct Connect, Vitiator.

ÖZ

RAMJET UYGULAMALARI İÇİN BORU BAĞLANTILI TEST DÜZENEGİ TASARIMI

SARIŞIN, Mustafa Nevzat

Yüksek Lisans, Makine Mühendisliği Bölümü

Tez Yöneticisi: Y.Doç.Dr. Abdullah ULAŞ

Ortak Tez Yöneticisi: Prof. Dr. Kahraman ALBAYRAK

Nisan 2005, 164 sayfa

Ramjet yanma odasının geliştirilmesi boru bağlantılı testler ile gerçekleştirilir. Boru bağlantılı test düzeneğinin seçilmesinin sebebi basınç, sıcaklık, Mach sayısı, hava debisi gibi parametlerin benzetiminin yapılmasının mümkün olmasıdır. Gerçek zamanlı yörüngede maruz kaldığı şartlar ve fırlatıcı motordan ramjet motorunun çalışmasına geçiş evresi bu düzenek ile test edilebilmektedir. Boru bağlantılı test düzeneğinin en önemli avantajı düşük operasyon maliyeti ve basitliğidir. Hava debisi gereksinimi diğer test tekniklerine göre çok daha azdır, bu sebeple sesüstü nozul ve yanma sonu gazları tahliye sistemi gibi elemanlara ihtiyaç duyulmamaktadır.

Bu tez kapsamında boru bağlantılı test düzeneği tasarımı gerçekleştirilmiştir. Üç ana alt sistem incelenmiştir; hava depolama sistemi, hava ısıtma sistemi ve test rampası.

Hava depolama sisteminin tasarımı basınç tankları ve akış kontrol sistemlerinin tasarımını içerir. Akış kontrol sistemleri sayesinde ramjet motorunun gerçek uçuş esnasında maruz kalacağı basınç ve debi miktarları benzetilir. Bu çalışmada akış kontrol sistemi alternatifleri değerlendirilmiştir. Tasarlanan hava tankları 50 bar basınçta ve 27.8 m³ hacminde olup 3 kg/s debide 200 saniye test imkanı sağlamaktadır.

Hava ısıtma sistemi uçuş sırasında ramjet hava alığından kaynaklanan aerodinamik ısınmanın benzetimi için kullanılmaktadır. Değişik yanma odası tasarımları yapılmış ve en efektif sistem seçilmiştir. Yanma analizleri FLUENT HAD (Hesaplamalı Akışkanlar Dinamiği) kodu ile yapılmıştır. Yanma ve yanma odası tasarımları deneysel verilerle doğrulanmıştır. Tasarlanan hava ısıtma sisteminin 1.5-8 kg/s hava debisi kapasitesi olup 2-8 bar arasında ve 400-1000 K arası sıcaklık üretebilmektedir.

Son olarak test rampası tasarımı ve ramjet motoru yanma odası analizleri yapılmıştır. Test rampasının 3 boyutlu CAD çizimleri yapılmıştır. Tasarlanan test düzeneğinde test edilecek olan ramjet yanma odasının modelleri oluşturulmuş ve yanma analizleri yapılmıştır. Analizlerde FLUENT HAD kodu kullanılmıştır. Ramjet motoru 16 km irtifa ve 3.5 Mach hız seyir şartları için tasarlanmıştır.

Anahtar Kelimeler: Hava solumalı motorlar, Ramjet, Boru bağlantı, direk bağlantı

To Eylem Kılıç SARIŞIN

ACKNOWLEDGEMENTS

I would like to express my deepest thanks and gratitude to Asst. Prof. Dr. Abdullah ULAŞ and Prof. Dr. Kahraman ALBAYRAK for their supervision, encouragement, understanding and constant guidance.

Also I would like to express my gratitude to Dr. H. Tuğrul TINAZTEPE for initializing and supporting this thesis.

I would like to thank to Mr. Emre ÖZTÜRK for his assistance on using the Fluent CFD flow solver.

I would like to express my sincere appreciation to Mr. Özdemir AYDIN, Mr. Uğur ARKUN, Dr. Mine YUMUŞAK and Dr. Atılgan TOKER for their crucial advises and invaluable efforts during the preparation of this thesis.

My gratitude is endless for my wife and my family, without whom this thesis would not have been possible.

TABLE OF CONTENTS

ABSTRACT	iv
ÖZ.....	vi
ACKNOWLEDGEMENTS.....	ix
TABLE OF CONTENTS.....	x
LIST OF TABLES	xiii
LIST OF FIGURES	xv
LIST OF SYMBOLS	xix
1. INTRODUCTION	1
1.1. LITERATURE SEARCH	2
1.1.1. HISTORY OF THE RAMJET ENGINES.....	2
1.1.2. CLASSIFICATION OF RAMJETS	3
1.1.3. OPERATION OF RAMJETS.....	6
1.1.4. RAMJET CONFIGURATIONS.....	7
1.1.5. RAMJET TEST FACILITY COMPONENTS	11
1.1.6. RAMJET TEST FACILITIES	17
1.2. VITIATED AIR HEATERS	26
1.2.1. HEATER REQUIREMENTS	27
1.2.2. HEATER PERFORMANCE.....	31
1.2.3. FLAME HOLDERS	31
1.3. TECHNICAL METHOD.....	35
1.3.1. DESIGN INPUTS.....	35
1.3.2. DESIGN METHODOLOGY.....	39
2. AIR STORAGE SYSTEM DESIGN.....	40
2.1. INTRODUCTION	40
2.1.1. SYSTEM REQUIREMENTS.....	40

2.1.2. SYSTEM COMPONENTS	40
2.1.3. AIR STORAGE SYSTEM DESIGN ALGORITHM.....	41
2.1.4. AIR STORAGE SYSTEM SIZING	41
2.2. PRESSURE VESSEL DESIGN.....	42
2.3. FLOW CONTROL SYSTEM.....	45
2.3.1. PRESSURE REGULATION BY VALVES.....	46
2.3.2. PRESSURE REGULATION FOR HIGH PRESSURE DROP	49
2.4. STORAGE SYSTEM CHOICE.....	49
2.4.1. EVALUATION OF STORAGE SYSTEM CASE 1	49
2.4.2. EVALUATION OF STORAGE SYSTEM CASE 2	50
2.5. COMPRESSOR TO CHARGE THE AIR TANK.....	51
3. AIR HEATER SYSTEM DESIGN	53
3.1. AIR HEATER DESIGN	53
3.1.1. VITIATOR ANALYSIS.....	53
3.1.2. EVALUATION OF STUDIED CASES.....	75
3.2. DETAILED ANALYSIS OF CASE 2	77
3.2.1. 2 D Analysis	77
3.2.2. 3D Analysis	80
4. TEST STAND DESIGN	91
4.1. TEST STAND DESIGN	91
4.1.1. REQUIREMENTS	91
4.1.2. COMPONENTS OF THE THRUST STAND.....	92
4.1.3. 3D CAD MODELING OF THE TEST CENTER.....	96
4.2. PIPING SYSTEM DESIGN	97
4.2.1. HEAD LOSS IN A PIPE	97
4.2.2. MINOR LOSSES IN PIPE SYSTEMS	98
4.2.3. PRESSURE DROP AT AN ELBOW.....	99
4.2.4. PRESSURE DROP IN A PIPE.....	100
4.2.5. MODELLING OF PIPING SYSTEM BY FLUENT	104
4.3. RAMJET COMBUSTOR DESIGN.....	105
4.3.1. Case 1	105
4.3.2. Case 2	109
5. CONCLUSION AND DISCUSSION	113
5.1. SUMMARY OF THE WORK	113
5.2. SUGGESTIONS FOR FUTURE WORK	114

5.3. CONCLUSION	115
REFERENCES.....	116
APPENDIX A : AIR TANK DESIGN.....	119
APPENDIX B: AIR TANK DESIGN CALCULATIONS.....	128
APPENDIX C: COMBUSTION MODELLING BY FLUENT	139
APPENDIX D: TEST CENTER DESIGN CODES	148
APPENDIX E: SAMPLE CALCULATIONS FOR PIPING SYSTEM.....	157

LIST OF TABLES

Table 1-1. Comparison of Properties between the Test Centers.....	27
Table 1-2. Compositions for Ideal Air	28
Table 1-3. Fuel and Oxidizers for Combusting Heaters [6].....	30
Table 2-1. Trade-Off Study for Tank Pressure Selection	42
Table 2-2. Pressure Vessel Sizing.....	43
Table 2-3. Cv Analysis for Case 1	48
Table 2-4. Cv Analysis for Case 2	49
Table 3-1. Case 1 Inputs for FLUENT Boundary Conditions	56
Table 3-2. Flow Properties at the Outlet Plane (Case 1).....	57
Table 3-3. Flow Properties at the Outlet Plane (Case 2).....	59
Table 3-4. Case 3 Inputs for FLUENT Boundary Conditions	61
Table 3-5. Flow Properties at the Outlet Plane (Case 3).....	62
Table 3-6. Flow Properties at the Outlet Plane (Case 4).....	63
Table 3-7. Flow Properties at the Outlet Plane (Case 5).....	66
Table 3-8. Flow Properties at the Outlet Plane (Case 6).....	68
Table 3-9. Flow Properties at the Outlet Plane (Case 7).....	70
Table 3-10. Flow Properties at the Outlet Plane (Case 8).....	72
Table 3-11. Flow Properties at the Outlet Plane (Case 9).....	75
Table 3-12. Outlet Plane Data Comparison	76
Table 3-13. Inlet-Off Design Performance Data.....	77
Table 3-14. Mass Fractions Corresponding to Mass Flow Rates	78
Table 3-15. Results of the Air Heater Off-Design Analysis	79
Table 3-16. Final Mass Flow Rate and Mass Fraction Data.....	79
Table 3-17. Results of the Air Heater Off-Design Analysis	80

Table 3-18. Case 1 Inputs for FLUENT Boundary Conditions	82
Table 3-19. Flow Properties at the Outlet Plane	84
Table 3-20. Case 2 Inputs for FLUENT Boundary Conditions	85
Table 4-1. Average Roughness of Commercial Pipes	97
Table 4-2. K Factors for Fittings.....	99
Table 4-3. Nominal Pipe Sizes for Standard Pipes	99
Table 4-4. Comparison of FLUENT Results with Experimental Results.....	106
Table 4-5. Comparison of FLUENT Results with Experimental Results.....	110
Table E-1. Summary of Results	Error! Bookmark not defined.

LIST OF FIGURES

Figure 1-1. Liquid Fuel Ramjet [5].....	3
Figure 1-2. Solid Fuel Ramjet [5].....	4
Figure 1-3. Ducted Rocket with Integrated Gas Generator [5].....	5
Figure 1-4. Missile Launch	6
Figure 1-5. Booster Phase	6
Figure 1-6. Transition and Ramjet Ignition	7
Figure 1-7. Schematic of a Connected-Pipe Test Setup.....	9
Figure 1-8. Free-Jet Testing of a Scaled Down Test Article	10
Figure 1-9. Jet Stretcher Concept.....	10
Figure 1-10. Product Tree of Connected Pipe Test Facility	11
Figure 1-11. Sketch of a SUE Heater.....	13
Figure 1-12. Tube Type Cross Counter Flow Heater [1].....	14
Figure 1-13. Pebble Bed Storage Heater.....	15
Figure 1-14. Sketch of NASA Langley Test Facility [8].....	18
Figure 1-15. Sketch of Chitose Semi-Free-Jet Ramjet Test Setup [9].....	22
Figure 1-16. ARC Connected Pipe Ramjet Test Centre [11].....	23
Figure 1-17. Sketch of ONERA Connected-Pipe Test Setup [12].....	24
Figure 1-18. Sketch of Hypersonic Test Setup of APTU [7].....	25
Figure 1-19. Sketch of U.S. Air Force Connected Pipe Facility [13].....	26
Figure 1-20. Recirculating Flow Behind a Sphere, a Gutter and a Strut	33
Figure 1-21. Flame Propagation Downstream of a Baffle: (a) For A Uniform Fuel-Air Mixture, (B) When The Fuel Is Confined To A Central Region.....	33
Figure 1-22. Flow Behind a Baffle	34
Figure 1-23. Stabilization Setup by Recirculation	34

Figure 1-24. The Stabilization Setups by Pilot Flames.....	35
Figure 1-25. Flight Trajectory of Missile X.....	36
Figure 1-26. Mach Number Evolution of Missile X.....	37
Figure 1-27. Mass Flow Rate Captured by Inlets vs. Time	37
Figure 1-28. Static Pressure at the Combustor Inlet vs. Time	38
Figure 1-29. Static Temperature at the Combustor Inlet vs. Time	38
Figure 1-30. Design Algorithm of the Connected Pipe Test Facility	39
Figure 2-1. Component Tree of Air Storage System	41
Figure 2-2. Air Storage System Design Algorithm	41
Figure 2-3. Pressure and Temperature Change During Discharge for Case 1	44
Figure 2-4. Pressure and Temperature Change During Discharge for Case 2	45
Figure 2-5. Pressure Regulation System	46
Figure 2-6. Scheme for Valve Calculations	47
Figure 2-7. Example of High Pressure Regulator	50
Figure 2-8. Example of High Pressure Compressor	52
Figure 2-9. Air Flow Rates of EHNX GT Compressor	52
Figure 3-1. Prediction of Temperature Using Different Grid Densities	56
Figure 3-2. Sketch of Case 1	56
Figure 3-3. Contours of Static Temperature of Case 1.	57
Figure 3-4. Sketch of Case 2	58
Figure 3-5. Contours of Static Temperature of Case 2.	59
Figure 3-6. Sketch of Case 3	60
Figure 3-7. Contours of Static Temperature of Case 3.	61
Figure 3-8. Sketch of Case 4	63
Figure 3-9. Contours of Static Temperature of Case 4.	64
Figure 3-10. Sketch of Case 5	65
Figure 3-11. Contours of Static Temperature of Case 5.	65
Figure 3-12. Sketch of Case 6	67
Figure 3-13. Contours of Static Temperature of Case 6.	67
Figure 3-14. Sketch of Case 7	69
Figure 3-15. Contours of Static Temperature of Case 7.	69

Figure 3-16. Sketch of Case 8.....	70
Figure 3-17. Contours of Static Temperature of Case 8.	71
Figure 3-18. Contours of Velocity Magnitude of Case 8.....	72
Figure 3-19. Sketch of Case 9.....	73
Figure 3-20. Contours of Static Temperature of Case 9.	74
Figure 3-21. Contours of Velocity Magnitude of Case 9.....	74
Figure 3-22. Mass Flow Rate Requirement of the Test Facility.....	77
Figure 3-23. Final Configuration of the Air Heater.....	80
Figure 3-24. Flame Holding Mechanism.....	81
Figure 3-25. Quarter of the Air Heater Combustion Chamber.....	81
Figure 3-26. Sketch of Combustion Chamber of Case 1.....	82
Figure 3-27. Contours of Static Temperature of Case 1.....	83
Figure 3-28. Contours of Static Temperature of Case 1 (Isometric View).....	83
Figure 3-29. Sketch of Combustion Chamber of Case 2.....	84
Figure 3-30. Contours of Static Temperature of Case 2.....	85
Figure 3-31. Sketch of Combustion Chamber of Case 3.....	86
Figure 3-32. Contours of Static Temperature of Case 3.....	87
Figure 3-33. Sketch of combustion chamber of Case 4.....	87
Figure 3-34. Fuel Injector Studied in Case 4.....	88
Figure 3-35. Contours of Static Temperature of Case 4.....	89
Figure 3-36. Contours of Static Temperature and Fuel Path Lines of Case 4.....	89
Figure 3-37. Final Configuration of the Vitiator.....	90
Figure 3-38. Fuel Injector Configuration.....	90
Figure 4-1. Wheel Configuration.....	93
Figure 4-2. Double Wheel Configuration.....	93
Figure 4-3. Cylindrical Rod and Sliding Pad Configuration.....	93
Figure 4-4. V-Blocks Configuration.....	94
Figure 4-5. Vitiator Table.....	95
Figure 4-6. Piping Systems.....	95
Figure 4-7. 3D Model of the Test Center.....	96
Figure 4-8. Sketch of an Elbow.....	100

Figure 4-9. Sketch of a Pipe.....	100
Figure 4-10. Piping Configuration Following the Vitiator	102
Figure 4-11. Piping Configuration Before the Vitiator.....	103
Figure 4-12. Temperature Contours on the Fluent Model of the Piping System..	104
Figure 4-13. Sketch of Case 1	106
Figure 4-14. Contours of Static Temperature of Case 1.	107
Figure 4-15. Contours of Mach Number of Case 1.....	108
Figure 4-16. Sketch of Case 2.....	109
Figure 4-17. Contours of Mach Number of Case 1.....	110
Figure 4-18. Contours of Static Temperature of Case 2.	111
Figure A-1. General Configuration for Vessel Shells and Head.....	124
Figure A-2. Nozzle Reinforcement.....	125
Figure B-1. Technical Drawing of Case	124
Figure B-2. Technical Drawing of Head 1.....	124
Figure B-3. Technical Drawing of Head 2.....	124
Figure B-4. Technical Drawing of Nozzle and Air Pipe.....	124
Figure B-5. Assembly Drawing of Pressure Vessel.....	124
Figure C-1. Schematic of the Combustor.....	143
Figure C-2. Grid Used in Fluent Analysis	143
Figure D-1. Main Window of the Program.....	148
Figure D-2. Pipe Code Window.....	149
Figure D-3. Main Window Following the Pipe Code Window	150
Figure D-4. Discharge Code Window.....	151
Figure D-5. Main Window Following the Discharge Code Window	152
Figure D-6. Replenishment Code Window.....	153
Figure D-7. Main Window Following the Replenishment Code Window	154
Figure D-8. Valve Code Window	155
Figure D-9. Final Window of the Code	156
Figure E-1. Pipe Configuration of the Test Center	157

LIST OF SYMBOLS

A	Surface area (m^2)
Q	Load on one saddle (N)
t_s	Wall thickness of shell (mm)
t_h	Wall thickness of head (mm)
θ	Contact angle of saddle (deg)
D_i	Inside diameter (mm)
D_o	Outside diameter (mm)
R_i	Inside radius (mm)
R_o	Outside radius (mm)
E	Joint efficiency
σ_x	Longitudinal stress (MPa)
σ_ϕ	Circumferential stress (MPa)
$\rho_{air@1atm}$	Density of air at 1 atm (kg/m^3)
Q_{CH_4}	Flow rate of CH_4 (m^3/s)
Q_{air}	Flow rate of air (m^3/s)
\dot{m}_{CH_4}	Mass flow rate of CH_4 (kg/s)
\dot{m}_{air}	Mass flow rate of air (kg/s)
T_{inlet}	Combustor inlet temperature (K)

ϕ	Equivalence Ratio
T_{wall}	Combustor wall temperature (K)
T	Temperature (K)
ρ_{air}	Density of air (kg/m^3)
M	Mach number
c	Speed of sound (m/s)
V	Velocity (m/s)
$scmh$	Standard cubic meter per hour
$scfh$	Standard cubic feet per hour
S	Allowable or calculated stress (MPa)
alt	Missile cruise altitude (m)
M_0	Missile cruise Mach Number
M_e	Inlet downstream Mach Number
T_e	Inlet downstream Static Temperature (K)
P_e	Inlet downstream Static Pressure (Pa)

CHAPTER 1

INTRODUCTION

It is more difficult to evaluate the performance of air breathing engines than conventional rockets, because they vary strongly with the flight conditions (Mach Number, altitude, atmospheric conditions, angle of attack, etc.). In the development of the combustor and the complete engine, direct connect testing and freejet testing techniques are used.

Many nations are conducting research and development of ramjets for supersonic, extended range missiles and projectiles. Supersonic air breathing test facilities are few in number. There has been a continuous improvement in techniques and capability.

Full simulation is unnecessary in conducting component development tests. For example, the aerodynamic and performance of inlets and exit nozzles can be established with reduced scale models in wind tunnels and similar facilities, which simulate the Mach and Reynold's number but not the temperature, pressure or fluid velocity. This approach is not possible with the combustor, where simulation of the later parameters is also important. As a result, unique simulation requirements are associated with direct connect testing and freejet testing involved in the development of the combustor and the complete engine. [1]

Test Center Design in this study will be based on the Ramjet Engine designed reported at [2].

1.1. LITERATURE SEARCH

Basic advantages of all ramjet configurations over conventional rocket propulsion systems are:

- They have higher specific impulse than the classical rocket motors.
- They have the potential to achieve an increased range.
- They offer increased effectiveness against maneuvering targets by maintaining thrust.
- They have lower fuel consumption than classical rocket motors. [3]

These advantages can be sufficient to justify the use of a ramjet over a conventional rocket motor in certain applications.

1.1.1. HISTORY OF THE RAMJET ENGINES

The ramjet concept was invented in 1911 by a French scientist, R. Lorin. R. Leduc applied it to the propulsion of aircraft, and subsonic tests were conducted in 1949. Before and during the Second World War, the Germans studied the application possibilities of the ramjet concept to the missiles. Between the end of the Second World War and the middle of the 60's, a large number of countries undertook a major research effort, which took the shape (in France) of many flight tests of experimental missiles called CT41, VEGA, R431 and Staltex; and operational developments of ground-to-air or surface-to-air missiles such as the BOMARC (1957) and the TALOS (1959) in the United States; the BLOODHOUND(1959) in Great Britain; and the SA4(1964) in the USSR. After that period, the research and the development efforts were focused on other propulsion systems. Activities began again around the 70's with, in particular, the following: introduction in Great Britain in 1975 of the SEA DART; the in-flight evaluation in the US of the ASLM (advanced strategic air-launched missile) and ALVRJ (advanced low-volume ramjet) experimental missiles; the development of the SLAT (supersonic low-altitude target) in 1991; and in France, the flight test of the ANS missile

(supersonic anti-ship) and the operational missile ASMP (medium range air-to-ground). [4].

1.1.2. CLASSIFICATION OF RAMJETS

Among the various configurations, a classification can be established according to the nature of the fuel, either liquid with its high performance, or solid with its operational simplicity and potentially lower cost.

1.1.2.1. Ramjets Using Liquid Fuel

The liquid fuel ramjet (Figure 1-1) can use classical kerosene, high density or slurry fuels. The liquid fuel dominates the operational applications, mainly because of its high throttle ability and excellent performance.

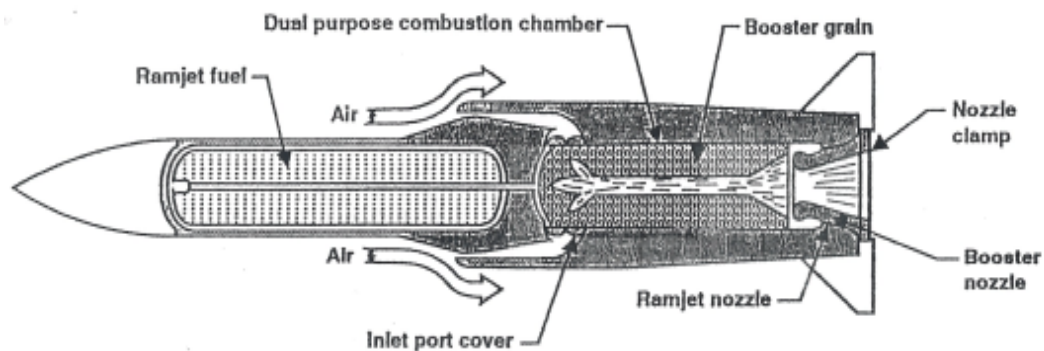


Figure 1-1. Liquid Fuel Ramjet [5]

1.1.2.2. Ramjets Using Solid Fuel

The solid fuel ramjet (SFRJ) has been considered as a propulsion device for missile since 1930's. It is possible to use special solid fuels in a solid fuel ramjet in order to obtain conditions of maintenance and storage similar to that of ordinary ammunitions or classical solid propellant rocket missiles. The engine uses only one chamber, resulting in a very simple construction. The solid fuel, which is produced without oxidizer, covers the wall of the combustor. By ablation in the hot air flow, it is transformed into gases, which burn in a combustion chamber. It is particularly well-suited for the high-acceleration environment of projectiles.

The SFRJ can provide specific impulse in the 900-1400 sec range and density impulse in the 1150-2300 gm-s/cm³ range. This results in a 200-400% increase in range over that of a solid rocket motor with comparable size and weight.

Figure 1-2 shows a classical configuration of the SFRJ. This configuration includes air inlet diffusers, which slow down the supersonic air to low subsonic speeds, raise the inlet air to a higher static temperature and pressure.

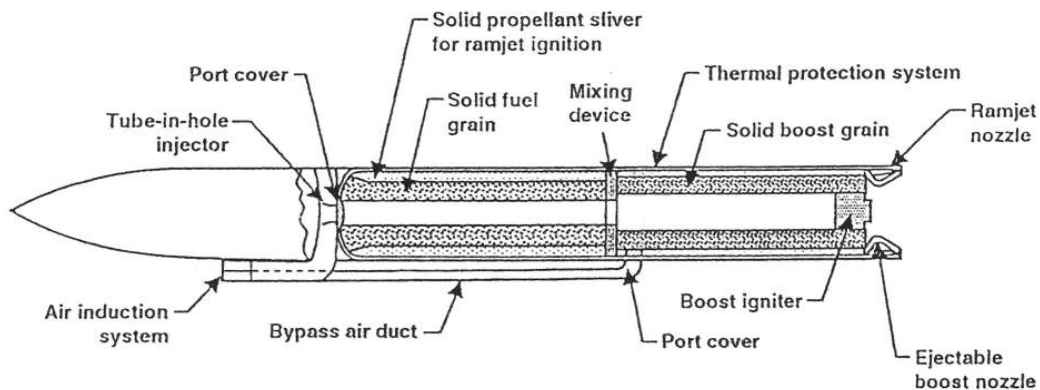


Figure 1-2. Solid Fuel Ramjet [5]

1.1.2.3. Ducted Rocket

The ducted rocket contains a solid propellant with a small portion of oxidizer (fuel rich solid propellant - Gas Generator). This small quantity of the oxidizer is just used to produce gases, which will be burned in the combustion chamber. The ducted rocket, like the solid fuel ramjet, has the maintenance and storage characteristics of a solid rocket motor. Like the liquid fuel ramjet, the ducted rocket may also have a throttling ability, but have higher acceleration and longer range than a liquid fuel ramjet. Two variants of the ducted rocket exist:

- Ducted rocket with separate gas generator: The fuel is stored in a separate container, or gas generator, which works like a rocket. The gases produced, relatively low in temperature, can be injected into the combustion chamber

through a control valve. As the burning rate of the solid fuel is influenced by pressure, it is possible to regulate the gas flow.

- Ducted rocket with integrated gas generator: It has a single chamber, fuel rich solid propellant being in direct contact with the combustion chamber. The altitude variation capability is large because of self-regulation qualities (as the burn rate is pressure dependant).

Figure 1-3 shows a classical ducted rocket with booster propellant. Booster propellant is consumed before the ramjet operation and the missile reach to high Mach numbers. At the end of booster operation, gas generator is ignited, booster nozzle is ejected and inlet port cover is removed. Air flowing through the inlet is mixed by the fuel generated at the gas generator and combustion occurs in the combustor. Then the hot combustion products are expanded in the nozzle to create the required thrust.

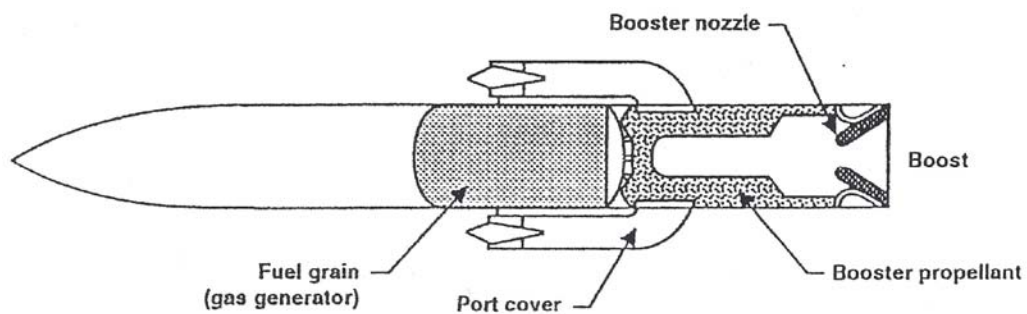


Figure 1-3. Ducted Rocket with Integrated Gas Generator [5]

1.1.2.4. The Scramjets (Supersonic combustion)

The ramjet is without any doubt the most suitable air-breathing propulsion system for hypersonic flight in the atmosphere. Efficient operation of a ramjet is reached by subsonic combustion up to vehicle Mach number of 6 or 7, and supersonic combustion beyond; in the latter case, the engine is designated as a scramjet.[6]

Theoretically, on the basis of its power performance, it could reach orbital velocities. In practice, it will be difficult to go beyond a hypersonic speed of about

Mach 10 to 12, because of the sensitivity of the engine thrust to small disturbances at higher Mach numbers.

1.1.3. OPERATION OF RAMJETS

Following the ignition of the missile (generally dropping from the aircraft fighter or firing from other platforms, Figure 1-4), the booster accelerates the missile up to the speed that allows the start of ramjet (around Mach 2.5), as shown in Figure 1-5. The booster is a conventional solid propelled rocket. The propellant grain that is placed in the ramjet combustor burns and the hot gases are expanded in the rocket nozzle. The rocket nozzle is fixed on the ramjet nozzle. Once the booster propellant is burnt, the rocket nozzle is ejected, and the ramjet nozzle becomes the missile operational nozzle (Figure 1-6). Since the missile has reached a sufficient velocity for the ramjet start, the caps that close the inlets are ejected, and air is swallowed in the combustor. This is called the transition phase that has to be tested in the freejet facility. Then, the ramjet combustion begins, and the missile follows its trajectory.

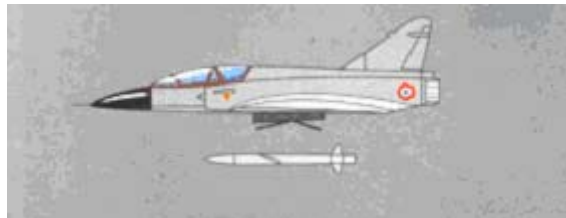


Figure 1-4. Missile Launch



Figure 1-5. Booster Phase

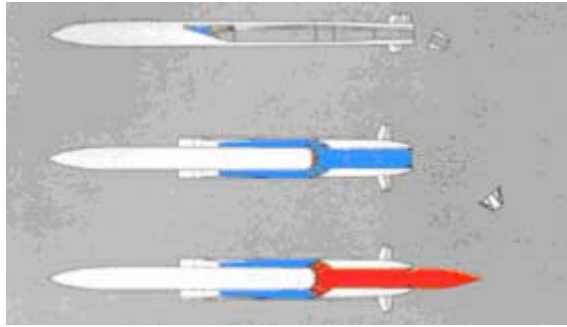


Figure 1-6. Transition and Ramjet Ignition

1.1.4. RAMJET CONFIGURATIONS

1.1.4.1. Main Stages of Ramjet Development

As for any propulsion system, developing a ramjet engine goes first through successive development phases, then through detailed design improvements and demonstrations, and finally acceptance testing under all flight conditions. This demands a great deal of experimental research and development.

For example, to debug one current operational ramjet powered missile and to qualify it with its requirement under all flight conditions, 600 test runs were required each year for seven years (90 % of blowdown tests lasted 30 seconds and 10% lasted longer), using nearly 80,000 kg of liquid fuel. [6]

The current trend is to qualify the missile on the ground, in the most realistic environment possible, so that the flight tests, which are always very costly, have a high probability of success.

During a ramjet development, the following steps are needed.

1.1.4.1.1. Design Test on Components

This includes tests of air intakes in a wind tunnel, optimization of the combustor with the help of flow visualization techniques.

1.1.4.1.2. Connected Pipe Tests

This is a very important step of a development. Before the full propulsion system is tested, ramjet combustors are generally tested alone. Hot subsonic air is ducted directly into the combustor. Figure 1-7 shows a connected-pipe test facility sketch.

Connected pipe testing is conducted primarily to demonstrate combustor thermal/structure design integrity and combustor performance, using a direct thrust stand measurement. Precise input conditions of airflow, inlet temperature and fuel flow to the combustor may be achieved during connected pipe tests using facility-supplied air and fuel flow; consequently, accurate combustor performance correlations may be derived from these tests.

In some connected pipe test facilities an entire trajectory time profile may be simulated using computer-controlled valves for airflow, heater fuel flow, and combustor fuel flow.

Fuel-injector arrangements may be altered in these tests to meet performance requirements. Insulation and other thermal protection system may be altered to meet endurance requirements.

Rocket-to-ramjet transition tests are also a major phase of development testing for Integral Rocket Ramjet propulsion systems.

1.1.4.1.3. Semi-Free Jet Tests

The engine, including air intakes, is supplied with supersonic air coming from nozzles just in front of each inlet. The air mass flow required is roughly 50% to 100% higher than in connected-pipe tests, due to external air flow.

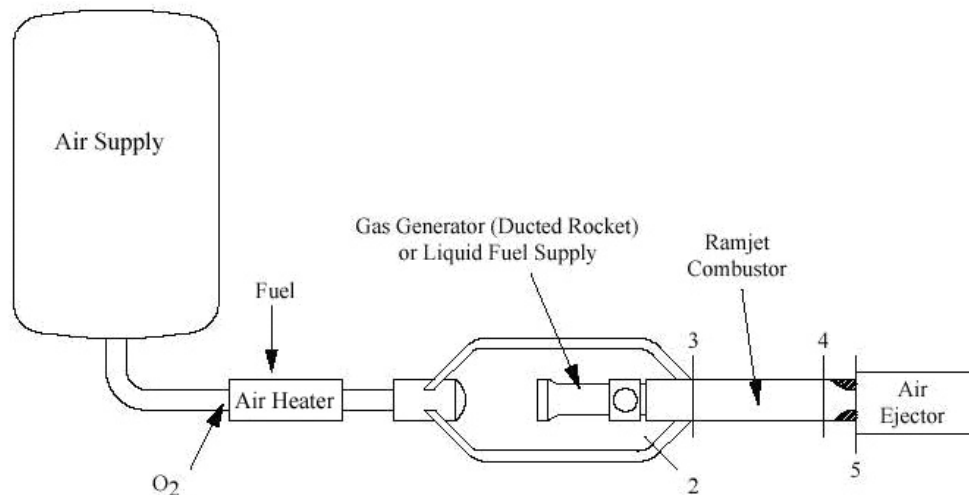


Figure 1-7. Schematic of a Connected-Pipe Test Setup

1.1.4.1.4. Free-Jet Tests

This is the best simulation, because the entire vehicle forebody is surrounded with supersonic air flow, as in flight.

Free-jet testing serves to integrate the whole propulsion system. Free-jet tests primarily are conducted to verify the functional operation and performance of the integrated propulsion system in a supersonic flowfield. Net engine thrust, combustor performance and interactions between ramburner and inlet can be evaluated in a free-jet facility. Flight-weight inlets can also be evaluated. Fuel management systems and fuel tank expulsion systems can also be optionally added.

To take full advantage of the free-jet tests, the test article should include as many flight designed systems as possible like vehicle forebody, equipment and telemetry systems, pyrotechnic and ignition systems, inlets, fuel management systems, auxiliary power systems, booster/combustor system, etc. Figure 1-8 shows a supersonic test of a missile during a free-jet test.

In the basic free-jet setup the entire missile is tested. For forward-mounted inlet configurations, the inlet is located in the nozzle test rhombus and exposed to the flow Mach number. Semi-free jet testing is often used for aft-mounted inlets since Mach numbers cannot be exactly reproduced at the aft end of the missile in the full free-jet mode. Generally, the forebody is omitted and free jet inlets are mounted directly in front of the inlets. This is also a cost effective technique for aft inlet configurations, since free-jet testing of the full vehicle would require either a scaled-down test article or an extra large facility with considerable airflow requirements.

A jet stretcher can also be used for aft mounted inlets. The jet stretcher (Figure 1-9) is an aerodynamically shaped surface, which simulates a free-jet streamline, extends the test rhombus of the free jet nozzle by precluding shock or expansion waves from the nozzle or jet boundary from being reflected into the flow upstream of the inlet.

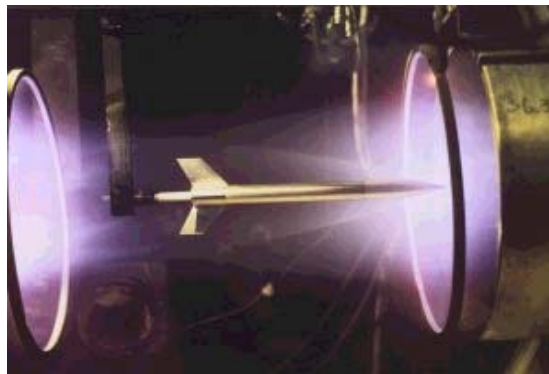


Figure 1-8. Free-Jet Testing of a Scaled Down Test Article

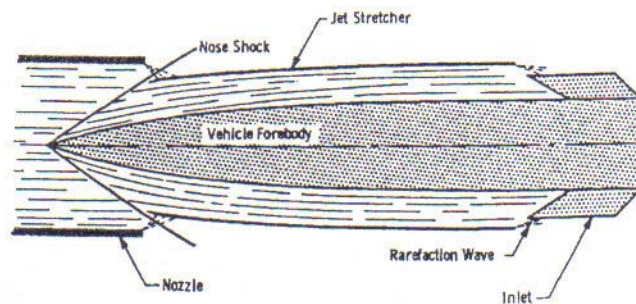


Figure 1-9. Jet Stretcher Concept

With the basic free-jet setup, both pitch and yaw angle of attack can be evaluated. In the other two setups, the testing is restricted effectively to zero-degree angle of attack.

1.1.4.1.5. Flight Tests

This is the final objective after several years of ground tests.

1.1.4.2. Test Facility Simulation

The followings are a number of parameters and flight conditions that are simulated in the test facility.

- Stagnation pressure
- Stagnation temperature
- Mach number
- Pressure ratio
- Air mass flow rate
- Trajectory conditions
- External heating
- Maneuver loads
- Angle of attack
- Fore body flow field
- Transition sequence

1.1.5. RAMJET TEST FACILITY COMPONENTS

The product tree of a typical connected pipe test facility is given in Figure 1-10.

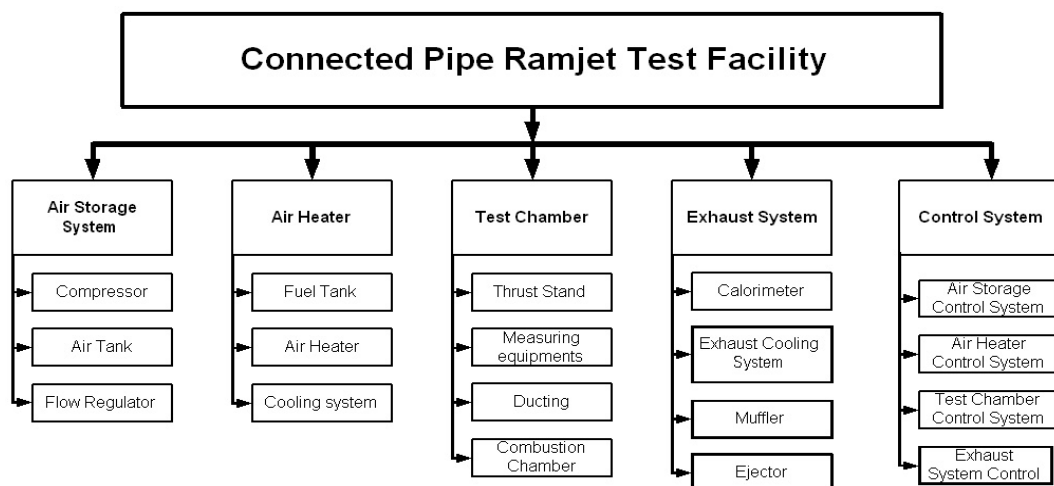


Figure 1-10. Product Tree of Connected Pipe Test Facility

1.1.5.1. Air Storage System

Power requirements for continuous air flow are prohibitive; therefore, ramjet test facilities are of the stored air blowdown type. The blowdown facility is an economical method of meeting the high air mass flow and pressure ratio requirements. Mass flow rate and test duration is limited with the air storage capacity. For example test center at "Arnold Engineering Development Center" store 450,000 lb (204 tons) of air at a maximum pressure of 4000 psi (275 bar) [7], which allows a run duration of the facility from approximately 3 minutes to over 12 minutes, depending on the free-jet nozzle selected and the altitude simulated in the test cell.

In direct connect testing, this run duration is higher due to the less pressure and airflow requirements.

1.1.5.2. Air Heater

Different air heating methods are used in ramjet testing. They may be grouped into three categories: combustors heaters (vitiators), non-combustors heaters (including heat exchangers), and combinations of these heaters.

1.1.5.2.1. Heater Types

a. Combustors Heaters (Vitiators):

Combustors heaters heat air directly with a fuel-oxidizer reaction. Fuel is burned in the air stream in a combustor similar to a ramjet combustor. The exhaust gases are used for ramjet testing after the consumed oxygen is replenished.

The main advantages:

- Low fuel flow requirement, low cost
- Simple operation and maintenance.

The disadvantages:

- The effects of air heater combustion products on ramjet combustion (unburned vitiator fuel can increase the ramjet performance)
- The changes of air properties like molecular weight.

The principle problem associated with vitiated air heater is that the resulting air, after heating by combustion and oxygen replenishment, contains higher mass fractions of water vapor and carbon dioxide than normal air. Fortunately, this has proved to be only a minor problem in ramjet engine testing [6]. A major advance in test technique, which facilities simulating low altitudes and high Mach numbers, was provided by the Sudden Expansion (SUE) heater. The sudden expansion vitiated air burner with oxygen replenishment was originally developed for ramjet testing and has since been adapted by several facilities. SUE heater is more compact than the other types. This permits it to be installed in close proximity to the free-jet nozzle. Figure 1-11 shows a sketch of a SUE heater [1].

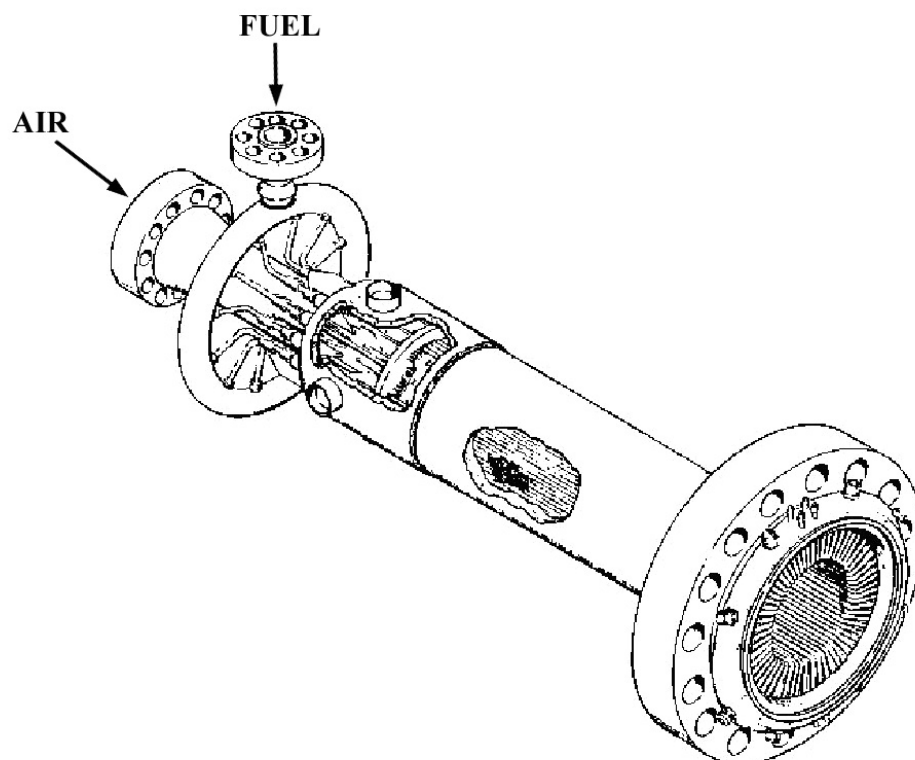


Figure 1-11. Sketch of a SUE Heater

b. Non-Combusting Heaters

Non-combusting heaters avoid contamination of the air stream with combustion products and deliver clean air to the ramjet combustor. Non-combusting heaters used in ramjet testing are as follows:

Tube Type Cross Counter Flow Heater: The tube heat exchanger type of heater can supply clean air up to (1000 K) 1200°F [1]. The heat source may be electrical resistance or combustion of a separate fuel and oxidizer. However structural and maintenance problems, as well as heat transfer considerations, limit the maximum operating temperature. Higher temperatures can be achieved by adding a vitiated air heater downstream. A sketch of tube type cross counter flow heater is given in Figure 1-12.

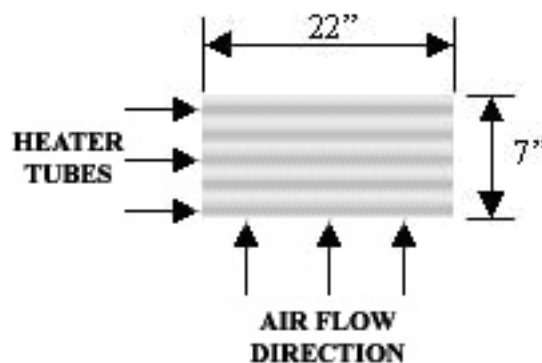


Figure 1-12. Tube Type Cross Counter Flow Heater [1]

Pebble Bed Storage Heater: Heat storage devices are heat exchangers of high thermal mass that are gradually heated to operating temperature and during a test run give up stored thermal energy to air passing through them. Commonly, large vessels filled with ceramic or metal pebbles are used, heated by either electrical resistance or hot combustion gases (Figure 1-13). These storage heaters can heat air to higher temperatures than conventional heat exchangers because the pebbles are

more resistant to thermal damage than fragile heat exchanger tubes. Nevertheless, repeated thermal expansion and contraction can rub the pebbles together and introduce dust particles into the air stream. Heater life span is lengthened by reducing the number and magnitude of these thermal cycles. The main challenge in designing heat storage devices is obtaining a constant output temperature for the required run time and range of test conditions. This usually results in large heaters with a high heat capacity so that only a small fraction of the energy is extracted during a run. [6]

Electric Air Heater: Electric arc heaters heat air through the release of energy produced by an electric arc between two electrodes. Arc heaters are capable of producing very high air temperatures. The facility capabilities depend primarily on the limits of the anode and cathode producing the arc. Due to the extremely high temperatures produced by the arc, ionized species are created that react to form NO_x and other undesired constituents that contaminate the air stream. The presence of these contaminants, and the fact that oxygen dissociation begins at approximately 2500K, sets the upper limits of combustion testing in arc facilities. Above this temperature, care must be taken to account for the chemical effects of the contaminants and dissociated species on combustion. The high power requirements of arc heaters make them very expensive to operate.

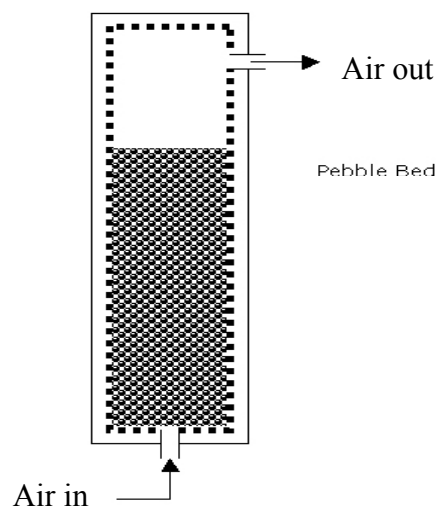


Figure 1-13. Pebble Bed Storage Heater

c. Combination Heaters

Combination heaters use a combination of the previously discussed methods to take advantage of the characteristic strengths of one method to offset the weaknesses of the other. For example, one could use a vitiator to boost the temperature from an electrically powered heat exchanger. This would allow higher temperatures without damaging the heating elements in electric heater, and would deliver lower levels of combustion products when compared to pure combustion heating. In addition this combination allows temperature variation during a run (transient simulations).

1.1.5.3. Combustion Chamber

In the connected pipe test, combustor is tested alone, to evaluate combustion efficiency, combustor pressure losses, fuel/air ratio flameout conditions, and thermal protection system durability. Fuel-injectors and flame holders may be used for these tests. Three types of combustors may be used:

- Heavy-wall performance combustors,
- Water-cooled performance combustors that can be run for longer time periods,
- Flight-weight combustors to evaluate performance and endurance with the flight thermal protection system.

1.1.5.4. Calorimeter

Energy losses through the various water-cooled components, coupled with the temperature measurements from a steam calorimeter allow calculation of combustion efficiency.

1.1.5.5. Ejector

The ejector system is used to evacuate the test cell volume to ensure that the desired altitude pressure is available in the free-jet nozzle test rhombus and to minimize the starting loads on the article during facility start-up. The ejector can sometimes be connected to the facility to eject hot gases.

In some systems the air storage system is used to drive the ejector system. A separate air source and steam generator may also be used for this application.

The ejector can also be connected to a muffler system to reduce the high intensity sound effects which can damage the test equipment or environment.

1.1.6. RAMJET TEST FACILITIES

Some major direct connect ramjet test facilities are as follows:

1.1.6.1. NASA Langley Direct Connect Supersonic Combustion Test Facility (USA)

Test Section and Performance: The Langley Direct-Connect Supersonic Combustion Test Facility (DCSCTF) [8] is used to test ramjet and scramjet combustor models in flows with stagnation enthalpies duplicating that of flight at Mach numbers between 4 and 7.5. A sketch of the facility is given in Figure 1-14.

The facility is located in a 4.9x4.9x15.8 m (16x16x52 ft) test cell with 0.6 m (2 ft) steel-reinforced concrete walls and forced-air ventilation. Test air is supplied from a high-pressure bottle field and is regulated to 38 bar (550 psia) (nominal) prior to entering the test cell. Gaseous hydrogen is supplied from 1700 m³ (60,000 ft³) tube trailers at a maximum pressure of 165 bar (2400 psia) and is regulated to 50 bar (720 psia). Oxygen is supplied from trailers at a maximum pressure of 165 bar (2400 psia) and is regulated to 50 bar (720 psia) prior to entering the test cell. A 20-percent silane and 80-percent hydrogen mixture (by volume) is supplied from

cylinders (maximum storage pressure of 165 bar (2400 psia)) for use as an igniter of the primary fuel in the combustor models.

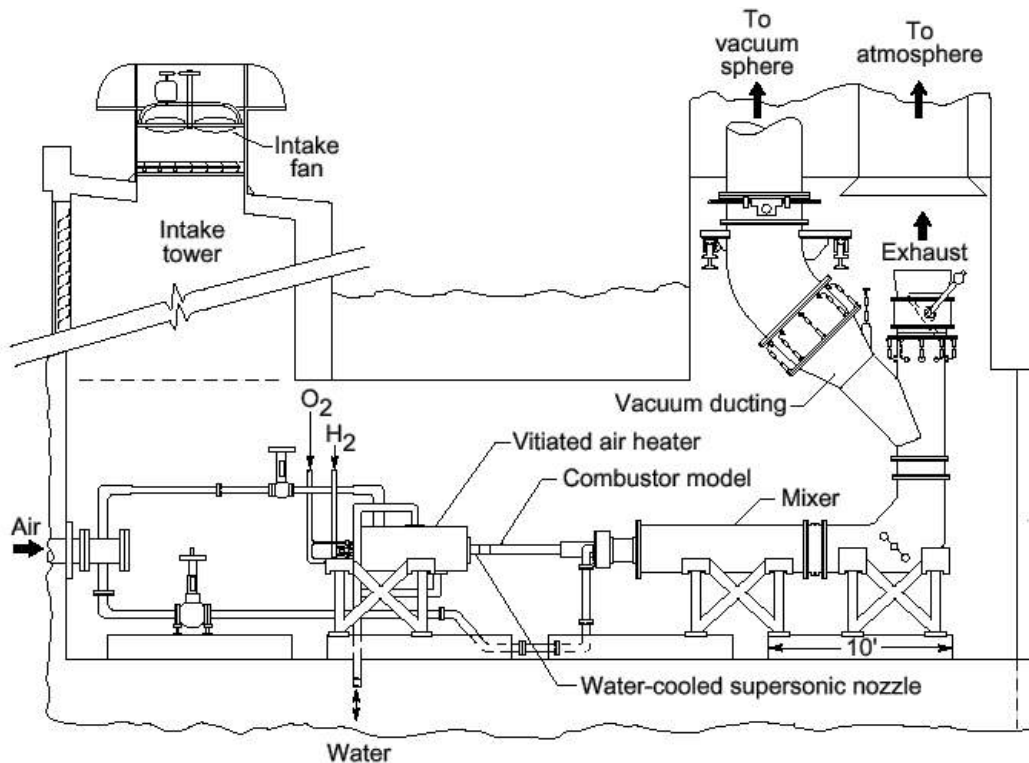


Figure 1-14. Sketch of NASA Langley Test Facility [8]

Results of the tests are typically used to assess the mixing, ignition, flame holding, and combustion characteristics of the combustor models.

The high stagnation enthalpy necessary to simulate flight is achieved through hydrogen-air combustion with oxygen replenishment to obtain a test gas with the same oxygen mole fraction as atmospheric air (0.2095). The flow at the exit of the facility nozzle simulates the flow entering the combustor of a ramjet or a scramjet in flight.

The facility normally operates at heater stagnation pressures between 7 and 35 bar and at heater stagnation temperatures between 850 and 2100 K. Test gas mass flow

rates range from 0.45 to 3 kg/s . The normal test schedule is 2 or 3 test days per week. Run duration averages 20 to 30 sec with multiple runs (5 to 20) per day.

The facility uses a hydrogen and air combustion heater with oxygen replenishment. During facility heater operation, oxygen is injected into the air stream from 12 in-stream injectors and premixed before injecting hydrogen. The hydrogen is injected into the air and oxygen mixture from 12 in-stream injectors centered in holes located in a baffle/mixing plate upstream of the water-cooled combustor section. The gas mixture is ignited by electric-spark-activated hydrogen and oxygen torch igniters.

Test gas compositions for the standard operating conditions of the DCSCTF are calculated with finite-rate chemistry during the expansion through the facility nozzle. The primary contaminant in the test gas is water vapor, which varies from 0.083 mole fraction at Mach 4 conditions to 0.358 at Mach 7.5 conditions. A small amount of nitric oxide (0.004 mole fraction) is also present in the test stream at the Mach 7.5 condition.

An air ejector or a 21.3 m (70-ft) diameter vacuum sphere and steam ejector system (requiring up to 6800 kg (15,000 lbm) per hr of steam) provides vacuum for altitude simulation. Gaseous hydrogen (at ambient temperature) is the primary fuel used in the combustors tested in the facility, although other types of gaseous fuels are used occasionally.

1.1.6.2. Chitose Ramjet Test Facility (Japan)

This is a facility to simulate an actual flight environment (altitude and the Mach number) for next-generation supersonic engines and to evaluate their thermal aerodynamic characteristics etc. on the ground. Main components of this facility are a compressor, air tanks, a burner, a cooler, a test chamber, a cooler for exhaust gas, ejectors, etc. High-pressure air generated by the compressor is accumulated in the air tanks and fed to an engine to be tested in a form of airflow corresponding to

the actual flight speed. A temperature of the airflow can be set according to the actual flight environment by the burner or cooler. In addition, the exhaust gas from the engine can be cooled by the exhaust gas cooler and depressurized by the ejectors so that a pressure in the test chamber can be set according to the actual flight altitude. Sketch of the facility is given in Figure 1-15 [9].

Features:

- This facility is available for the comprehensive control of airflow simulating the actual flight environment (flight altitude and the Mach number).
- This is available for the comprehensive evaluation of engine performance (thrust etc.) in the actual flight environment.
- Adoption of a hydrogen-combustion heating method for generating high-temperature air.
- Adoption of a liquid nitrogen spraying method for generating cold air.
- Adoption of a method that water is injected into kerosene-combustion gas for generating ejector drive gas.

1.1.6.3. Kakuda Space Propulsion Laboratory (Japan)

This is the only facility in Japan that can be used to test ramjet and scramjet engines under simulated flight conditions of Mach 4, 6 and 8 at altitudes of 20, 25 and 35km, respectively [10].

In this facility, Ram/Scramjet engine systems can be tested under the simulated flight conditions at hypersonic velocity and high altitude. It can be utilized also for testing other types of hypersonic air breathing engines and various materials/structures under severe aero-thermodynamic environment.

The thermal storage body "Core-de-bric" made of alumina with many holes along the length is piled up internally. Air is thrown after this thermal storage body, which is heated with the gas of LPG burner.

The flow of air becomes supersonic while passing through the nozzle. The nozzle for testing condition Mach 8 is cooled by water because it is exposed to high heat.

The engine is installed in the low pressure room, and is operated in a high-speed current of air which spouts from the nozzle, and thrust, pressure, and the temperature, etc. are measured.

The nozzle outlet size is 51 cm x 51 cm.

1.1.6.4. Atlantic Research Corporation Facilities (USA)

Features of the Airbreathing Facility (Figure 1-16):

- Three ramjet test cells.
- 2500 N (600-lbm) propellant capacity.
- Altitude simulation.
- Full transition and mission simulation capable.

Features of the Eight static test cells

- 1350 kg (3,000 lbm) propellant capacity.
- 1100 kN (250,000-lbf) thrust capacity.
- 40,000-rpm spin capability.
- High Speed X-ray.
- High Altitude Chambers:
 - Altitude simulation up to 55000 m (180,000 ft).
 - 11 kg (25-lbm) propellant capacity.

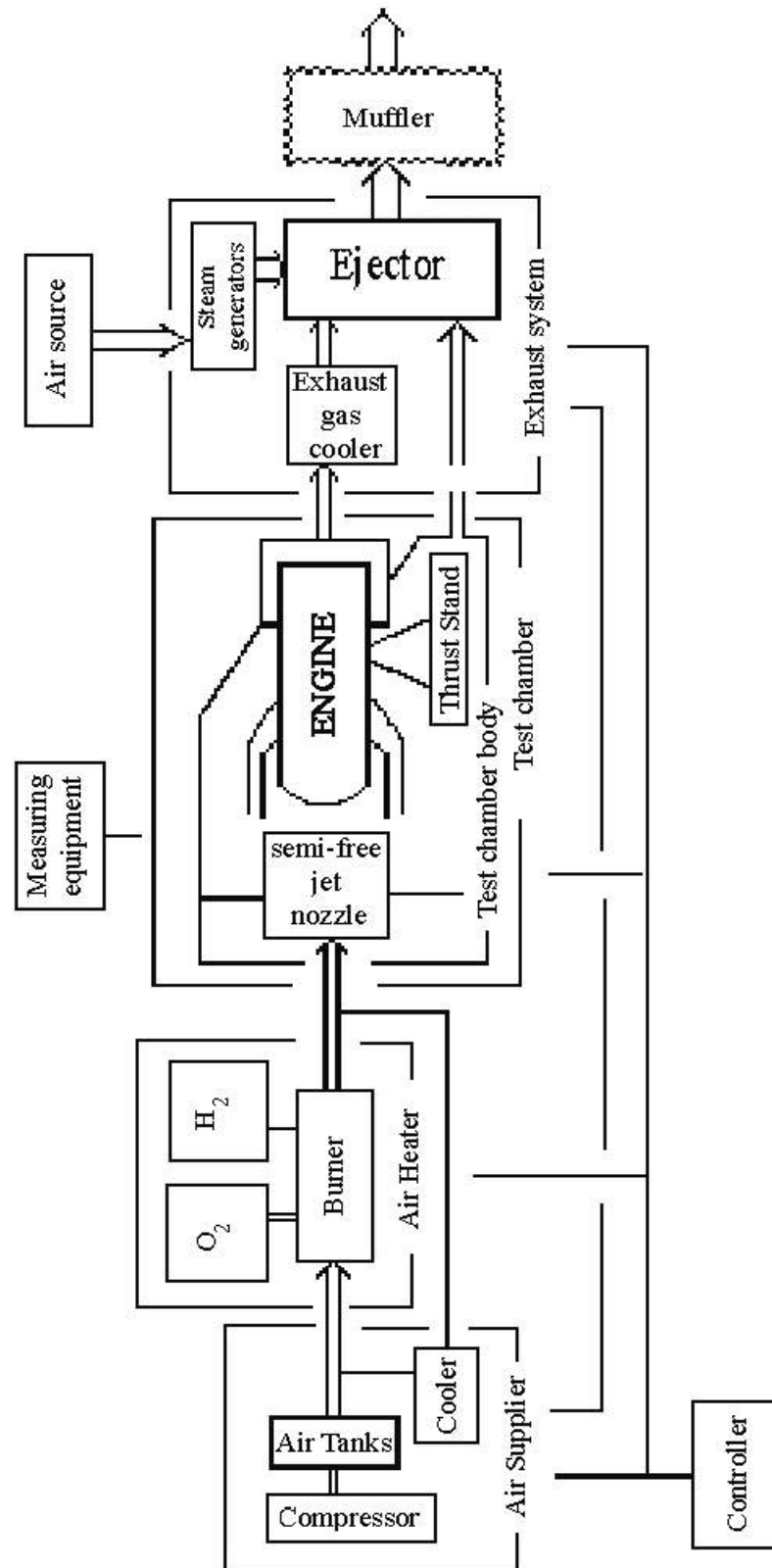


Figure 1-15. Sketch of Chitose Semi-Free-Jet Ramjet Test Setup [9]

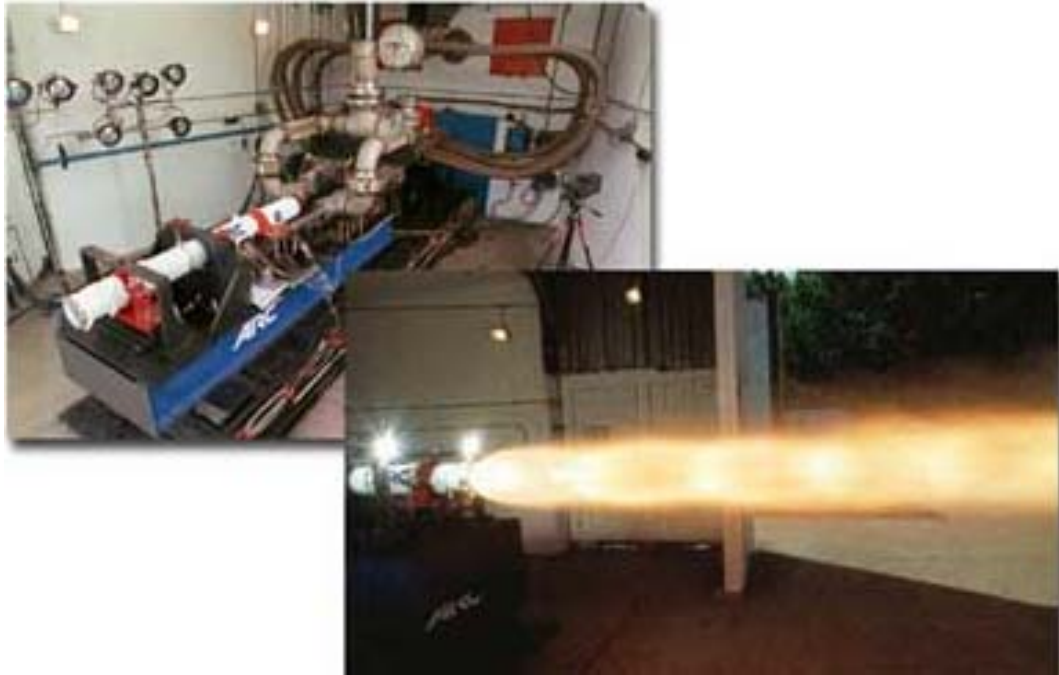


Figure 1-16. ARC Connected Pipe Ramjet Test Centre [11]

1.1.6.5. Onera S4MA Wind Tunnel (France)

The main features (Figure 1-17) [12]:

- The facility produces an air flow at a maximum stagnation pressure of 150 bars and a maximum stagnation temperature of 1800 K
- Usable run duration up to 90s (with vacuum downstream tank of 8000 m³ at 10 mbars).
- The accumulation heater contains 11 tons of alumina pebbles, heated before the run by propane combustion.
- During the run, the air from the heater, dry and non-vitiated, passes through a 10 µm mesh dust filter upstream of nozzle (available for stagnation temperature below 1250 K).
- 3 interchangeable nozzles; the throat of each nozzle is water cooled.
- A quick model introduction device is used to protect the model from flow initiation and breakdown effects.

- The model is mounted with sting and mast on a moving table (angle of attack range 27° at a maximum rate $5.5^\circ/\text{s}$, sideslip range 150° at a maximum rate $11^\circ/\text{s}$).
- Possible use of the facility as a hot gas generator, dry and clean, for ramjet testing, with exhaust to atmosphere.

Typical Tests

- Force measurements (6 components) on complete models.
- Force measurements and hinge moment measurements on model elements and control surfaces.
- Wall pressure measurements, air intake probing (pressure, flow angularities).
- Heat flux measurements (on complete models or model elements).
- Mechanical or thermal testing of real elements (e.g. coating).

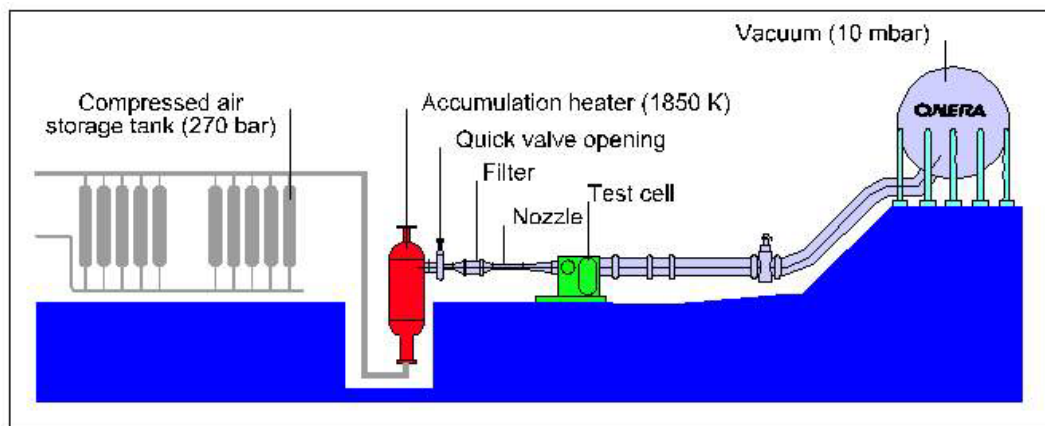


Figure 1-17. Sketch of ONERA Connected-Pipe Test Setup [12]

1.1.6.6. Arnold Aerodynamic and Propulsion Test Unit (APTU-USA)

APTU is a blowdown free-jet test facility designed for true temperature aerodynamic, propulsion and material/structures free-jet testing. A vitiated air

heater (VAH) provides the required temperature. Liquid oxygen (LOX) is added upstream of the VAH to provide the correct oxygen mole fraction at the free-jet exit plane for use by the test article. The facility is completely computer controlled during a run, and very rapid transitions in pressure and temperature can be accomplished. A sketch of the facility is given in Figure 1-18.

A 620 m^3 ($22,000 \text{ ft}^3$) air storage system, pressurized to 260 bar (3800 psia), allows a run duration of the facility from approximately 3 minutes to over 12 minutes, depending on the free-jet nozzle selected and the altitude simulated in the test cell. The test capability upgrade for APTU plans to use an existing high-enthalpy Sudden Expansion (SUE) burner that is currently in storage at AEDC. This burner was designed to provide a flow total temperature of 2500 K (4700°R) at a total pressure as high as 193 bar (2800 psia).

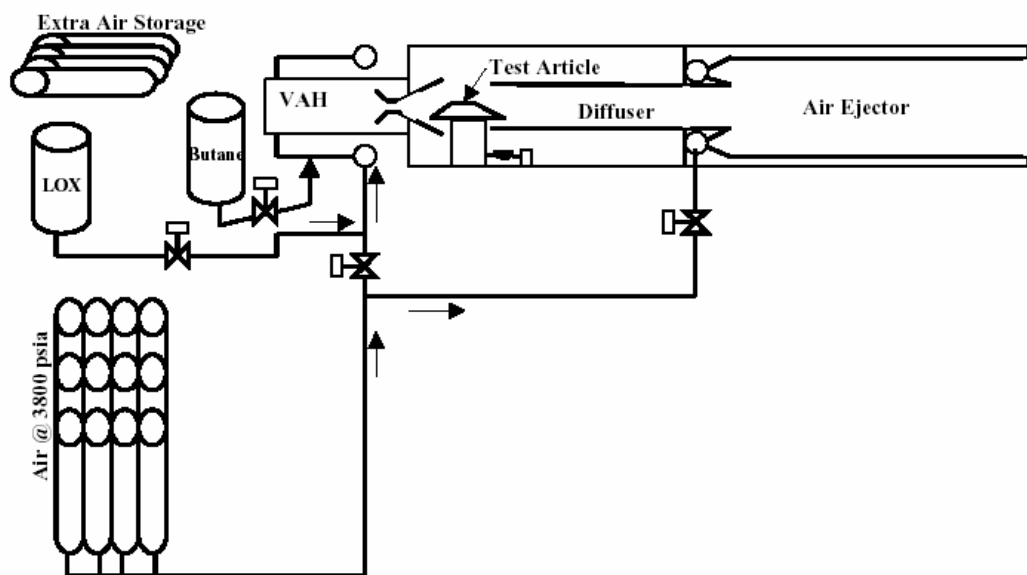


Figure 1-18. Sketch of Hypersonic Test Setup of APTU [7]

1.1.6.7. U.S. Air Force Direct Connect Research Laboratory (USA)

This test facility provides combustor inlet flow conditions corresponding to flight Mach numbers between 3.5 and 5, at dynamic pressures up to 95.8 kPa. The test

cell receives continuous airflow of 13.6 kg/s at 5.17 MPa and a maximum temperature of 922K with 20.7 kPa continuous exhaust from the research air facility. A recirculated cooling water system provides 158 l/s at 483 kPa; raw dump water at 2.41 MPa is also available. A variety of conventional and advanced instrumentation, including a steam calorimeter and a thrust stand, exist for accurate documentation of combustor inlet and exit condition and performance parameters. A sketch of the facility is given in Figure 1-19. [13]

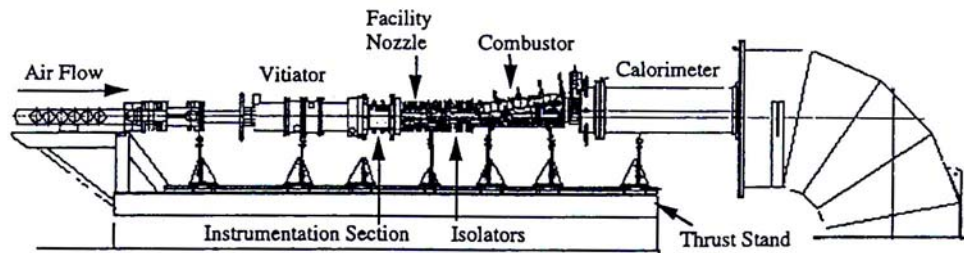


Figure 1-19. Sketch of U.S. Air Force Connected Pipe Facility [13]

1.1.6.8. Comparison of Test Centers

Comparison of test centers is given in Table 1-1.

1.2. VITIATED AIR HEATERS

Free stream air entering to the inlet of a ramjet goes through aerodynamic compression process. This process increases the static temperature of the air. For realistic simulation, air heating system has to be integrated to the test facility to obtain the elevated temperatures caused by aerodynamic compression.

Since combustor inlet Mach numbers are quite low, the static temperature is almost equal to the stagnation temperature. At a flight Mach number of 4, the combustor inlet temperature is approximately 1000K, at Mach 6 it is near 2000K, and at Mach 8 the temperatures are in the 3000 K range. The precise amount of heating required to simulate true flight conditions also varies with altitude. In order to examine combustion performance at realistic flight conditions these combustor inlet

temperatures must be reproduced in test facilities, and a method for producing this heated air must be found.[1]

Table 1-1. Comparison of Properties between the Test Centers

	NASA	Chitose	Kakuda
Simulated Flight Mach number	4-7.5	4	4 - 6 - 8
Nozzle Exit/ Combustor Inlet Mach number	2 - 2.7	-	-
Test gas	Hydrogen	Hydrogen	-
Heater	Vitator	Vitator	Pepple Bed Storage Heater
Total pressure	8 - 35 bar	0.7 - 37 Bar	10, 50, 100 bar
Total temperature	800 - 2100 K	250 - 930 K	800,1500, 2500 K
Airflow	0.4 - 3.5 kg/s	150 kg/s	-
Air Storage	-	-	-

	ONERA	APTU	USAF
Simulated Flight Mach number	6 - 12	3 - 7	
Nozzle Exit/ Combustor Inlet Mach number	2 - 4	2 - 4	3.5 - 5
Test gas	-	Butane	
Heater	Pepple Bed Storage Heater	Vitator	Vitator
Total pressure	150 bar	200 bar	50 bar
Total temperature	1800 K	2500 K	920 K
Airflow	-	80 kg/s	13.6 kg/s
Air Storage	270 Bar 29 m ³	260 Bar 600 m ³	-

1.2.1. HEATER REQUIREMENTS

The air heater should operate on different mass flow rates. It should supply the air in a wide temperature and pressure ranges. Another requirement is that, the heater should operate on different test durations. The air delivered should have a uniform temperature profile and low turbulence levels and be free of air contaminants. Ignition and control of the output flow should be simple and steady state conditions

should be achieved quickly. The heater should be small and have low operation and maintenance costs. The fuel or energy source should also be economical, safe and available. The heater should also be easy, safe and affordable to use.

It is difficult to achieve all these criteria together. An optimum solution has to be found.

1.2.1.1. Special Considerations for Vitiators

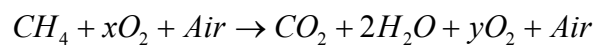
1.2.1.1.1. Make-up Oxygen

While heating the air in a vitiator, combustion process depletes part of the available oxygen. In order to conduct combustion experiments, the oxygen content of the flow must be restored to the proper percentage.

Table 1-2. Compositions for Ideal Air

Species	O ₂	N ₂	Ar
Composition of dry air by volume %	20.95	78.07	0.98
Composition of dry air by weight %	23.19	75.46	1.35
Mean molecular weight of air	28.97		

The aim is to calculate the make-up oxygen flow rate so that the mole fraction of oxygen in the vitiator products is equal to that in atmospheric air. Compositions for ideal air are given in Table 1-2 [14]. To get this mole fraction the stoichiometric chemical reaction for the vitiator fuel and oxidizer combination must be examined. For a methane - air vitiator the reaction is:



Maintaining the mole fraction of oxygen preserves its partial pressure, and therefore reaction rates which may be important at low combustor pressures or high combustor Mach numbers. If the mass fraction of oxygen is maintained instead, the oxygen available to react in the combustor will be less.

The make-up oxygen may be mixed into the flow at any point upstream of the ramburner. However, it is usually helpful to add the oxygen upstream of the vitiator to ensure good mixing and help raise the heater's efficiency and broaden its operating range.

1.2.1.1.2. Air Contaminants

The use of vitiated air instead of ideal air to study ramjet combustion in connected-pipe testing will have an effect not only on the experimental performance but also on the theoretical performance prediction.[1]

The most important problem associated with vitiated air tests is the influence of the contaminants on the combustion process. Unreacted vitiator fuel will add energy to the ramjet and species such as CO and H₂O can change ignition, combustion efficiency and flame holding characteristics measured in the combustor.

Concerning the theoretical performance, contaminants complicate the problem of calculating properties such as the molecular weight, specific heat ratio and the enthalpy of the air entering the combustor. However, if the air heater operates efficiently these thermodynamic properties can be calculated with computer codes, assuming the heater products are at equilibrium by the time they enter the combustor.

1.2.1.1.3. Fuel and Oxidizer Choices

The choice of a fuel and oxidizer combination for heating in a particular test facility is complicated by all the concerns listed in 1.2.1. Table 1-3 lists some common fuels and oxidizers together with some of their positive and negative attributes.

1.2.1.2. Heater Installation and Use

The performance of a heater is significantly affected by the way it is installed in the facility. [6]

The flow quality of air to the ramjet combustor under test can be modified by means of flow strengtheners, screens or plenums to reduce turbulence and spatial variations in flow pressures and temperatures from the heater. If water cooling is necessary for the heater and the ducting to the combustor, heat loss may induce a temperature gradient in the flow. Insulating the hardware to limit heat loss minimizes this problem.

Table 1-3. Fuel and Oxidizers for Combusting Heaters [6]

Hydrogen	<p>Advantages:</p> <ul style="list-style-type: none"> • Wide flammability and ignition ranges • Efficient combustion <p>Disadvantages:</p> <ul style="list-style-type: none"> • Water vapor and low molecular weight in exhaust
Hydrocarbon (liquid or gaseous)	<p>Advantages:</p> <ul style="list-style-type: none"> • Minimal safety requirements <p>Disadvantages:</p> <ul style="list-style-type: none"> • Carbon dioxide and water vapor in exhaust
NH ₃	<p>Disadvantages:</p> <ul style="list-style-type: none"> • Water vapor in exhaust • Toxicity
NO ₂	<p>Advantages:</p> <ul style="list-style-type: none"> • Exhaust is similar to air • Heat release upon decomposition <p>Disadvantages:</p> <ul style="list-style-type: none"> • Special handling required
N ₂ O ₂	<p>Disadvantages:</p> <ul style="list-style-type: none"> • Toxicity

Acoustic decoupling of the air heater from the fuel and oxidizer feed lines and the ramjet combustor is often necessary to avoid introducing acoustic oscillations unique to the facility installation of the ramjet under test. A basket diffuser having

many small holes is often used in the air heater to suppress these pressure oscillations. Sonic orifices between the combustor and heater prevent feed back from the ramburner to the vitiator. This solution, however, requires higher vitiator supply pressures for the air, fuel and make-up oxygen, which necessitates higher pressure supply tanks and/or pumps.

1.2.2. HEATER PERFORMANCE

1.2.2.1. Performance Parameters

Combustion efficiency is the most important heater performance parameter since unburned heater fuel will affect the results obtained with the ramjet tested.

Uniform temperature and pressure profiles in the vitiator exhaust are desirable.

The heater should have a smooth combustion behavior with a minimum of pressure oscillations and be free of distinct resonance frequencies.

Heat loss to the heater structure or downstream devices is a performance related parameter since it increases heater fuel flow and subsequently the air contaminants.

The envelope of heater operation should be wide enough to allow for the temperature and mass flow variations needed for flight trajectory simulations.

1.2.3. FLAME HOLDERS

Typical velocities in vitiators or Ramjet combustors are greater than 30 m/s , which exceed the flame speed of hydrocarbon and air mixtures. Any flame initiated in a high velocity region would be swept downstream. Consequently, to stabilize a flame in the combustor, a low velocity region is required. [15]

It is of very great use that the flame-stabilization process is seen as nothing but the interaction of high-temperature reaction kinetics with the aerodynamics of the recirculation.

If the fluid stream is a gas capable of sustaining an exothermic reaction, moving at an average velocity greatly in excess of the speed of laminar flame propagation of the mixture, a steady flame can exist only if a flame-stabilising device is provided in the stream. [16]

1.2.3.1. Common Flame Stabilizing Devices

- A jet of hot gas injected into the steam in the direction of flow
- A jet of gas at the same temperature as the oncoming stream, at such an angle to it that recirculation is provoked
- A stream-lined surface, heated by external means to a high temperature
- A stream-lined catalytic surface, heated by the reaction of main-stream gases in contact with it
- A steady stream of sparks

1.2.3.2. Flame Stabilization by Bluff Bodies

The most common flame-stabilising device is the “bluff body”. A “bluff body” is a solid object of such a shape that, when it is suspended in a fluid stream, a re-circulatory flow is formed in its immediate wake as shown in Figure 1-20. Examples are:

- a sphere,
- a circular-sectioned cylinder with its axis at right angles to the direction of flow,
- a cone with its axes parallel to the direction of flow,
- a V-sectioned “gutter” with its edges at right angles to the flow direction.

The essential feature is the recirculation found in the immediate wake of the body. Another name for “bluff-body flame-stabilizer” is “baffle”.

If the whole fluid stream is combustible, the stabilization region is normally followed by a propagation region, in which the flame spreads from the bluff-body

stabilizer to the wall. If the fuel air ratio of the stream is non-uniform, this propagation may be of only limited extent (Figure 1-21).

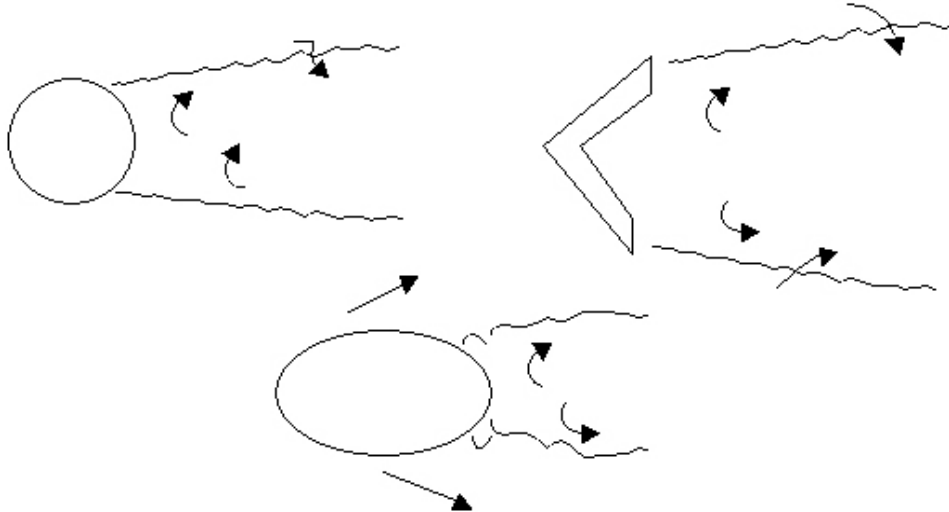


Figure 1-20. Recirculating Flow Behind a Sphere, a Gutter and a Strut

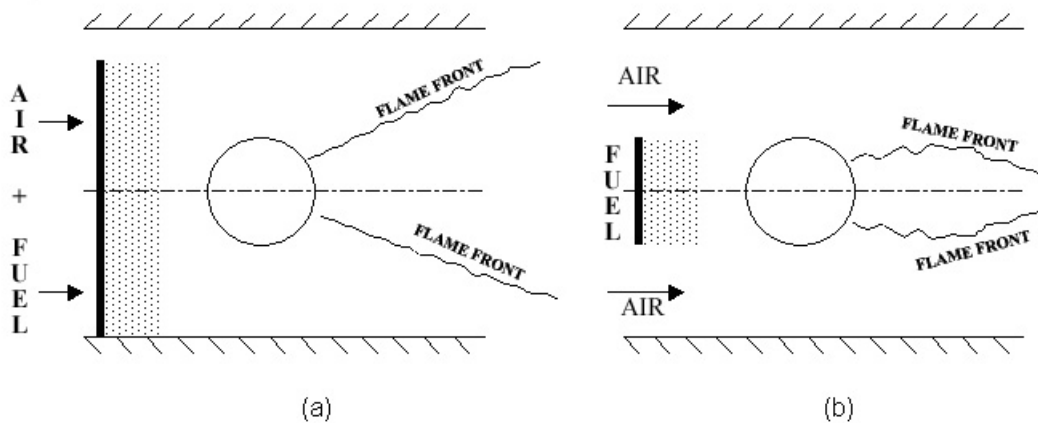


Figure 1-21. Flame Propagation Downstream of a Baffle: (a) For A Uniform Fuel-Air Mixture, (B) When The Fuel Is Confined To A Central Region.

1.2.3.3. Flow Pattern Behind a Bluff Body

The pattern of stream lines is roughly as shown in Figure 1-22. The reverse-flow region is usually between two and five body widths long. The fluid within the closed stream lines is highly turbulent at the velocities which are encountered in flame-stabilization practice.

1.2.3.4. Flame Stabilization by Recirculation

An alternative to a bluff body is a recess in the wall of the combustor. Recesses with leading edges that are adequately sharp produce flow separation to establish a recirculation zone in the recess. The stabilization mechanism is like that of the bluff body. The length of the wall recess plays the same role as the length of the bluff-body recirculation zone in stabilization. The design is a duct with a small cross-sectional area expanding coaxially into a duct with a larger cross-sectional area (Figure 1-23). The flame is stabilized by the recirculation region that forms at the step. Designs of this type are becoming popular since they offer benefits such as reduced losses in total pressure; associated wall-heating problems are solvable, for example, by transpiration cooling if necessary.[17]

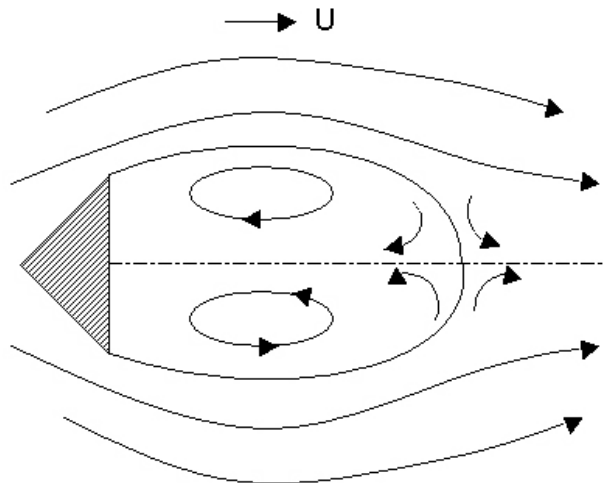


Figure 1-22. Flow Behind a Baffle

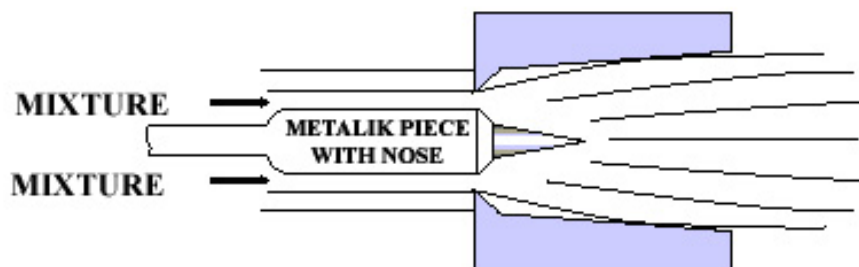


Figure 1-23. Stabilization Setup by Recirculation

1.2.3.5. Pilot Flames

The immediate expansion of the mixture as soon as it leaves the central orifice of the nozzle creates some depression around it. Secondary air is necessary both for stabilizing the pilot flame and complete the combustion of gas. The combined effect of the pressure drop through the pilot ports and the impact of the flames on the outer rails act as a stabilizer on the flame. This type of construction prevents the burner from overheating. Design alternatives for flame stabilization by pilot flames are given in Figure 1-24.[17]

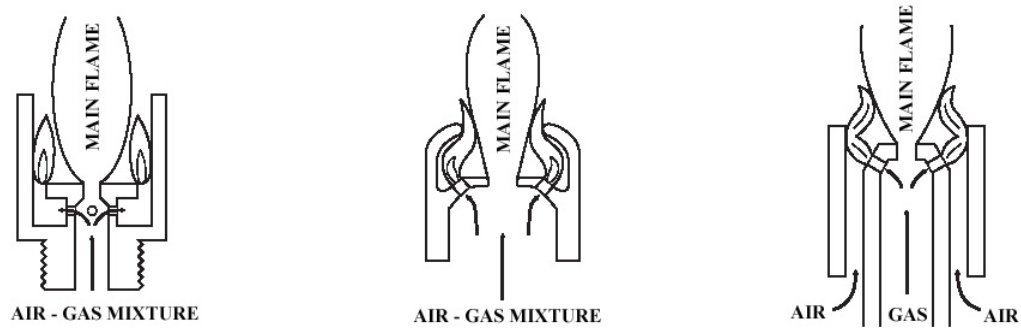


Figure 1-24. The Stabilization Setups by Pilot Flames

1.3. TECHNICAL METHOD

The design of the connected pipe ramjet test facility is based on the conceptual design a ramjet missile which is reported in [2].

1.3.1. DESIGN INPUTS

The trajectory and flight data of the ramjet engine has been determined by guidance study. The trajectory and Mach number evolution during flight is given in Figures 1-25 and 1-26.

Notice that for the chosen trajectory, the ramjet engine will stop at 200 s of flight. After that it will fly horizontally by increasing its angle of attack and will start diving at 250 s.

Design of the inlet of Missile X is performed for cruise conditions; flight altitude of 16 km and Mach number of 3.5. Off-design analysis of the inlet is also performed. For the trajectory and Mach number evolutions presented in Figures 1-25 and 1-26, the pressure, temperature and air mass flow rate values at the combustor inlet are evaluated for entire flight. Pressure, temperature and air mass flow rate variation versus time graphs are presented in Figures 1-27, 1-28 and 1-29, respectively.

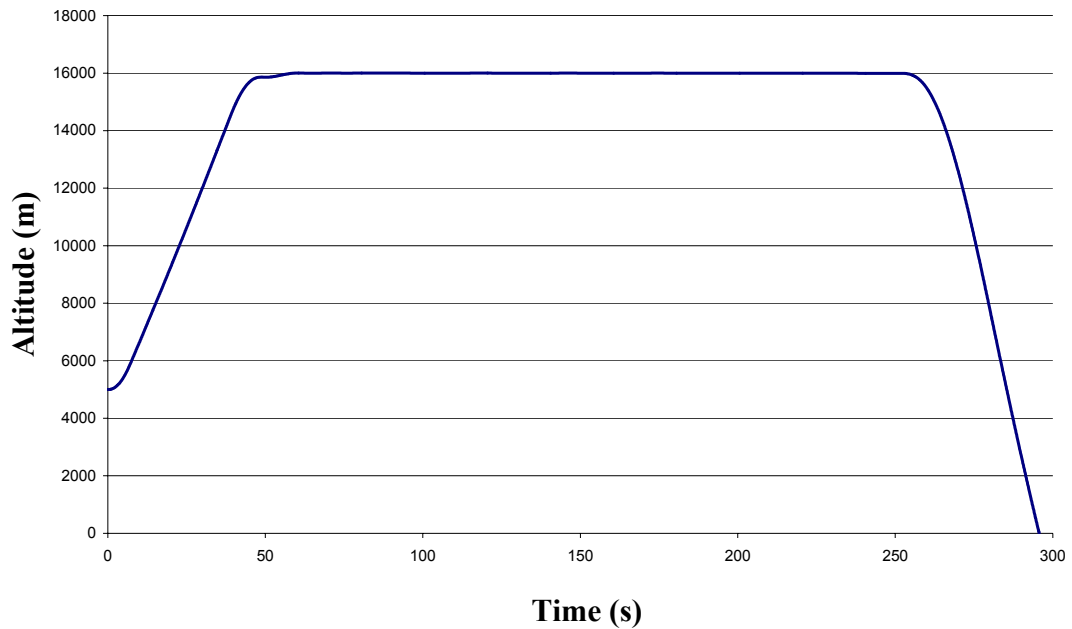


Figure 1-25. Flight Trajectory of Missile X.

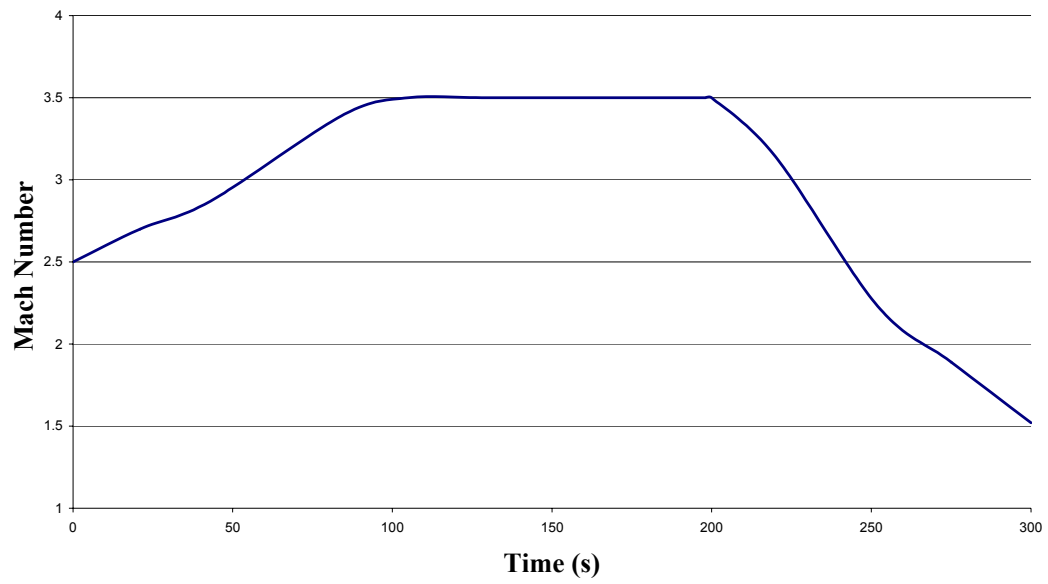


Figure 1-26. Mach Number Evolution of Missile X.

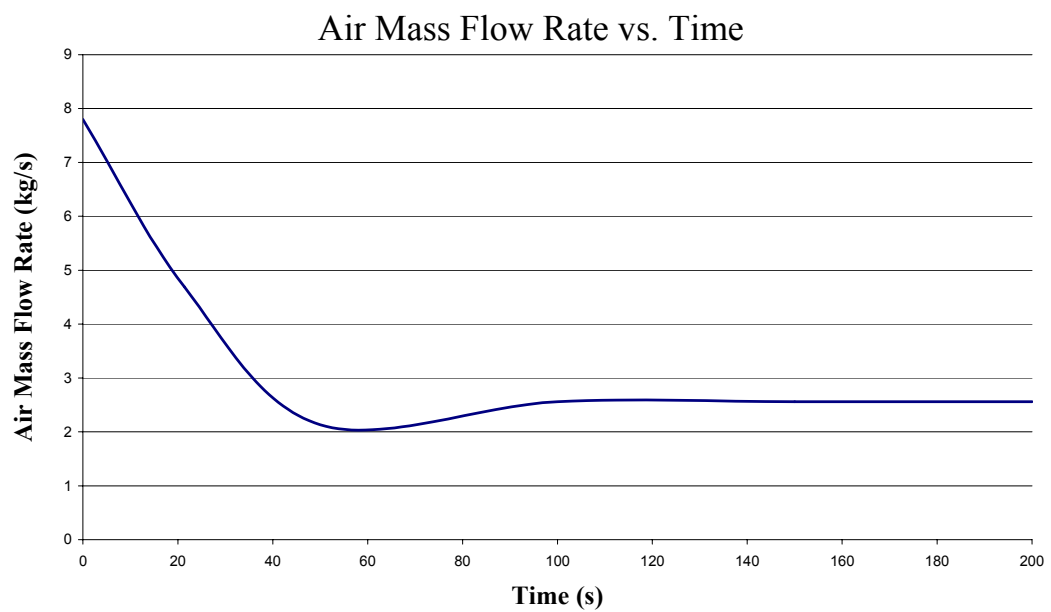


Figure 1-27. Mass Flow Rate Captured by Inlets vs. Time

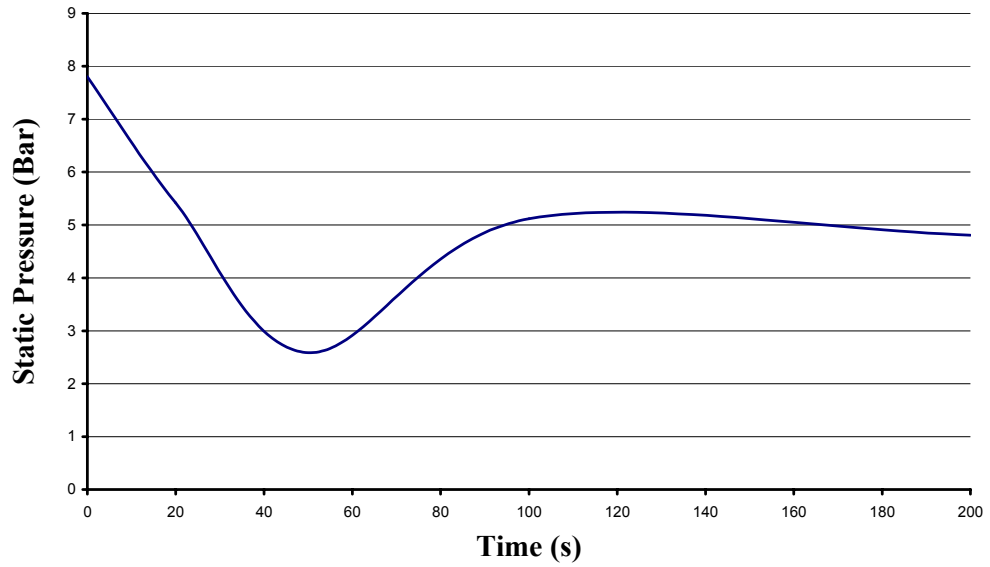


Figure 1-28. Static Pressure at the Combustor Inlet vs. Time

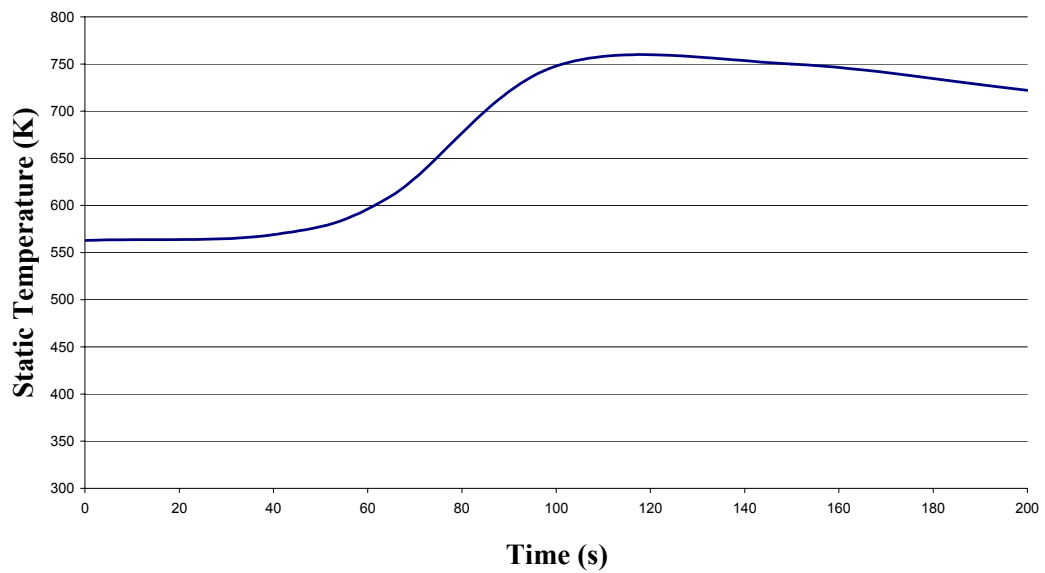


Figure 1-29. Static Temperature at the Combustor Inlet vs. Time

Test facility designed in this study will be able to provide the air mass flow rate, temperature and pressure variation presented in Figures 1-27, 1-28 and 1-29 for test duration of 200 s.

Ramjet combustor air inlet area is 3673.4 cm^2 .

1.3.2. DESIGN METHODOLOGY

During design process three subsystems have been analyzed; air storage system, air heater system and test chamber. Exhaust system is not considered in this test facility. Design algorithm followed during the design process is given in Figure 1-30.

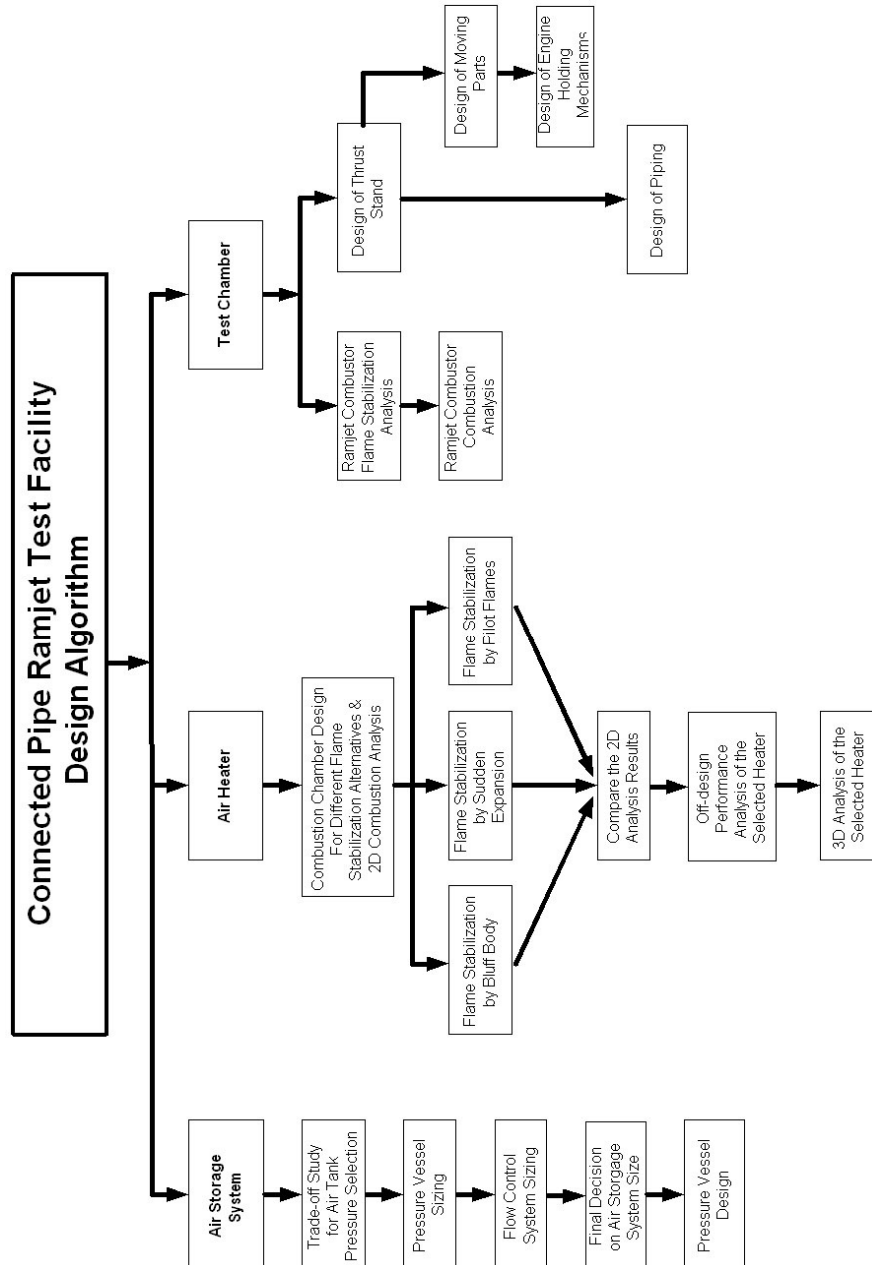


Figure 1-30. Design Algorithm of the Connected Pipe Test Facility

CHAPTER 2

AIR STORAGE SYSTEM DESIGN

2.1. INTRODUCTION

In this chapter, design of the air storage system is considered. Design of the pressure vessel is initiated by vessel sizing for different pressures and wall thickness. After an evaluation of the designed cases, some of the alternatives are eliminated because of the high manufacturing cost, material limitation and difficult manufacturing operations. Then the flow control system is designed for the remaining alternatives and finally the best solution for pressure vessel and flow control system is selected. Pressure vessel design is based on ASME Codes. Design methodology and equations of ASME Code are given in Appendix A. Details of pressure vessel design is given in Appendix B.

2.1.1. SYSTEM REQUIREMENTS

Air storage system should be able to supply the air mass flow rate profile presented in Figure 1-27 and the pressure profile presented in Figure 1-28.

2.1.2. SYSTEM COMPONENTS

Component tree of air storage system is given in Figure 2-1. Main components of the air storage system are as follows:

- Pressurized air tanks (to store air which is needed during the ground testing)
- Compressor (to charge the air tank with air)

- Flow regulation system (to receive the air at the required pressure and the mass flow rate)

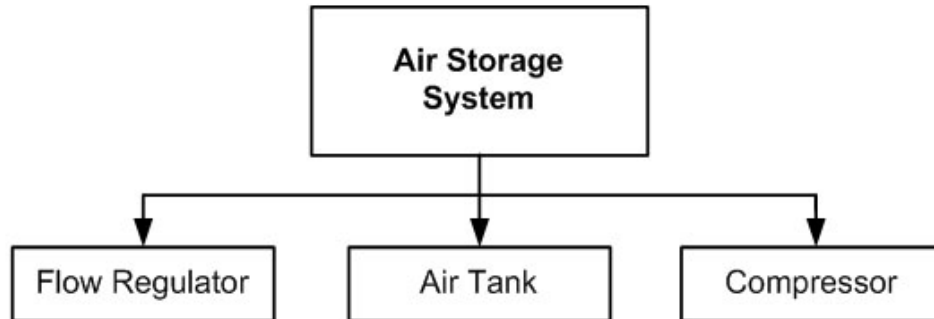


Figure 2-1. Component Tree of Air Storage System

2.1.3. AIR STORAGE SYSTEM DESIGN ALGORITHM

Air storage system design algorithm is given in Figure 2-2.

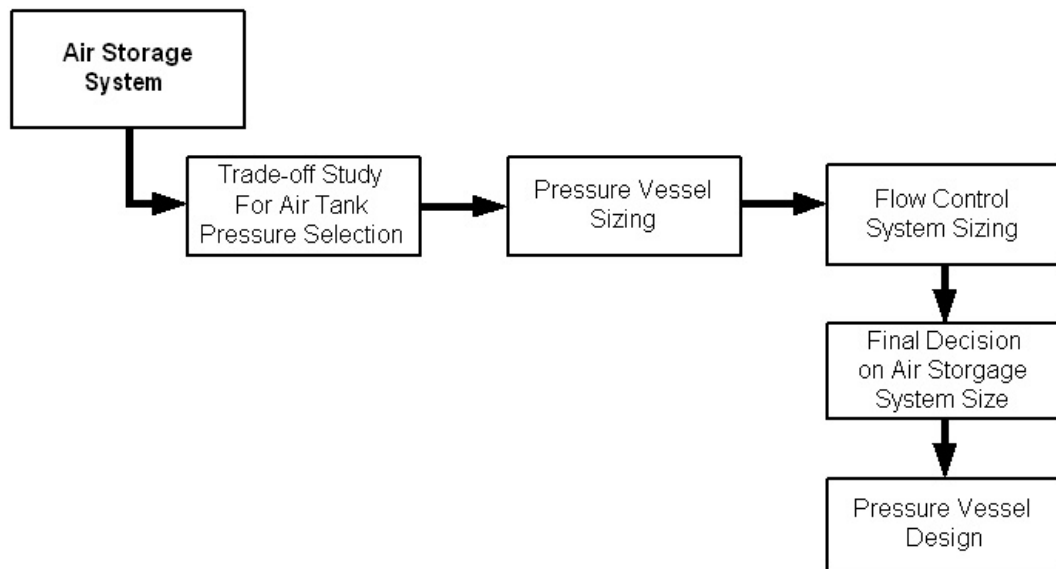


Figure 2-2. Air Storage System Design Algorithm

2.1.4. AIR STORAGE SYSTEM SIZING

2.1.4.1. Design Parameters

Average mass flow rate: 2.77 kg/s

Test duration: 200 seconds

Total mass of air needed: 550 kg

Safety factor: 3

Total air to be stored: 1650 kg

Air critical temperature: 132.65 K [18]

Air critical pressure: 37.71 bar [18]

2.1.4.2. Sizing

Pressure of the air storage tank has to be determined to design the pressure vessels and pressure regulation system. A tradeoff study is performed to choose the best configuration for the present case. The results of the study are given in Table 2-1. For four pressures alternative (50, 100, 150 and 200 bar), density and volume required to store 1650 kg of air are calculated.

Table 2-1. Trade-Off Study for Tank Pressure Selection

	Case 1	Case 2	Case 3	Case 4
Pressure (bar)	50	100	150	200
Reduced Pressure	1.326	2.65	3.97	5.29
Reduced Temperature	2.25	2.25	2.25	2.25
Compressibility Factor	0.9865	0.986	0.9982	1.022
Density (kg/m ³)	59.26	118.5	175.7	228.8
Volume (m ³)	27.8	14	9.39	7.21

Case 1 to Case 4 is studied during the air tank design.

2.2. PRESSURE VESSEL DESIGN

Case 1 to 4 given in Table 2-1 is studied in detail in this section. In the analysis, quenched/tempered alloy steel is used. Ultimate Tensile Strength of the material is 828 MPa. Safety factor for the shell and head are taken as 3 and 4, respectively.

Shell contains a welding seam longitudinally and the head is connected to shell by welding. The thickness of the shell and the head is limited by the weld technology. In order to ease welding operation, thickness of the shell and the head is limited to 15 mm. Two conditions are considered, thickness for 10 and 15 mm. Then, the volume of the tank is evaluated using the calculated radius. Length of the tank is taken as 2 meters. Results are tabulated in Table 2-2.

Table 2-2. Pressure Vessel Sizing

Cylindrical Section	Case 1		Case 2		Case 3		Case 4	
Pressure (bar)	50		100		150		200	
Volume (m ³)	27.8		14		9.39		7.21	
Thickness (mm)	10	15	10	15	10	15	10	15
Vessel Radius (mm)	546	819	270	405	178	267	132	198
Unit Vessel Volume (m ³)	1.87	4.21	0.46	1.03	0.2	0.45	0.11	0.25
Number of Vessels	22	10	44	20	75	34	100	44
Elliptic Head Thickness (mm)	14	20.6	14	21.5	14.6	22	15.5	23

As the internal pressure increases, the vessel radius decreases and the number of vessel increases. On the other hand, the production is easy to handle for vessels that are smaller in size. Also for high pressure vessels, pressure regulation is more complicated.

Case 3 and Case 4 is eliminated at this point because of the high number of vessels to be manufactured. Also the head with thickness greater than 20 mm is not easy to manufacture. Pressure vessel alternatives will be considered as Case 1 and Case 2 with thickness 10 mm from this point on.

A computer code (Discharge Code) is written to evaluate the pressure and temperature change during discharge. First law of thermodynamics and compressible flow properties are used in this code. Details on the discharge code are given in APPENDIX D. Results are given in Figures 2-3 and 2-4 for Case 1 and Case 2, respectively.

Temperature at the end of 200 seconds is 255 K for both Case 1 and Case 2. Pressure vessel material properties can perform efficiently between these operation temperatures, 298 K to 255 K.

Vessel choice is also depends on the pressure regulation system.

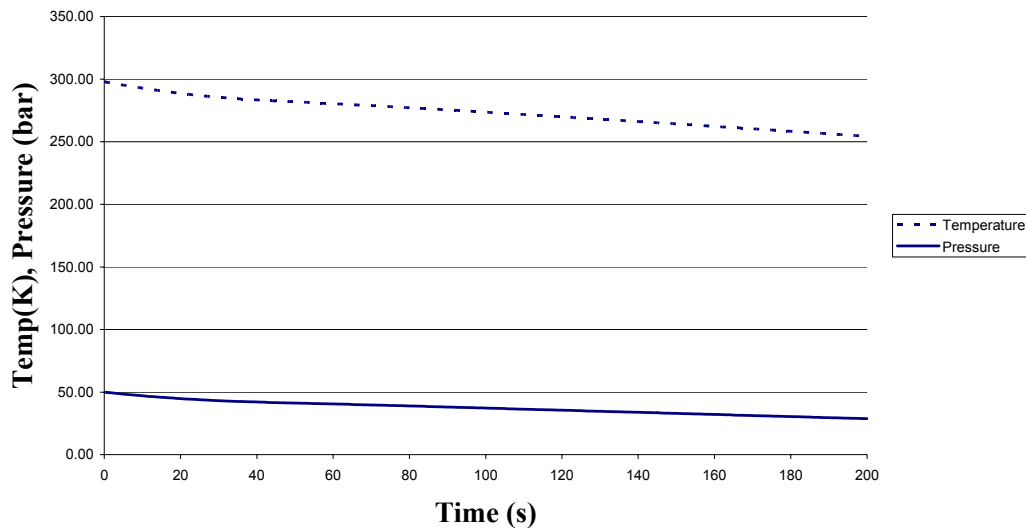


Figure 2-3. Pressure and Temperature Change During Discharge for Case 1

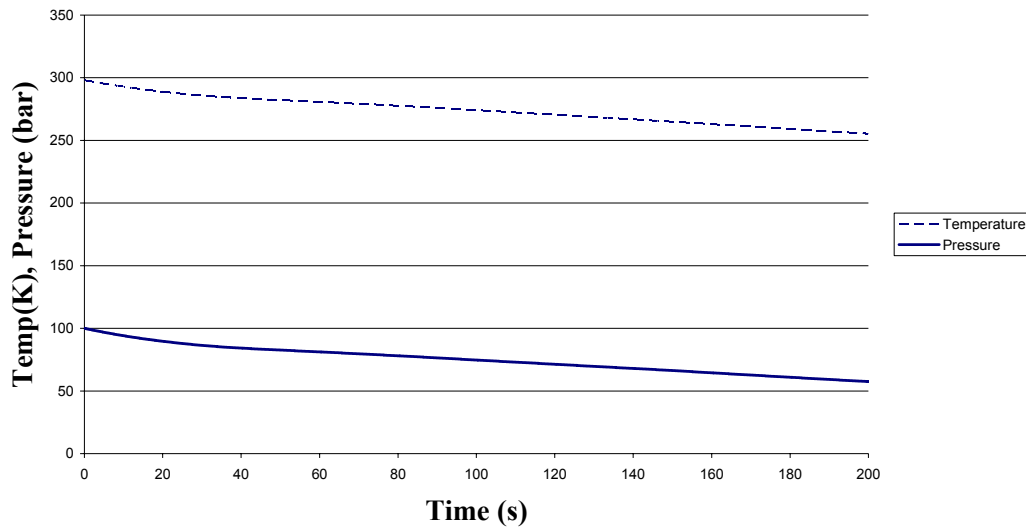


Figure 2-4. Pressure and Temperature Change During Discharge for Case 2

2.3. FLOW CONTROL SYSTEM

In the connected pipe test stand, pressurized air has to be supplied to the heater. Pressure of air stored in the vessel is higher than required. To obtain the required pressure along with the required mass flow rate, a flow regulation system should be used. Regulation can be obtained by using valve series. Air to be supplied to the ramjet engine is around 5 bar. The valves available in the market offers pressure drop between 5-25 bar. For pressure vessel pressure higher than 50 bar, special flow regulators as well as a bundle of pipe that contains on-off control valves can be used to decrease the pressure down to acceptable level to be handled by the valve series. To couple pressure regulator and the valves, a resting chamber can be utilized (Figure 2-5).

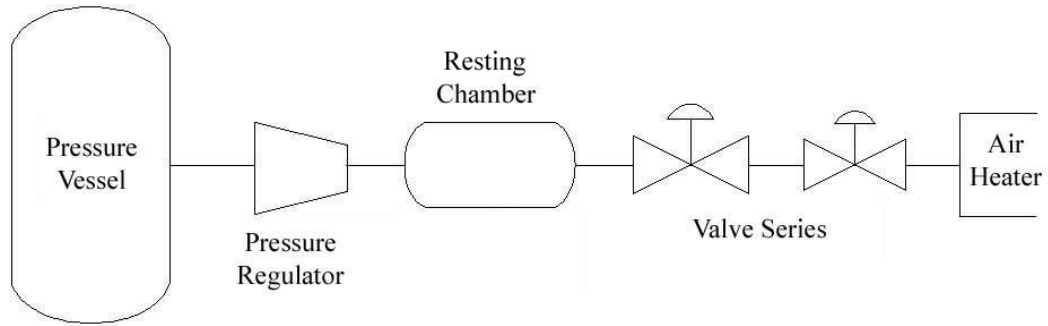


Figure 2-5. Pressure Regulation System

Flow regulation components are as follows:

- Pressure regulator (special regulator or bundle of pipe)
- Resting chamber
- Regular Valves for flow control

2.3.1. PRESSURE REGULATION BY VALVES

Mass flow rate and pressure of air can not be adjusted by one regulating valve. A series of valves should be used as shown in Figure 2-5.

A valve can supply a certain pressure drop for specific mass flow rate. For two valves with different characteristics, required pressure and mass flow rate can be obtained.

2.3.1.1. Valve Sizing

2.3.1.1.1. Terminology

dp: Differential pressure across test valve, measured in kPa (psi).

Flow coefficient (Cv): The number of standard cubic meters of air (air at standart pressure and temperature) per minute that can flow through the valve at a pressure drop of one psi. (Note: The maximum Cv is determined with the valve in a fully open position. However, intermediate flow coefficients can also be determined.)

N: The numerical constant for the units of measurement used in the general sizing equations. N is 4.17 when q is expressed in m³/h, P is expressed in kPa, and T is expressed in K. [Note: N is 1,360 when q is expressed in scfh, P in psia, and T in °R.]

P: Absolute pressure at upstream test manifold tap, expressed in kPa (psia). [P(abs) = P(gauge) + barometric pressure]

q: Volumetric flow rate (scmh).

Sg: The specific gravity of a gas relative to air, Sg approximately equals the ratio of the mass of a gas to the mass of an equal volume of air at a specified temperature. [Specific gravity of air =1.0 at 15.6°C(60°F).]

T: Absolute temperature of test gas, K (or °R).

x: the ratio of differential pressure to absolute inlet static pressure, dP/P.

Scheme for valve calculations is given in Figure 2-6.

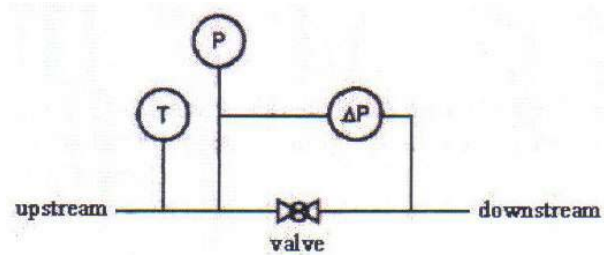


Figure 2-6. Scheme for Valve Calculations

$$C_v = \frac{q}{N.P} \left(\frac{T.S_g}{x} \right)^{0.5} \quad [19]$$

2.3.1.1.2. Valve Selection

The C_v value should be used as a guide in the valve selection. A valve that is less than half the pipe size shouldn't be used. Also using the lower 10% and upper 20% of the valve stroke should be avoided. The valve is much easier to control in the 10-80 % stroke range.

2.3.1.2. Pressure Regulation for Case 1

In this case, two valves are directly connected to pressure vessel one after each other. Tank pressure and temperature given in Figure 2-3 is used in C_v analysis. Results are given in Table 2-3.

Table 2-3. C_v Analysis for Case 1

	1 st valve	2 nd valve
$C_{v_{\max}}$	8.8	6.0
$C_{v_{\min}}$	33.2	22.2
ΔP_{\max}	17 bar	30.5 bar
ΔP_{\min}	17 bar	7 bar

2.3.1.3. Pressure Regulation for Case 2

For Case 2, it is not possible to obtain required pressure regulation by only regular valve series. In this situation, a prior regulation is required (First 100 bar will be reduced to 50 bar). A resting chamber can be placed between the regulator and the valves. Resting chamber helps to control the flow and ease the calculations. The special regulator will keep the pressure of the resting chamber at a constant value (50 bar) and the other two valves will act as in Case 1 to obtain the pressure profile given in Figure 1-28.

Air temperature at the resting chamber is assumed to be the same with the vessel temperature given in Figure 2-4. Results of the C_v values obtained are tabulated in Table 2-4:

Table 2-4. C_v Analysis for Case 2

	1 st valve	2 nd valve
$C_{v_{\max}}$	8.8	7.3
$C_{v_{\min}}$	36.5	39.15
ΔP_{\max}	20 bar	12.5 bar
ΔP_{\min}	20 bar	7.45 bar

2.3.2. PRESSURE REGULATION FOR HIGH PRESSURE DROP

Pressure regulation between tank pressure and resting chamber pressure can be obtained by special pressure regulators for Case 2. Such regulators are available on the market. An example is given in Figure 2-7.

Flow rate at standard conditions are calculated as:

$$Q_{\max} = 390 \text{ scmh}$$

$$Q_{\min} = 90 \text{ scmh}$$

Max Primary Pressure = 100 bar

Secondary Pressure (resting chamber) = 35 bar

2.4. STORAGE SYSTEM CHOICE

2.4.1. EVALUATION OF STORAGE SYSTEM CASE 1

- Internal pressure of the main tank is 50 bar. Pressure is easy to control.
- 22 tank with 546 mm radius can be used. Less tank is needed than Case 2.
- Radius is greater than Case 2. Manufacturing is more difficult.
- Pressure regulation is simple. It can be achieved by two regular valve.

Dome Pressure Regulator

Directly effective dome pressure regulator for mounting in pressure lines.

Medium:

Air, gas

Standard features:

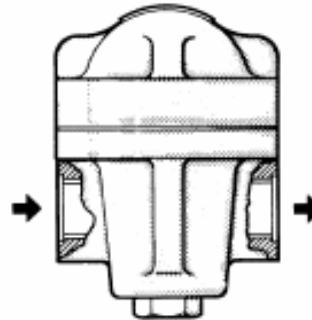
Housing and dome made of forged aluminium bronze, valve seat made of stainless steel, valve seat soft gasket, which ensures a tight seal when the valve is closed.

Ambient temperature:

+ 5 °C to + 45 °C

Temperature range of medium:

- 20 °C to +100 °C, (special version to - 50 °C)



We recommend the BAUER particle filter, N 4817, which reliably absorbs particles through his precision work of 20 mm. That guarantees a long life of the pressure reducer.

Recommended filter:

N 4817 for PN 420

Order- Number	Max. primary pressure bar	Secondary pressure bar	Flow rate * m3/min	H mm	Diame- ter mm	Thread	Order- number repair kit
N 4801	420	0,1 - 280	160	160	120	G 1	N 6294
N 4802	315	0,1 - 175	612	260	260	G 2	N 6295
N 16014	310	0,4 - 175	505	244	171	G 1 1/2	sur de- mande

* with 42 bar primary pressure and max. secondary pressure rel. to +20°C and 1 bar abs.

Figure 2-7. Example of High Pressure Regulator

2.4.2. EVALUATION OF STORAGE SYSTEM CASE 2

- Internal pressure of the tank is 100 bar. Pressure is more difficult to control.
- 44 tank with 270 mm radius can be used.
- Manufacturing is easier for small size.
- Pressure regulation is more complex. A regulator and resting chamber is needed in addition to the other two regular valve.

When Case 1 and Case 2 are compared, it is more feasible to employ Case 1. Design method and equations are given in Appendix A. Details for mechanical design is given in the Appendix B.

2.5. COMPRESSOR TO CHARGE THE AIR TANK

The compressor should be able to compress the air up to 50 bar which is the pressure of the selected air tank. Such compressors are available on the market. Technical data of one compressor manufactured by Atlas Corpo which can be used in the system is as follows:

Gas: hydrocarcon, air, carbone dioxide, nitrogen

Compressor shaft power: 30-1500 kW / 40-2040 HP

Compressor speed: ≤ 1000 rpm

Maximum working pressure:

- 100 % oil-free: $P_{\max} = 90$ bar / 1300 psi
- Mini-lub : $P_{\max} = 200$ bar / 3000 psi
- Full lubrication : $P_{\max} = 350$ bar / 5000 psi

Minimum pressure ratio: 1.2

Minimum working pressure: 2 bar / 30 psi

Minimum suction temperature: -50°C / -60°F

A picture of the compressor is given in Figure 2-8 and air flow rates supplied by the compressor is shown in Figure 2-9.



Figure 2-8. Example of High Pressure Compressor

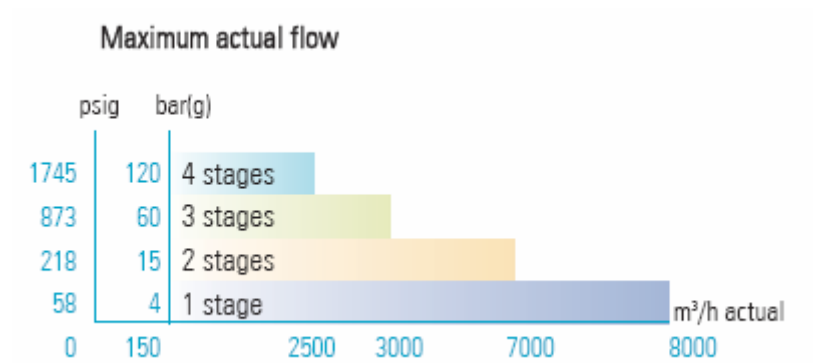


Figure 2-9. Air Flow Rates of EHNX GT Compressor

CHAPTER 3

AIR HEATER SYSTEM DESIGN

3.1. AIR HEATER DESIGN

For the current study, the best way to achieve temperature variation that simulates the flight conditions is to use a vitiator or a combination of vitiator and electric heaters.

Solutions for transient simulations can be as follows:

- A single vitiator with adjustable fuel flow rate: Computer controlled valves adjusts the fuel flow rate. By adjusting the correct air to fuel ratio, the required air temperature is obtained. The response of the fuel flow rate on the output temperature is very quick.
- A vitiator following an electric resistance heater: An electric heater has limiting conditions such as material strength and operation cost. On the other hand, temperature variation can be controlled easily by electric heater. This solution eliminates the need for computer controlled valves but fast response from electric heater for air temperature can not be obtained.

3.1.1. VITIATOR ANALYSIS

Several different vitiator design alternatives are studied for the three flame holding mechanisms stated in section 1.2.3. Combustion analyses are performed by using FLUENT CFD code. Modeling methodology and verification of FLUENT

combustion module is presented in APPENDIX C. Analysis are performed to obtain the most suitable design by using the experimental results given in [6]. Measured test data from [6] are as follows:

Vitiation fuel: CH₄

Air: 79% N₂ – 21%O₂ (mass fraction of O₂ is 23.19%)

- Mass flows rates:

$$\dot{m}_{vf} = 0.047 \text{ kg/s}$$

$$\dot{m}_{O_2} = 0.262 \text{ kg/s}$$

$$\dot{m}_{air} = 6.383 \text{ kg/s}$$

- Pressures and temperatures:

$$P_2 = 650200 \text{ Pa}$$

$$T_{t2} = 606 \text{ K}$$

Air inlet size is designed such that the flow Mach Number at the inlet is 0.3.

3.1.1.1. FLUENT MODELLING

In combustion analysis, Finite rate chemistry model is used. Species transport model is selected for species handling and volumetric reactions are considered. **Eddy-Dissipation** (for turbulent flows, computes the mixing rate) is chosen for the “Turbulence – Chemistry Interaction” model. Mixture properties which are already available in FLUENT database are used.

For physical properties of the species in the mixture like molecular weight, viscosity, thermal conductivity etc., default values from the FLUENT database are used.

A turbulent model has to be specified. The realizable k-ε model is used.

3.1.1.1.1. Boundary Conditions:

Operating Pressure: Input the pressure that combustion takes place

Inlet (for premixed flow):

- mass flow rate of the mixture is defined
- mass fractions of fuel and oxygen are defined
- turbulence parameters are defined

Outlet: only turbulence parameters are defined

3.1.1.1.2. Properties of the Grids Used in CFD Analysis

Analyses are performed to see the effect of mesh size on the CFD solutions. Figure 3-1 shows prediction of static temperature for Case 2 presented in section 3.1.1.2.2, at radial location 50 mm after the flame holder. The solutions predicted by the 3000 and 5000 cases were nearly identical. But solutions predicted by 1000 cell case was slightly different from those predicted by the finer grid calculations. The solution predicted by the 5000 cell case is considered to be sufficient. For 2D analysis an average element number of 5000 is used.

For 3D analysis, analysis are performed using 100,000 hybrid cells (structured and unstructured used together at different parts of the model).

3.1.1.2. FLAME STABILISATION BY BLUFF BODY

3.1.1.2.1. CASE 1

The vitiator fuel is mixed with the air and the replenished O₂ before the vitiator inlet. A sketch of the vitiator is given in Figure 3-2 (dimensions are in mm). Inputs for FLUENT are given in Table 3-1.

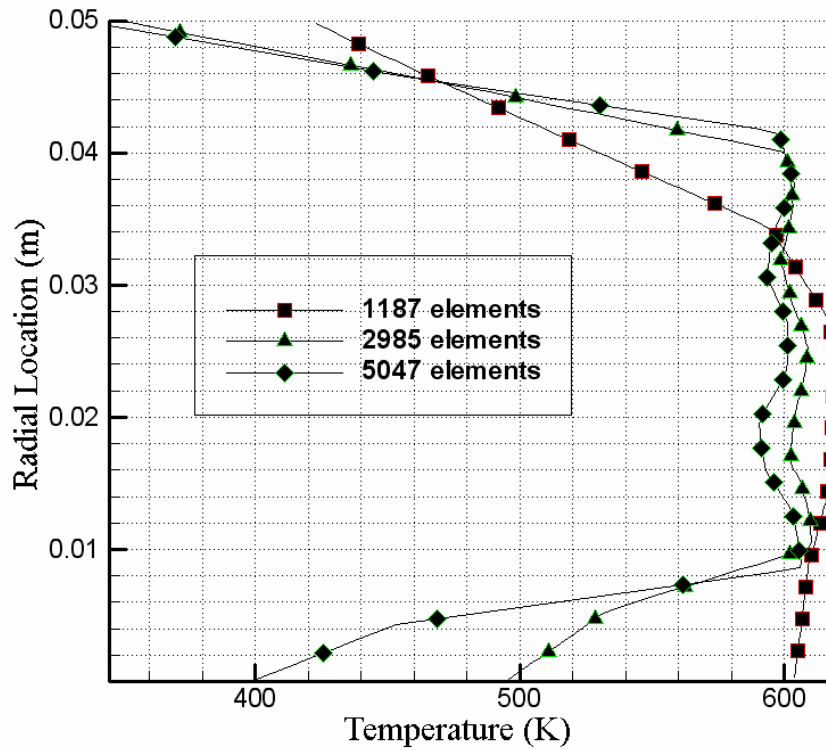


Figure 3-1. Prediction of Temperature Using Different Grid Densities

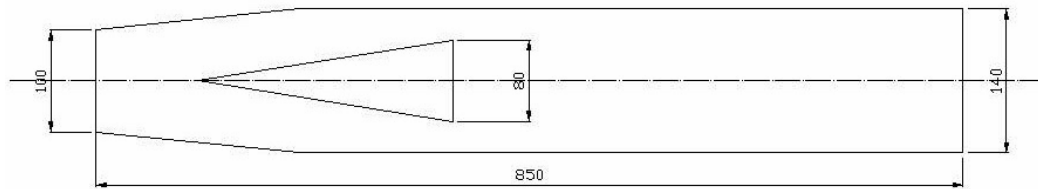


Figure 3-2. Sketch of Case 1

Table 3-1. Case 1 Inputs for FLUENT Boundary Conditions

	Inlet	O ₂	CH ₄
$\dot{m}_{air} \text{ (kg/s)}$	6.383	1.48	
$\dot{m}_{O_2} \text{ (kg/s)}$	0.262	0.262	
$\dot{m}_{vf} \text{ (kg/s)}$	0.047		0.047
$\dot{m}_{total} \text{ (kg/s)}$	6.692	1.742	0.047
Mass fraction		26%	0.7%

NOTE: Mass flow rate of O₂ (1.48 kg/s) is calculated by mass flow rate of air x 0.2319 (mass fraction of O₂ in air as given in Table 1-2).

Contours of static temperature obtained from FLUENT are given in Figure 3-3.

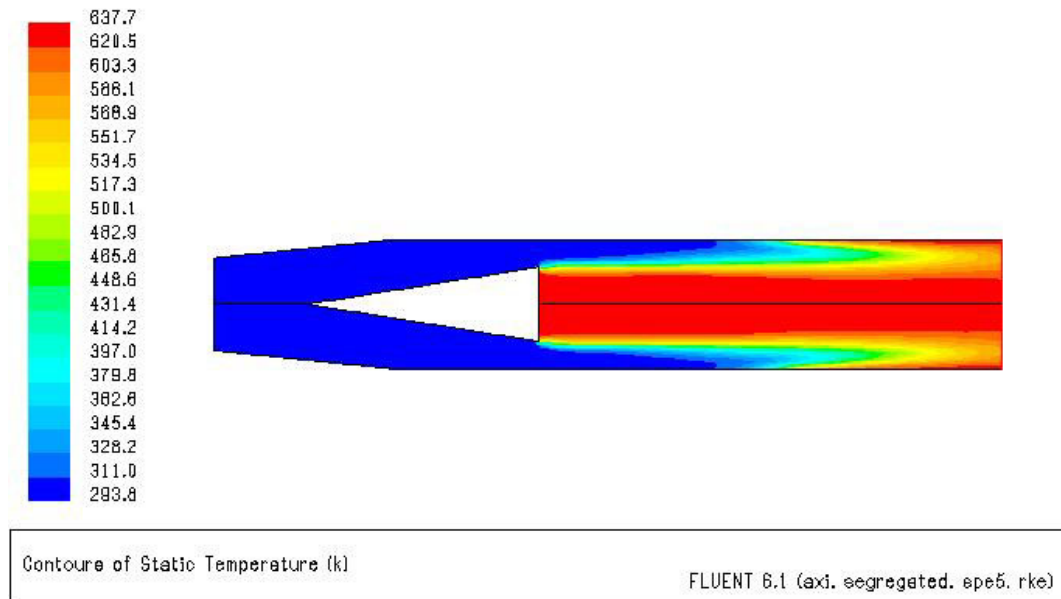


Figure 3-3. Contours of Static Temperature of Case 1.

Table 3-2. Flow Properties at the Outlet Plane (Case 1)

Static Pressure	650209.1 Pa
Static Temperature (Average)	613.07 K
Mole fraction of O ₂	21.040 %
Mole fraction of CH ₄	0.083 %
Mole fraction of H ₂ O	2.347 %
Mole fraction of CO ₂	1.173 %
Mole fraction of N ₂	75.356 %
Max. Temp.	633.45 K
Min. Temp.	582.71

Results

- Since the flow speed is higher than the flame speed, combustion starts after the bluff body where the circulation occurs.
- Almost uniform temperature profile is obtained at the outlet.
- Mole fraction of oxygen at the exit plane is very close to the ideal air conditions.

Comments

The results obtained from one single bluff body are acceptable. To obtain a better temperature profile at the outlet plane, another configuration of bluff body flame stabilization is studied in Case 2.

3.1.1.2.2. CASE 2

The vitiator fuel is mixed with the air and the replenished O₂ before the vitiator inlet. A sketch of the vitiator is given in Figure 3-4 (dimensions are in mm). Inputs for FLUENT Boundary Conditions are the same with Case 1 (Table 3-1). Contours of static temperature obtained from FLUENT are given in Figure 3-5.

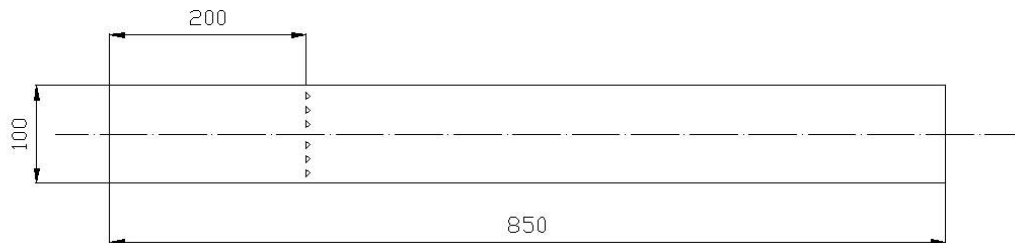


Figure 3-4. Sketch of Case 2

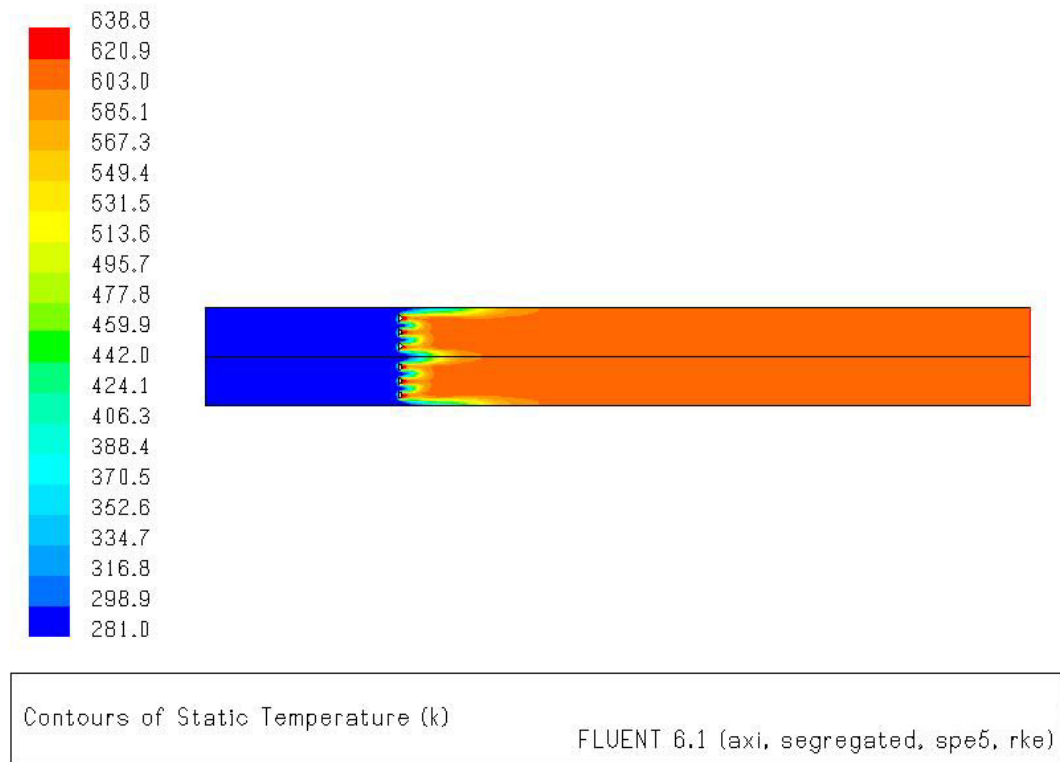


Figure 3-5. Contours of Static Temperature of Case 2.

Table 3-3. Flow Properties at the Outlet Plane (Case 2)

Absolute Pressure	650121.6 Pa
Static Temperature	609.44 K
Mole fraction of O ₂	20.880 %
Mole fraction of CH ₄	0.000 % (less than 10 ⁻⁹)
Mole fraction of H ₂ O	2.512 %
Mole fraction of CO ₂	1.256 %
Mole fraction of N ₂	75.350 %
Max. Temp.	614.68 K
Min. Temp.	606.86

Results

- Since the flow speed is higher than the flame speed, combustion starts after the bluff body where the circulation occurs.
- Uniform temperature profile is obtained at the outlet.
- Mole fraction of oxygen at the exit plane is very close to the ideal air conditions.
- No unburned fuel.

Comments

Results obtained from Case 2 are much better than those of Case 1.

In Case 1 and Case 2, air and fuel was premixed before entering the vitiator. In Case 3, fuel will be injected from a nozzle inside the vitiator.

3.1.1.2.3. CASE 3

In this case, the vitiator fuel is injected behind the bluff body. The air and the replenished O_2 are fed to the combustor from the vitiator inlet. A sketch of the vitiator is given in Figure 3-6 (dimensions are in mm). Inputs for FLUENT are given in Table 3-4.

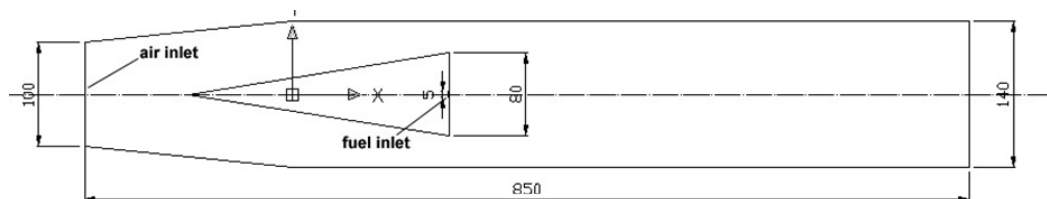


Figure 3-6. Sketch of Case 3

Table 3-4. Case 3 Inputs for FLUENT Boundary Conditions

	Inlet	O ₂	CH ₄
$\dot{m}_{air} \text{ (kg/s)}$	6.383	1.48	
$\dot{m}_{O_2} \text{ (kg/s)}$	0.262	0.262	
$\dot{m}_{vf} \text{ (kg/s)}$			0.047
$\dot{m}_{total} \text{ (kg/s)}$	6.65	1.742	0.047
Mass fraction		26.2 %	100 %

Contours of static temperature obtained from FLUENT are given in Figure 3-7.

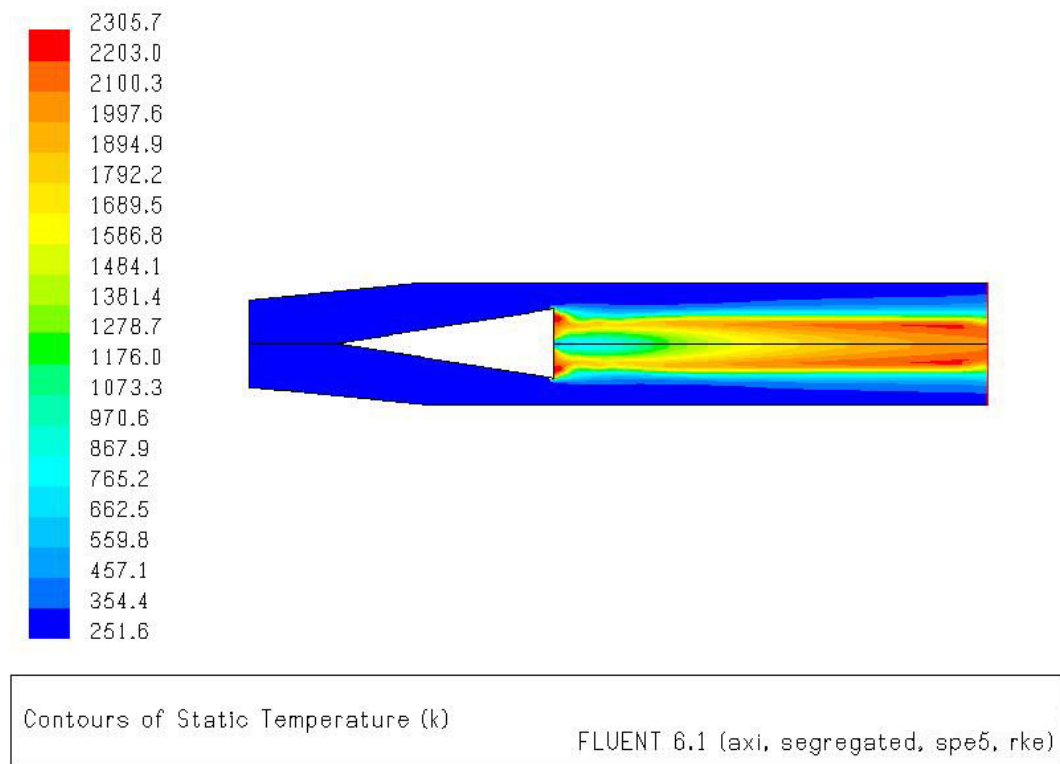


Figure 3-7. Contours of Static Temperature of Case 3.

Table 3-5. Flow Properties at the Outlet Plane (Case 3)

Absolute Pressure	650201.8 Pa
Static Temperature	741.05 K
Mole fraction of O ₂	19.100 %
Mole fraction of CH ₄	0.967 %
Mole fraction of H ₂ O	3.911 %
Mole fraction of CO ₂	1.958 %
Mole fraction of N ₂	74.064 %
Max. Temp.	2165.85
Min. Temp.	310.67

Results

- Combustion starts after the bluff body since the fuel is injected there.
- Temperature profile is not uniform at the outlet.
- Mole fraction of oxygen at the exit plane is lower than ideal air conditions.
- Unburned fuel percent is high.
- Maximum flame temperature is 2310 K, which is very high. For this case, material selection for combustion chamber case is critical. Also insulation is required to handle the high temperatures.

Comments

Injecting the fuel at the point of recirculation caused the combustion to start at that place. Near the nozzle, air to fuel ratio reached close to stoichiometric value so that the temperature reached to 2310 K. Also, the temperature at the exit plane is not uniform.

For flame stabilization by bluff body, Case 2 supplied us the best results.

3.1.1.3. FLAME STABILISATION BY RECIRCULATION

3.1.1.3.1. CASE 4

For this case, the vitiator fuel is fed to the combustor from the fuel inlets. Air and the replenished O_2 are supplied to the vitiator from the air inlet. A sketch of the vitiator is given in Figure 3-8 (dimensions are in mm).

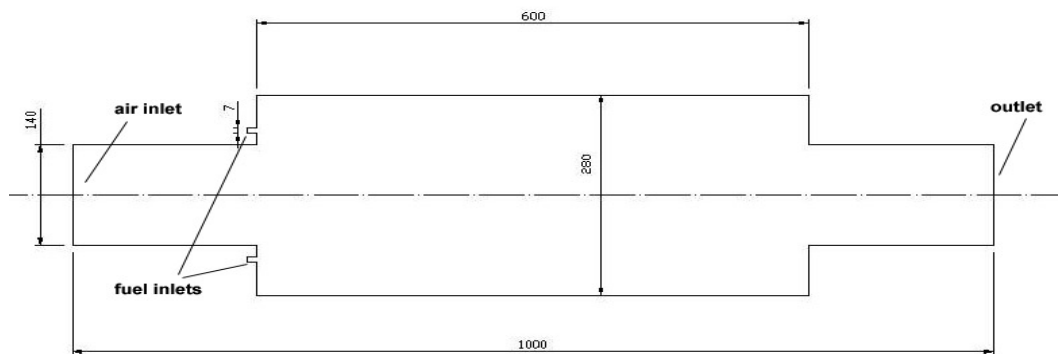


Figure 3-8. Sketch of Case 4

Inputs for FLUENT Boundary Conditions are the same with Case 3 (Table 3-4).

Contours of static temperature obtained from FLUENT are given in Figure 3-9.

Table 3-6. Flow Properties at the Outlet Plane (Case 4)

Absolute Pressure	650187.5 Pa
Static Temperature	692.78 K
Mole fraction of O_2	20.370 %
Mole fraction of CH_4	0.000 %
Mole fraction of H_2O	3.003 %
Mole fraction of CO_2	1.501 %
Mole fraction of N_2	75.125 %
Max. Temp.	943.46
Min. Temp.	325.30

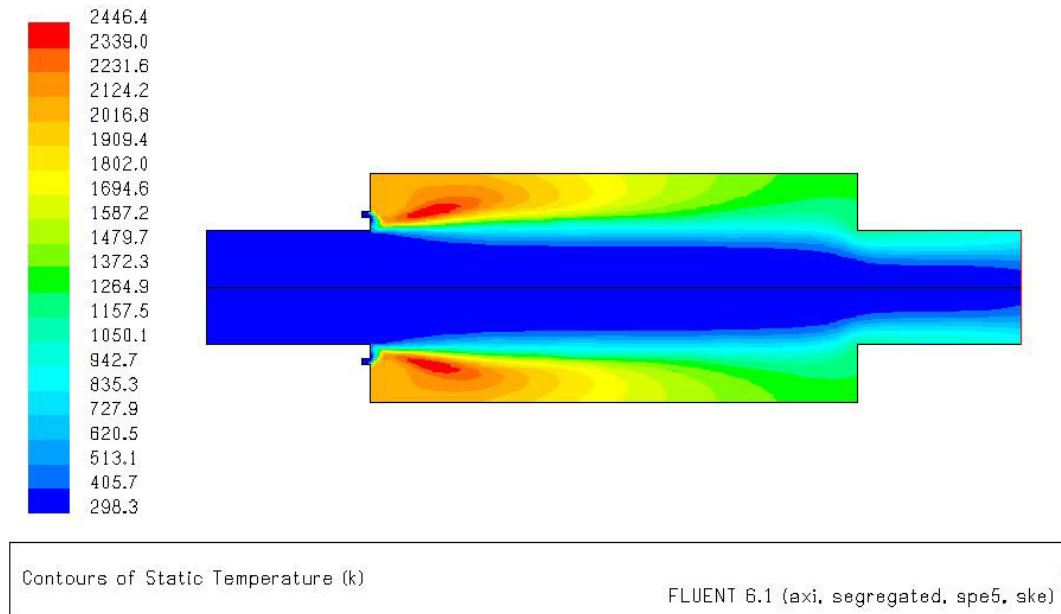


Figure 3-9. Contours of Static Temperature of Case 4.

Results

- Combustion starts after the fuel inlets.
- Temperature profile is not uniform at the outlet.
- Mole fraction of oxygen at the exit plane is close to ideal air conditions.
- Unburned fuel percent very small (less than $1e-6$)
- Maximum flame temperature is 2470 K, which is very high. For this case, material selection for combustion chamber case is critical. Also insulation is required to handle the high temperatures.

Comments

The situation encountered at Case 4 is similar to that of Case 3. Near the fuel injection nozzle, air to fuel ratio is close to stoichiometric value so that maximum temperatures has reached to 2470. This is not desired. On the other hand, combustion efficiency is high, there is no unburned fuel at the exit plane. In the next study, the same configuration with premixed flow will be considered.

3.1.1.3.2. CASE 5

The vitiator fuel is mixed with the air and the replenished O₂ before the vitiator inlet. A sketch of the vitiator is given in Figure 3-10 (dimensions are in mm).

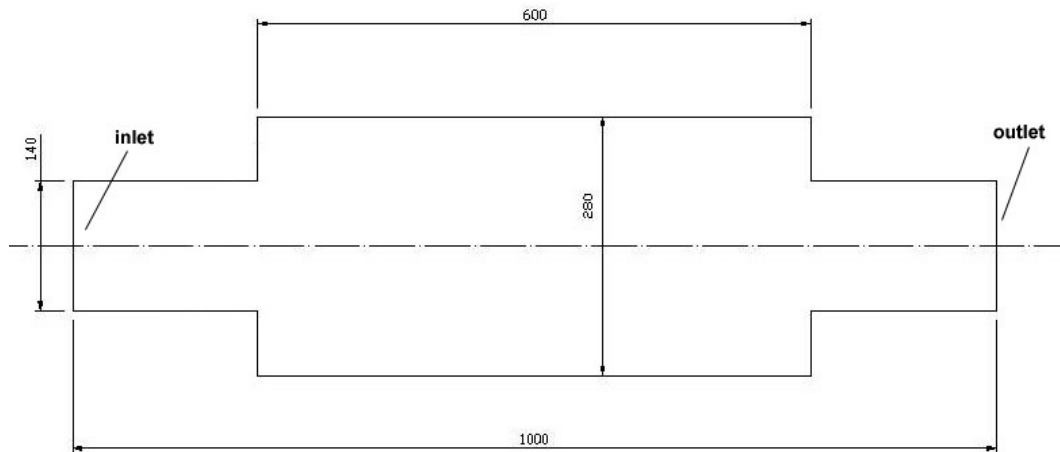


Figure 3-10. Sketch of Case 5

Inputs for FLUENT Boundary Conditions are the same with Case 1 (Table 3-1). Contours of static temperature obtained from FLUENT are given in Figure 3-11.

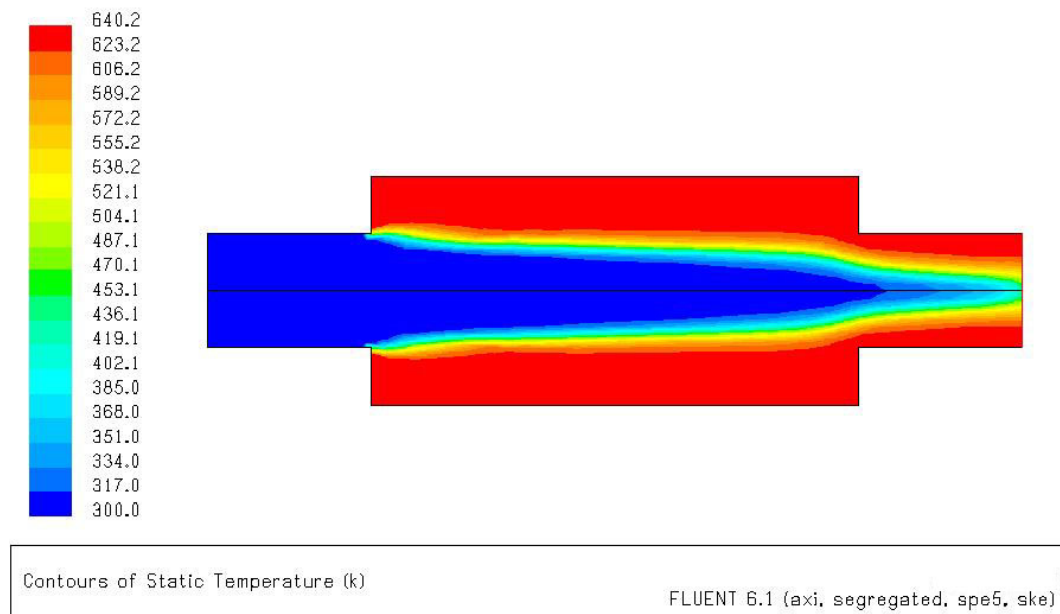


Figure 3-11. Contours of Static Temperature of Case 5.

Table 3-7. Flow Properties at the Outlet Plane (Case 5)

Absolute Pressure	650199.7 Pa
Static Temperature	610.07 K
Mole fraction of O ₂	21.080 %
Mole fraction of CH ₄	0.090 %
Mole fraction of H ₂ O	2.316 %
Mole fraction of CO ₂	1.158 %
Mole fraction of N ₂	75.356 %
Max. Temp.	640.02
Min. Temp.	454.7

Results

- Combustion starts after the area expansion where the recirculation occurs.
- Temperature profile is not uniform at the outlet.
- Mole fraction of oxygen at the exit plane is slightly higher than ideal air conditions.
- There are some unburned fuel at the exit.

Comments

The air/fuel mixture entering the combustion chamber from the center of the inlet leaves the combustion chamber without entering a combustion process. As a result, oxygen and fuel mole fractions are higher than desirable.

At this point, a new combustion chamber design based on flame stabilization with sudden expansion is studied.

3.1.1.3.3. CASE 6

The vitiator fuel is mixed with the air and the replenished O₂ before the vitiator inlet. A sketch of the vitiator is given in Figure 3-12 (dimensions are in mm).

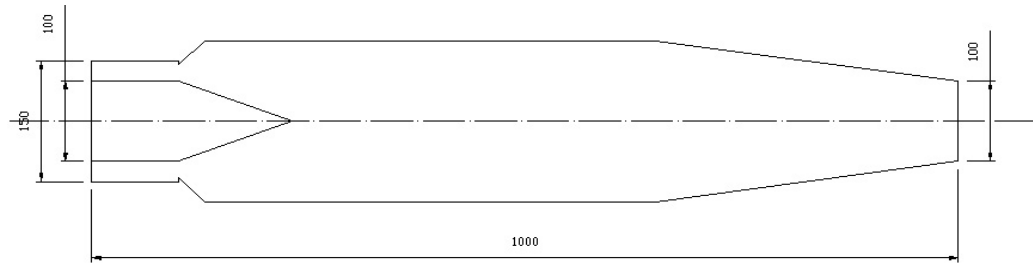


Figure 3-12. Sketch of Case 6

Inputs for FLUENT Boundary Conditions are the same with Case 1 (Table 3-1). Contours of static temperature obtained from FLUENT are given in Figure 3-13.

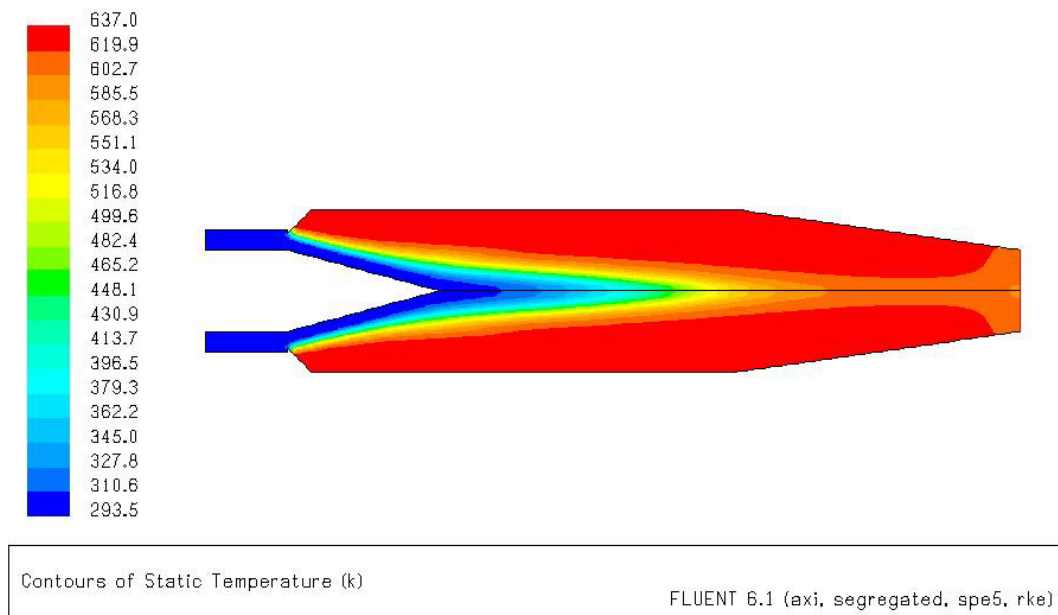


Figure 3-13. Contours of Static Temperature of Case 6.

Table 3-8. Flow Properties at the Outlet Plane (Case 6)

Absolute Pressure	650500.9 Pa
Static Temperature	634.19 K
Mole fraction of O ₂	21.070 %
Mole fraction of CH ₄	0.001 %
Mole fraction of H ₂ O	2.511 %
Mole fraction of CO ₂	1.255 %
Mole fraction of N ₂	75.161 %
Max. Temp.	611.78
Min. Temp.	600.90

Results

- Combustion starts after the sudden expending section.
- Temperature profile is uniform at the outlet.
- Mole fraction of oxygen at the exit plane is slightly higher than ideal air conditions.
- Unburned fuel percent is low.

Comments

The results obtained are close to the desired values.

To alter the results of case 6, a similar combustor design is developed for Case 7. The cone at the middle is reversed to obtain another circulation zone.

3.1.1.3.4. CASE 7

The vitiator fuel is mixed with the air and the replenished O₂ before the vitiator inlet. A sketch of the vitiator is given in Figure 3-14 (dimensions are in mm).

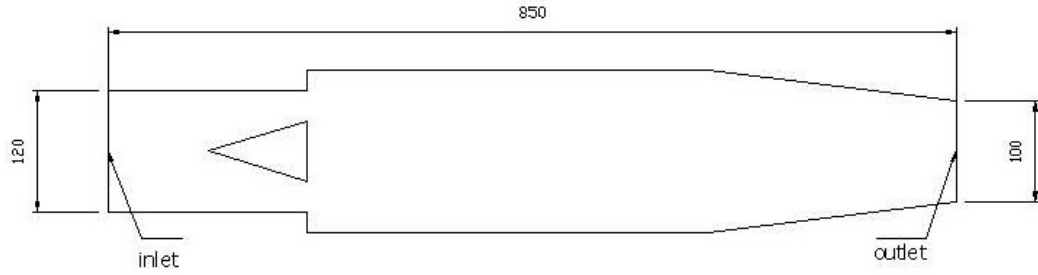


Figure 3-14. Sketch of Case 7

Inputs for FLUENT Boundary Conditions are the same with Case 1 (Table 3-1). Contours of static temperature obtained from FLUENT are given in Figure 3-15.

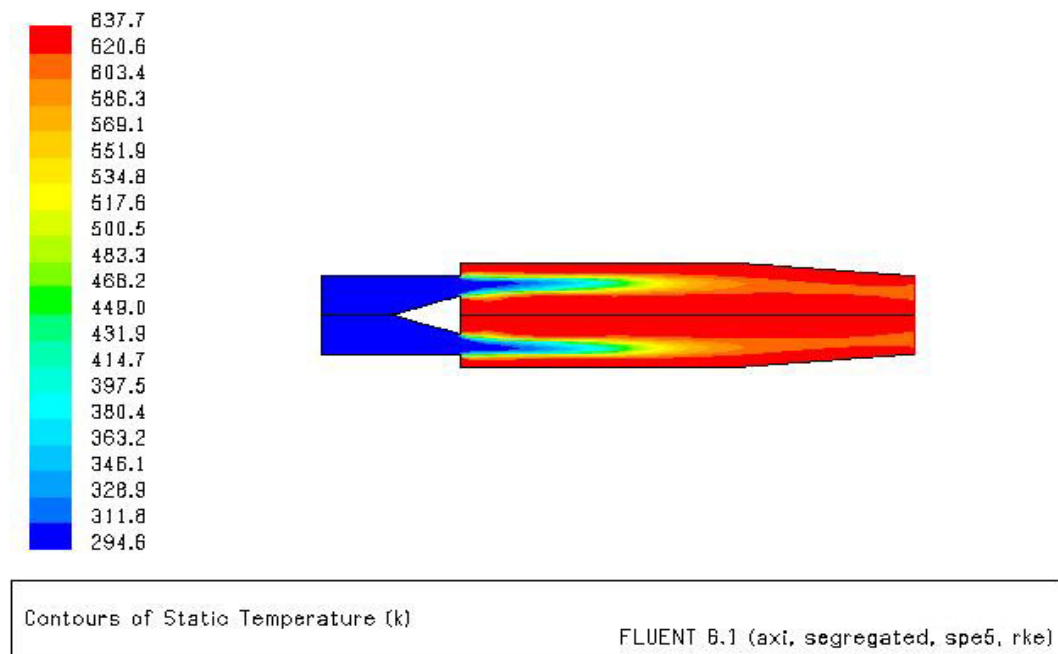


Figure 3-15. Contours of Static Temperature of Case 7.

Results

- Combustion starts after the sudden expanding section.
- Temperature profile is uniform at the outlet.
- Mole fraction of oxygen at the exit plane is close to that of ideal air.
- Unburned fuel percent is very low.

Table 3-9. Flow Properties at the Outlet Plane (Case 7)

Absolute Pressure	650258.6 Pa
Static Temperature	621.22 K
Mole fraction of O ₂	20.890 %
Mole fraction of CH ₄	0.004 %
Mole fraction of H ₂ O	2.505 %
Mole fraction of CO ₂	1.253 %
Mole fraction of N ₂	75.348 %
Max. Temp.	627.30 K
Min. Temp.	616.56 K

Comments

The results obtained are close to the desired values. This configuration (Case 7) is the best design for flame holding by sudden expansion.

3.1.1.4. FLAME STABILISATION BY PILOT FLAMES

3.1.1.4.1. CASE 8

The vitiator fuel is mixed with the air and the replenished O₂ before the vitiator inlet. A sketch of the vitiator is given in Figure 3-16.

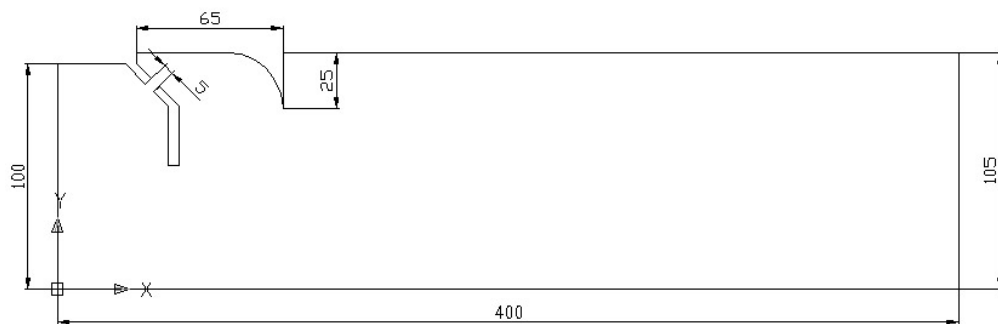


Figure 3-16. Sketch of Case 8

Inputs for FLUENT Boundary Conditions are the same with Case 1 (Table 3-1).

Contours of static temperature and velocity magnitude obtained from FLUENT are given in Figure 3-17 and Figure 3-18 respectively.

Results

- Temperature profile is not uniform at the outlet.
- Mole fraction of oxygen at the exit plane is close to ideal air conditions.
- Unburned fuel percent is high.

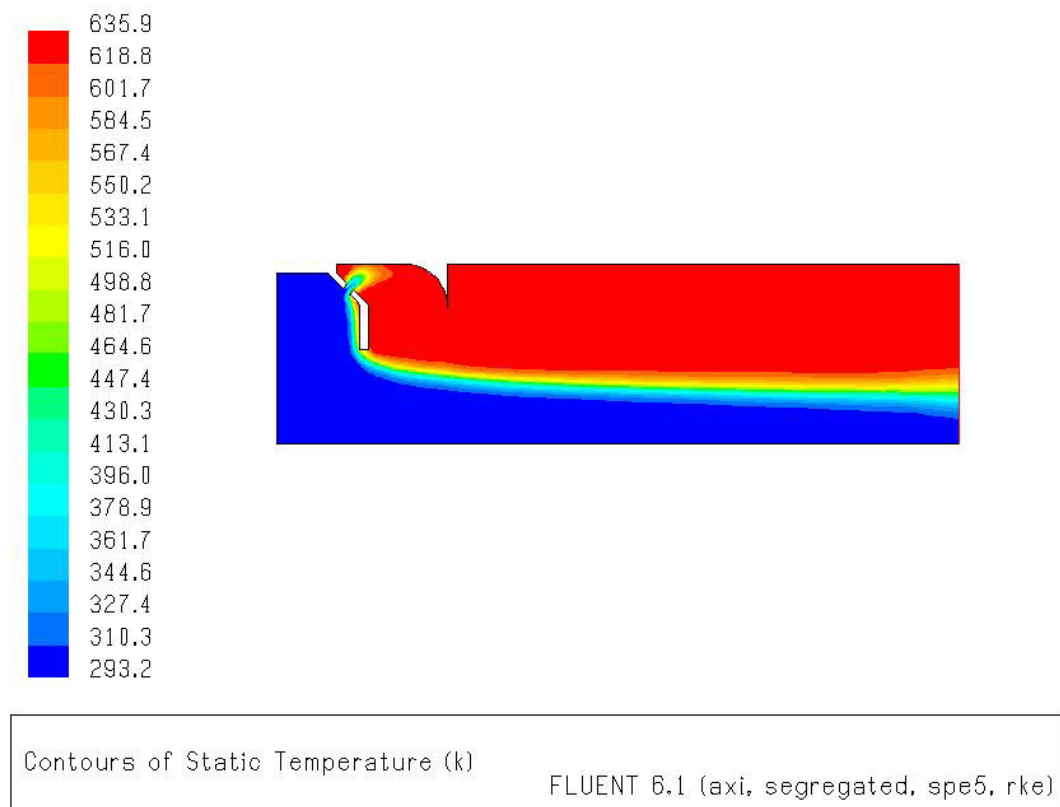


Figure 3-17. Contours of Static Temperature of Case 8.

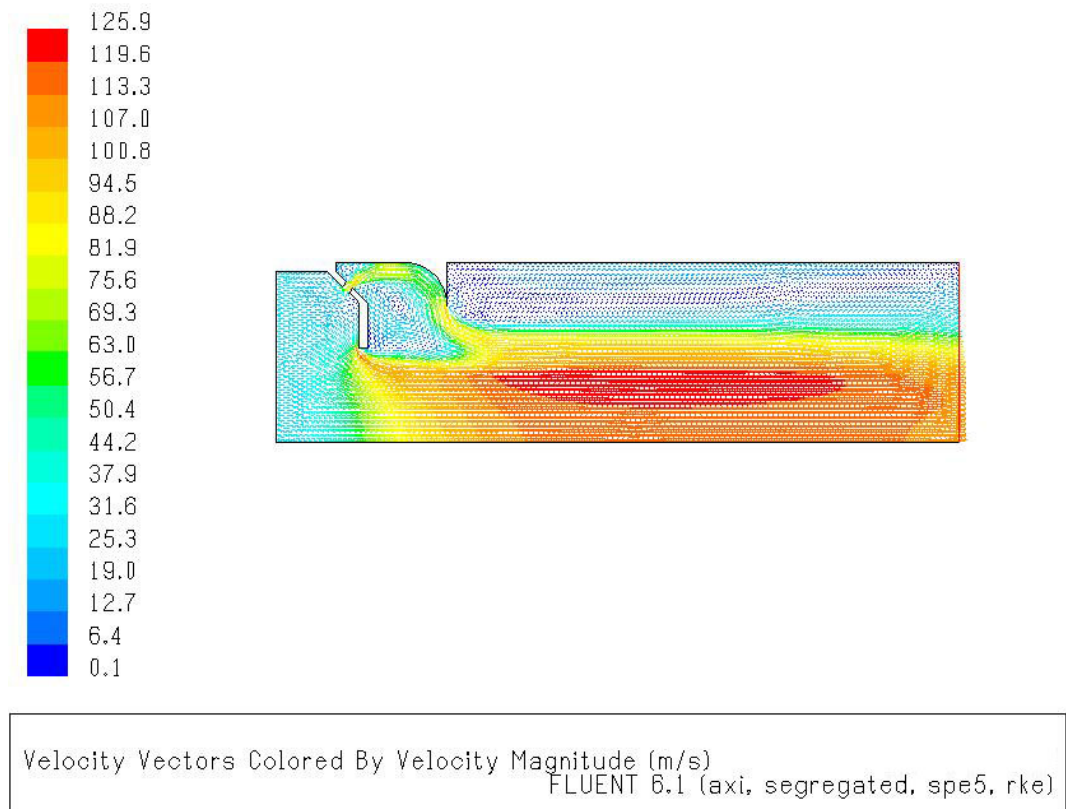


Figure 3-18. Contours of Velocity Magnitude of Case 8.

Table 3-10. Flow Properties at the Outlet Plane (Case 8)

Absolute Pressure	650200.9 Pa
Static Temperature	602.22 K
Mole fraction of O ₂	20.140 %
Mole fraction of CH ₄	0.110 %
Mole fraction of H ₂ O	3.388 %
Mole fraction of CO ₂	1.691 %
Mole fraction of N ₂	74.671 %
Max. Temp.	633.91
Min. Temp.	296.24

Comments

Unburned fuel percent is higher than desired value. Also, the air/fuel mixture entering the combustion chamber from the center of the inlet leaves the combustion chamber without entering a combustion process.

3.1.1.4.2. CASE 9

The vitiator fuel is mixed with the air and the replenished O₂ before the vitiator inlet. A sketch of the vitiator is given in Figure 3-19.

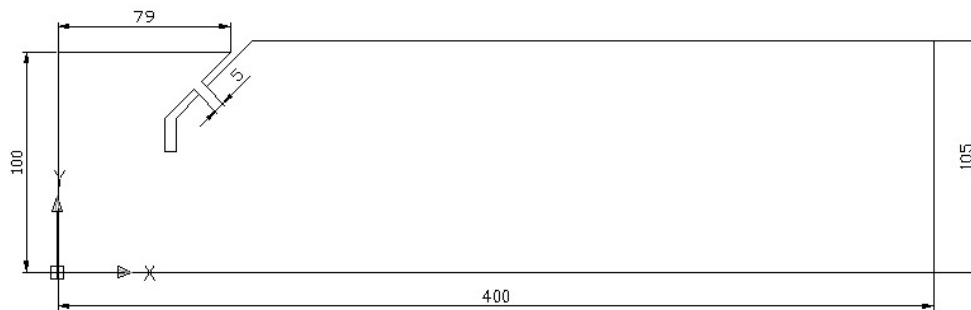


Figure 3-19. Sketch of Case 9

Inputs for FLUENT Boundary Conditions are the same with Case 1 (Table 3-1).

Contours of static temperature and velocity magnitude obtained from FLUENT are given in Figure 3-20 and Figure 3-21 respectively.

Results

- Temperature profile is not uniform at the outlet.
- Mole fraction of oxygen at the exit plane is lower than the ideal air.
- Unburned fuel percent is high.

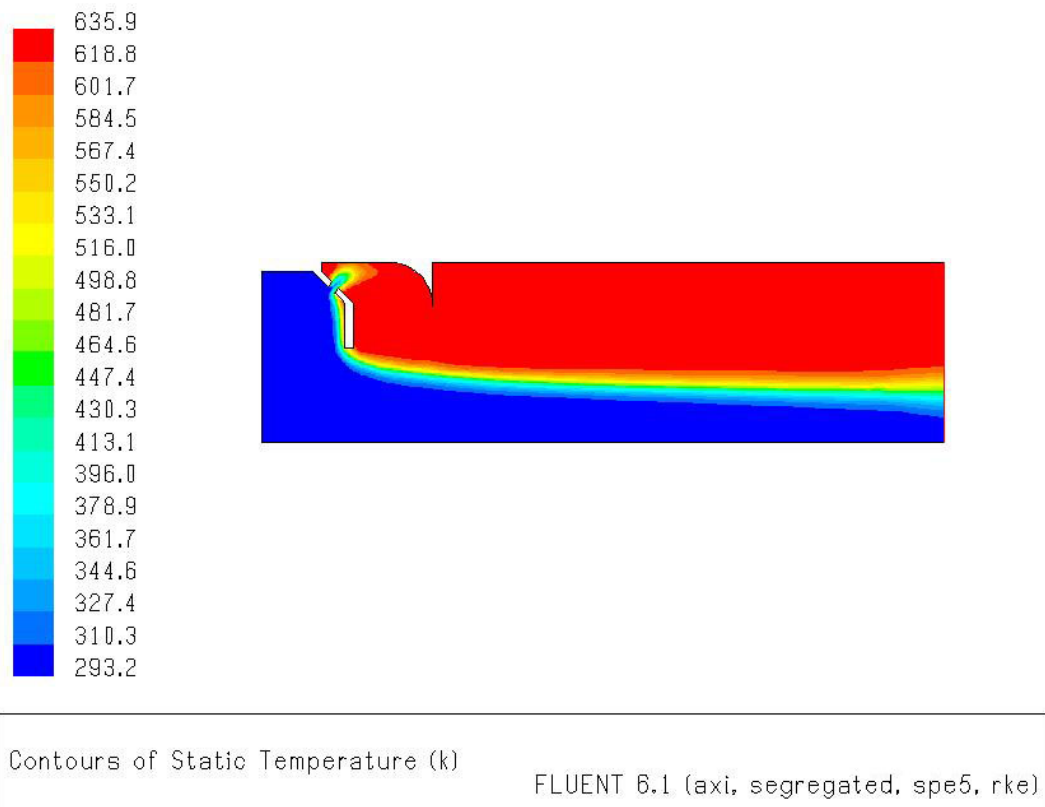


Figure 3-20. Contours of Static Temperature of Case 9.

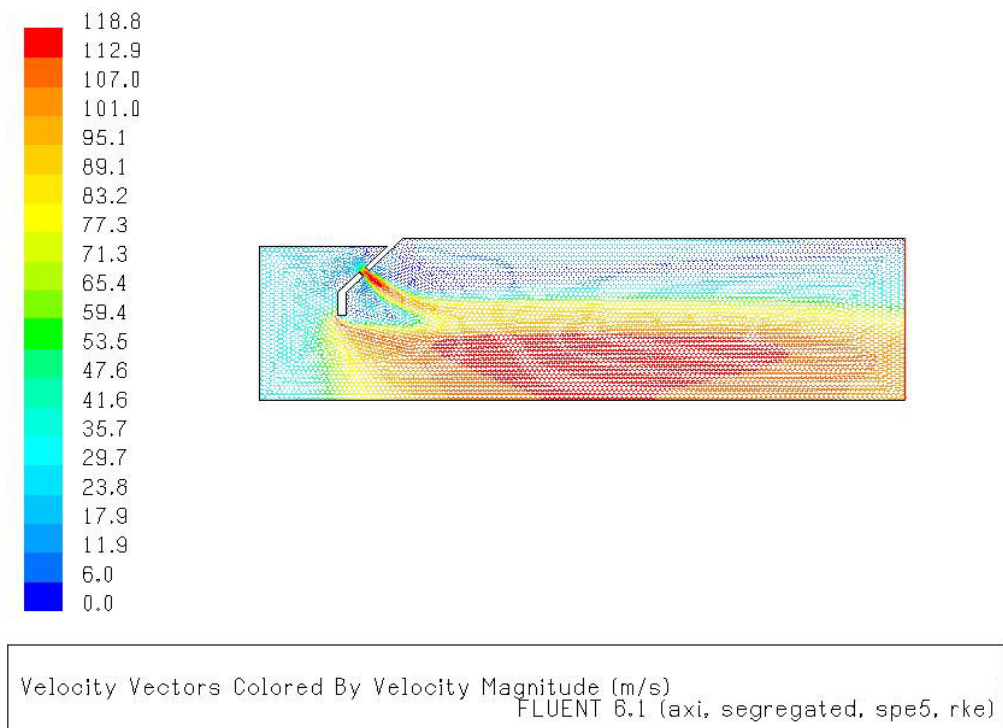


Figure 3-21. Contours of Velocity Magnitude of Case 9.

Table 3-11. Flow Properties at the Outlet Plane (Case 9)

Absolute Pressure	650199.7 Pa
Static Temperature	596.93 K
Mole fraction of O ₂	19.953 %
Mole fraction of CH ₄	0.133 %
Mole fraction of H ₂ O	3.540 %
Mole fraction of CO ₂	1.767 %
Mole fraction of N ₂	74.607 %
Max. Temp.	634.56
Min. Temp.	296.35

Comments

Oxygen mole fraction at the exit plane is lower than the desired values. Also, the air/fuel mixture entering the combustion chamber from the center of the inlet leaves the combustion chamber without entering a combustion process.

3.1.2. EVALUATION OF STUDIED CASES

Nine different designs have been presented in the previous section. Case 1 to Case 3 were based on flame stabilization by bluff bodies, Case 4 to case 7 were based on flame stabilization by recirculation, and Case 8 and Case 9 were based on flame stabilization by pilot flames.

The results of these designs are compared with the experimental results and tabulated in Table 3-12.

Table 3-12. Outlet Plane Data Comparison

	Experiment	Case 1	Case2	Case3
Static Pressure	650200.0 Pa	650209.1 Pa	650121.6 Pa	650201.8 Pa
Static Temp. (T_{out})	606 K	613.07 K	609.44 K	741.05 K
Mole fraction of O ₂	20.946 %	21.040 %	20.880 %	19.100 %
Mole fraction of CH ₄	0.0 %	0.083 %	0.000 %	0.967 %
Mole fraction of H ₂ O	2.532 %	2.347 %	2.512 %	3.911 %
Mole fraction of CO ₂	1.295 %	1.173 %	1.256 %	1.958 %
Mole fraction of N ₂	74.339 %	75.356 %	75.350 %	74.064 %
Max. Temp.	-	633.45 K	614.68 K	2165.85
Min. Temp.	-	582.71	606.86	310.67
Uniformity		95.04 %	99.14 %	0 %

	Experiment	Case 4	Case 5	Case 6
Static Pressure	650200.0 Pa	650187.5 Pa	650199.7 Pa	650500.9 Pa
Static Temp. (T_{out})	606 K	692.78 K	610.07 K	634.19 K
Mole fraction of O ₂	20.946 %	20.370 %	21.080 %	21.070 %
Mole fraction of CH ₄	0.0 %	0.000 %	0.090 %	0.001 %
Mole fraction of H ₂ O	2.532 %	3.003 %	2.316 %	2.511 %
Mole fraction of CO ₂	1.295 %	1.501 %	1.158 %	1.255 %
Mole fraction of N ₂	74.339 %	75.125 %	75.356 %	75.161 %
Max. Temp.	-	943.46	640.02	611.78
Min. Temp.	-	325.30	454.7	600.90
Uniformity		46.95 %	74.53 %	94.75 %

	Experiment	Case 7	Case 8	Case 9
Static Pressure	650200.0 Pa	650258.6 Pa	650200.9 Pa	650199.7 Pa
Static Temp. (T_{out})	606 K	621.22 K	602.22 K	596.93 K
Mole fraction of O ₂	20.946 %	20.890 %	20.140 %	19.953 %
Mole fraction of CH ₄	0.0 %	0.004 %	0.110 %	0.133 %
Mole fraction of H ₂ O	2.532 %	2.505 %	3.388 %	3.540 %
Mole fraction of CO ₂	1.295 %	1.253 %	1.691 %	1.767 %
Mole fraction of N ₂	74.339 %	75.348 %	74.671 %	74.607 %
Max. Temp.	-	627.30	633.91	634.56
Min. Temp.	-	616.56	296.24	296.35
Uniformity		95.83 %	49.19 %	49.64 %

Uniformity is defined as $\frac{\text{Max deviation in Temp} + T_{out}}{T_{out}} \times 100$

When compared to the experimental data, the best results are obtained at Case 2. This case is modified for the flow requirements of this study and analyzed for different flight conditions in the next section.

3.2. DETAILED ANALYSIS OF CASE 2

3.2.1. 2 D Analysis

Air mass flow rate requirement of the ramjet missile [2] is given in Figure 3-22.

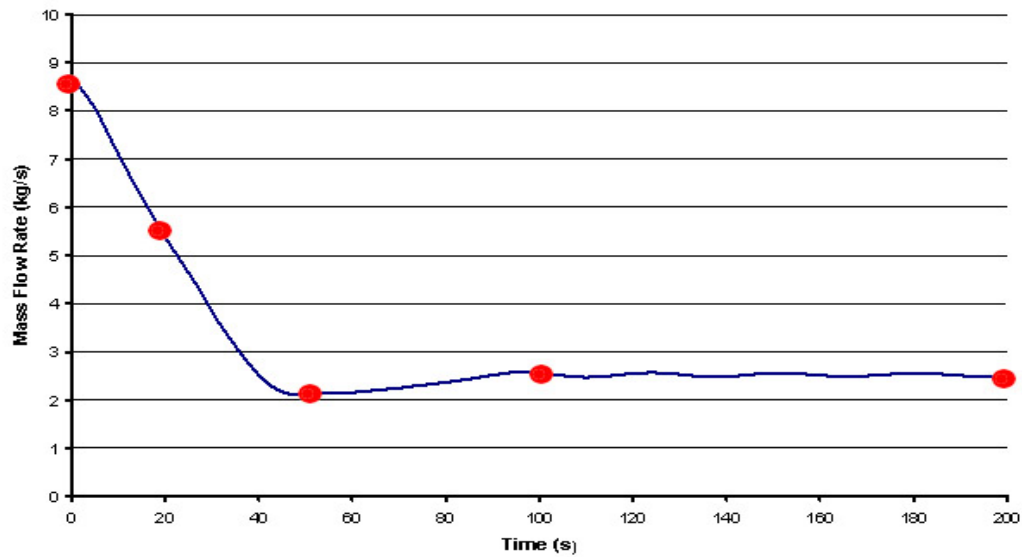


Figure 3-22. Mass Flow Rate Requirement of the Test Facility

Five different points from the missile flight trajectory is selected for heater performance analysis. These points are marked on Figure 3-22. Inlets off design analysis for the selected points are given in Table 3-13 [2].

Table 3-13. Inlet-Off Design Performance Data

time	Alt (m)	M_0	M_e	T_e (K)	P_e (Pa)	\dot{m}_{air} (kg/s)
0	5000	2.49	0.35	560.2	783400	8.66
20	9250.0	2.6	0.34	540.6	542860	5.38
50	15850.0	2.8	0.32	567.8	258810	2.13
100	16000.0	3.5	0.30	748.6	512080	2.56
200	16000.0	3.4	0.30	722.8	481560	2.50

The heater should be able to operate on the conditions stated in Table 3-13. Design of the vitiator should be based on the cruise condition to get the most efficient performance during the entire testing. Conditions at time =100 s is selected for vitiator design.

$$\begin{aligned}
 P &= 512080 \text{ Pa} & T &= 748.6 \text{ K} & \dot{m}_{air} &= 2.56 \text{ kg/s} \\
 \rho_{air} &= \frac{P}{ZRT} = 6 \frac{\text{kg}}{\text{m}^3} & M &= 0.3 & c &= \sqrt{\gamma RT} = 346 \text{ m/s} \\
 V &= M \ c = 100 \text{ m/s} & A &= \frac{\dot{m}}{\rho_{air} V} = 4616 \text{ mm}^2 & D &= 76 \text{ mm}
 \end{aligned}$$

To obtain a flow at Mach number 0.3, the area of heater inlet should be around 76mm. For analysis, diameter is taken as 80 mm to provide a better dimensioning. Grid used in Case 2 is scaled by 0.8 to get the inlet diameter 80 mm.

Using the NASA CET93 FORTRAN code [20], the amount of fuel to heat the incoming air up to the required inlet exit temperature is calculated. With an additional subroutine, iterations on the air to fuel (CH₄ methane) ratio are performed, the appropriate mix ratio for each time step is obtained. Details for mass flow rate of air and fuel, mass fractions of CH₄ and O₂ are given in Table 3-14.

Table 3-14. Mass Fractions Corresponding to Mass Flow Rates

<i>time</i> (s)	\dot{m}_{air} (kg/s)	\dot{m}_{fuel} (kg/s)	$\dot{m}_{rep.O_2}$ (kg/s)	X_{fuel}	X_{O_2}
0	8.66	0.049	0.273	0.55 %	25.41 %
20	5.38	0.027	0.155	0.50 %	25.24 %
50	2.13	0.012	0.069	0.56 %	25.48 %
100	2.56	0.026	0.147	0.96 %	27.10 %
200	2.50	0.024	0.134	0.91 %	26.87 %

Analyses using the data in Table 3-14 are performed and the results obtained are tabulated in

Table 3-15.

Table 3-15. Results of the Air Heater Off-Design Analysis

$time (s)$	$Te (K)$	$Te (required)$	Y_{O_2}
0	511.07	560.2	20.90 %
20	495.89	540.6	20.93 %
50	543.04	567.8	20.91 %
100	728.25	748.6	20.92 %
192	708.46	722.8	20.90 %

Results of the initial analysis are not satisfying because the pressure differences between the required and obtained values are quite high for high mass flow rates. The reason for this is that, the heater is designed for mass flow rate value of 2.77 kg/s whereas at time=0, air mass flow rate is 8.66 kg/s. So an iterative analysis is performed to get the required temperatures. Several runs are performed with different mass fractions of CH₄ and O₂. Final mass fractions obtained after these iterations are given in Table 3-16 and the results are tabulated in Table 3-17.

Table 3-16. Final Mass Flow Rate and Mass Fraction Data

$time (s)$	\dot{m}_{air}	\dot{m}_{fuel}	$\dot{m}_{rep.O_2}$	\dot{m}_{total}	X_{fuel}	X_{O_2}
0	8.384	0.056	0.228	8.66	0.65 %	25.83 %
20	5.217	0.032	0.131	5.38	0.60 %	25.63 %
50	2.069	0.013	0.055	2.13	0.63 %	25.78 %
100	2.432	0.026	0.105	2.56	1.01 %	27.29 %
192	2.383	0.023	0.094	2.50	0.93 %	26.97 %

Table 3-17. Results of the Air Heater Off-Design Analysis

<i>time (s)</i>	<i>Te (K)</i>	<i>Te (required)</i>	<i>Y_{O₂}</i>
0	557.01	560.2	20.94 %
20	543.04	540.6	20.91 %
50	567.87	567.8	20.94 %
100	747.64	748.6	20.95 %
192	721.03	722.8	20.90 %

Results obtained after iterations are quite satisfying. This configuration is good enough for this study. Final configuration of the air heater is given in Figure 3-23 (dimensions are in mm).

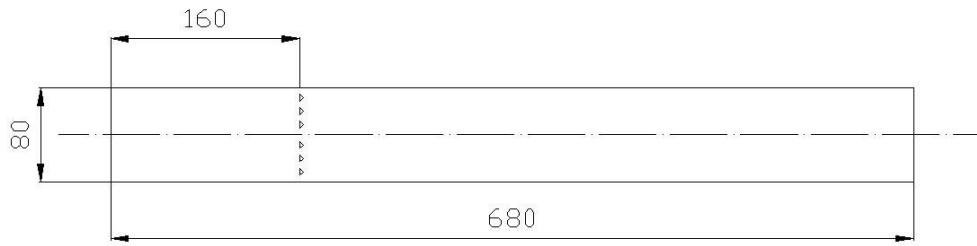


Figure 3-23. Final Configuration of the Air Heater

3.2.2. 3D Analysis

3.2.2.1. Case 1

The flame holding mechanism used in 2D analysis is transformed into 3D. The best solution is to use cylindrical bars and torus, which will exactly match the axisymmetric solution of 2D analysis. A sketch of the flame holder is given in Figure 3-24. Premixed air and fuel entering the combustor is studied in the first case. Combustor configurations are shown in Figure 3-25 and Figure 3-26.

Symmetry boundary condition is specified on the side walls so, $\frac{1}{4}$ of the total combustion chamber is studied. Analyses are performed for the properties at

time=100 seconds (cruise condition of the ramjet missile). Mass flow rates given in Table 3-16 are used. Inputs to the code are given in Table 3-18.

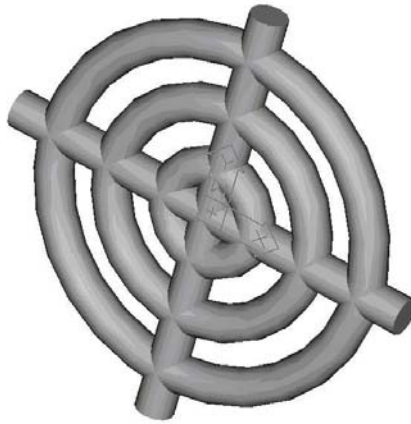


Figure 3-24. Flame Holding Mechanism

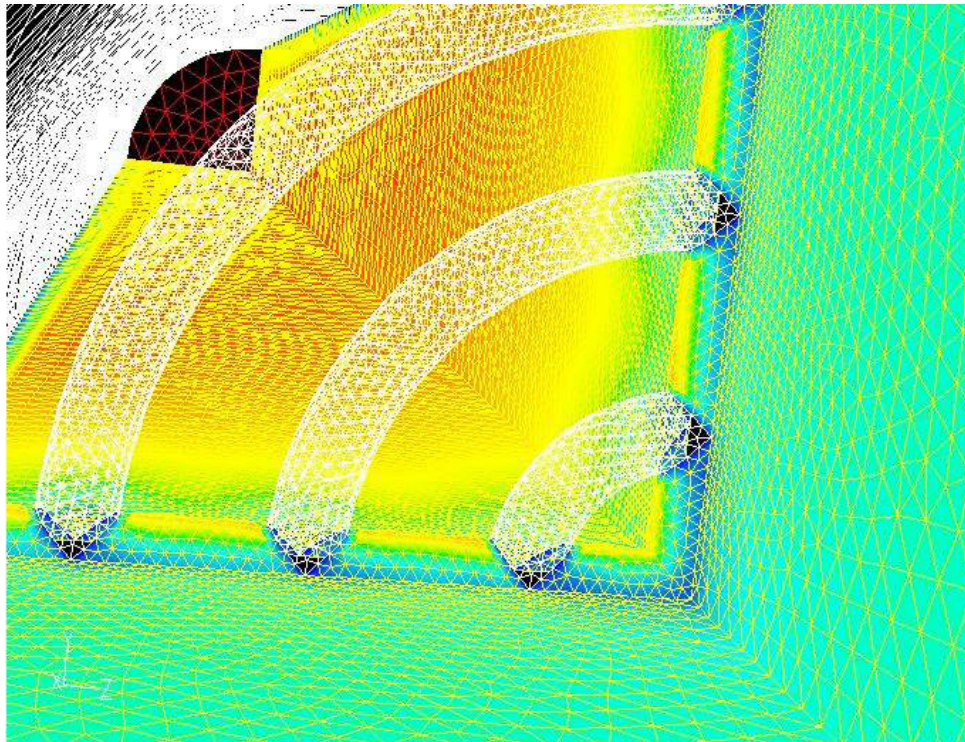


Figure 3-25. Quarter of the Air Heater Combustion Chamber

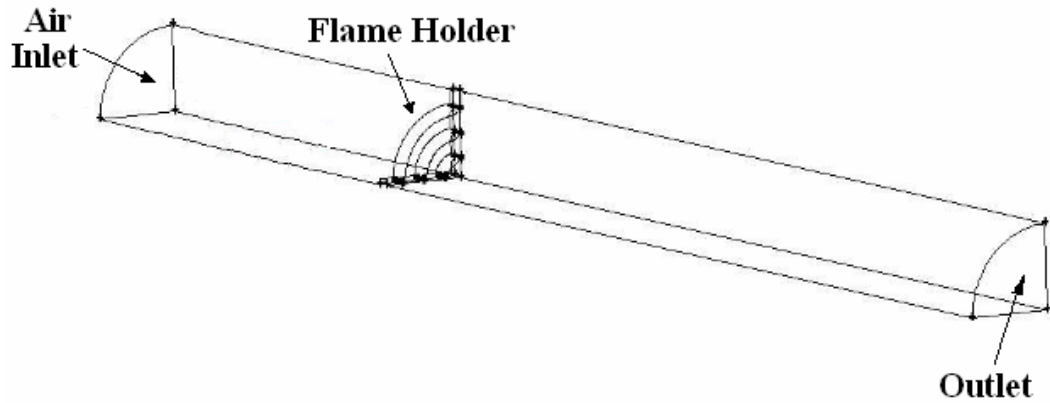


Figure 3-26. Sketch of Combustion Chamber of Case 1

Contours of static temperature obtained from FLUENT are given in Figure 3-27 and Figure 3-28.

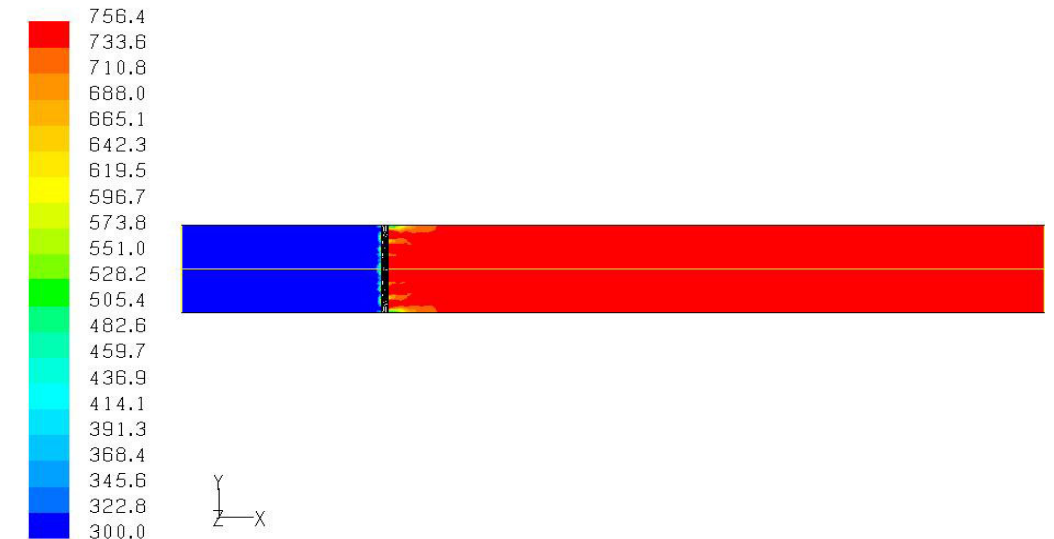
Table 3-18. Case 1 Inputs for FLUENT Boundary Conditions

	Inlet	O ₂	CH ₄
$\dot{m}_{air} \text{ (kg/s)}$	2.56	0.59	
$\dot{m}_{O_2} \text{ (kg/s)}$	0.147	0.147	
$\dot{m}_{vf} \text{ (kg/s)}$	0.026		0.026
$\dot{m}_{total} \text{ (kg/s)}$	2.733	0.738	0.026
<i>Mass fraction</i>		27%	0.951%

Results

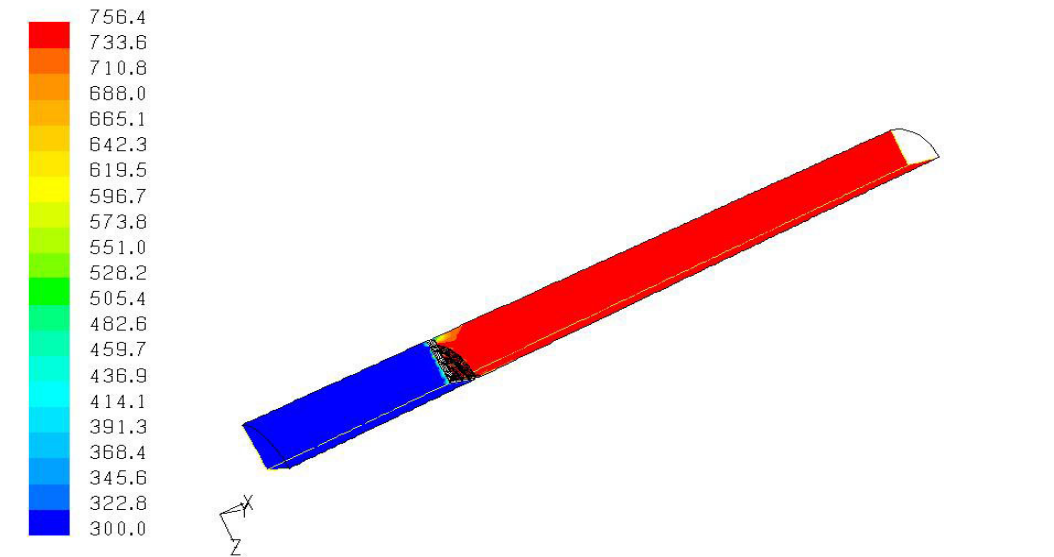
- Since the flow speed is higher than the flame speed, combustion starts after the bluff body where the circulation occurs.
- Almost uniform temperature profile is obtained at the outlet. Temperature calculated by fluent (747.36 K) at the outlet plane is close to the expected value (748.6 K).

- Mole fraction of oxygen at the exit plane is very close to the ideal air conditions.
- There is no unburned fuel.



Contours of Static Temperature (k) FLUENT 6.1 (3d, segregated, spe5, rke)

Figure 3-27. Contours of Static Temperature of Case 1



Contours of Static Temperature (k) FLUENT 6.1 (3d, segregated, spe5, rke)

Figure 3-28. Contours of Static Temperature of Case 1 (Isometric View)

Table 3-19. Flow Properties at the Outlet Plane

Absolute Pressure	510688.2 Pa
Static Temperature	747.36 K
Mole fraction of O ₂	20.970 %
Mole fraction of CH ₄	0.000 %
Mole fraction of H ₂ O	3.413 %
Mole fraction of CO ₂	1.706 %
Mole fraction of N ₂	73.910 %
Max. Temp.	747.58
Min. Temp.	747.16

Comments

The results obtained are satisfactory. In the following cases, fuel injection is considered instead of premixed flow.

3.2.2.2. Case 2

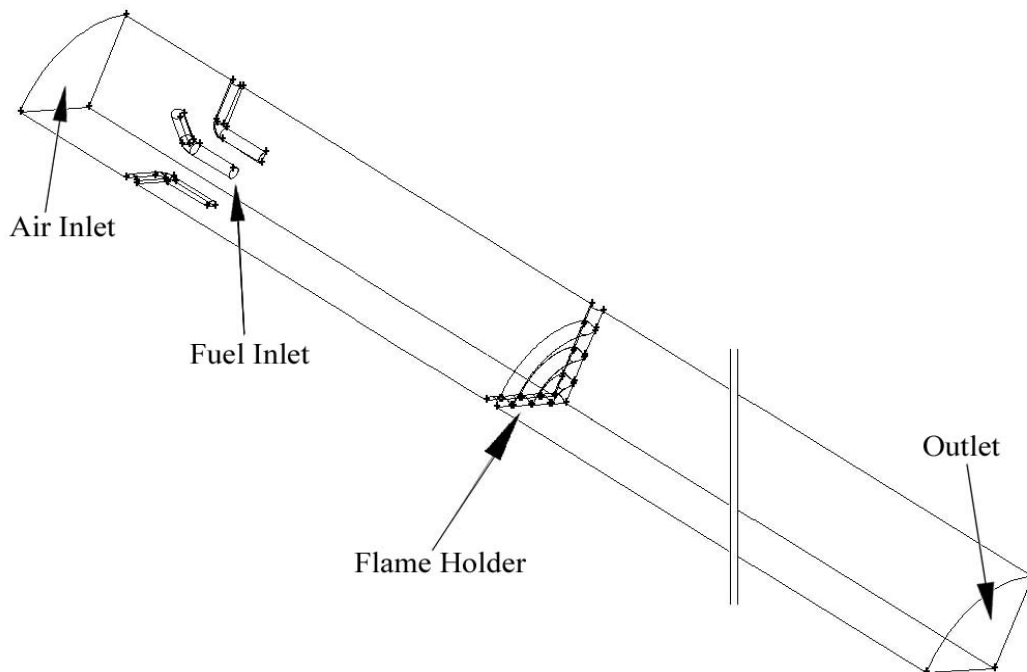


Figure 3-29. Sketch of Combustion Chamber of Case 2

Sketch of the combustor geometry studied in this case is given in Figure 3-29. Eight fuel pipes are placed before the flame holder. Quarter of the combustor is modeled to decrease computation time. Inputs for the FLUENT code are as given in Table 3-20.

Table 3-20. Case 2 Inputs for FLUENT Boundary Conditions

	Inlet	O ₂	CH ₄
$\dot{m}_{air} \text{ (kg/s)}$	2.56	0.59	
$\dot{m}_{O_2} \text{ (kg/s)}$	0.147	0.147	
$\dot{m}_{vf} \text{ (kg/s)}$			0.026
$\dot{m}_{total} \text{ (kg/s)}$	2.707	0.738	0.026
Mass fraction		27.26 %	100 %

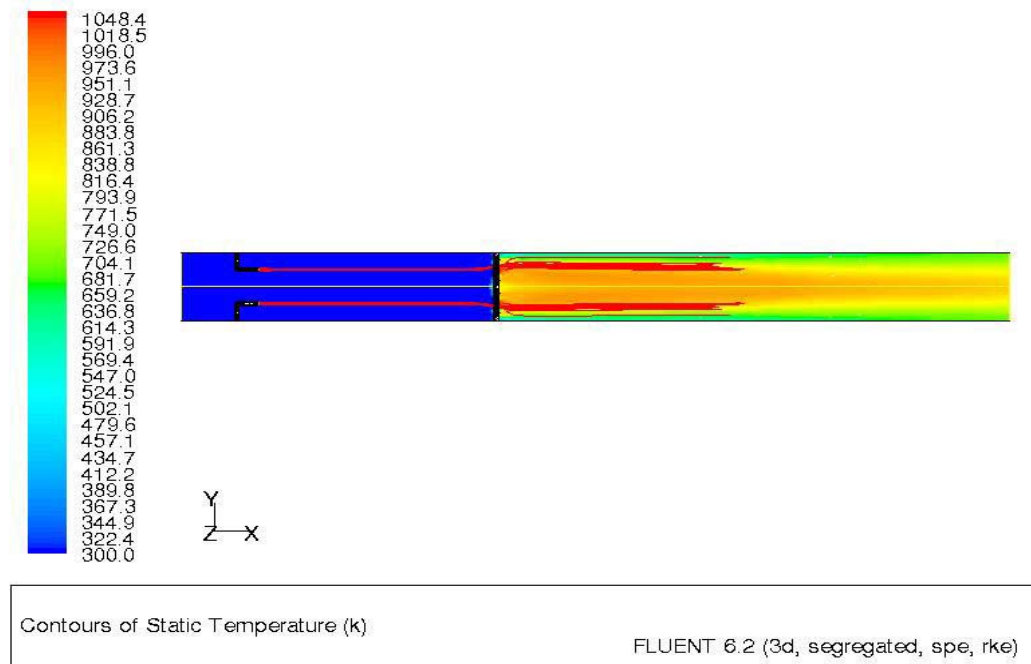


Figure 3-30. Contours of Static Temperature of Case 2

Fuel path lines are shown on the temperature contours on Figure 3-30. Fuel does not mix with the incoming air before the flame holder. At the points where fuel

paths intersect the flame holder, fuel to air ratio is close to 1 so at those locations, temperature reach up to 1050 K. Average temperature at the exit is 776 K whereas the required temperature is 747 K. Temperature at the exit is not uniform.

To improve the mixing, another fuel injector configuration is studied.

3.2.2.3. Case 3

In this case, four nozzle are placed at the end of the fuel lines studied in Case 2.

The temperature contours obtained is given in Figure 3-32.

A similar temperature profile is obtained as Case 2. Average temperature at the exit is 774 K whereas the required temperature is 747 K. Temperature at the exit is not uniform. Another fuel injector configuration is studied in case 4.

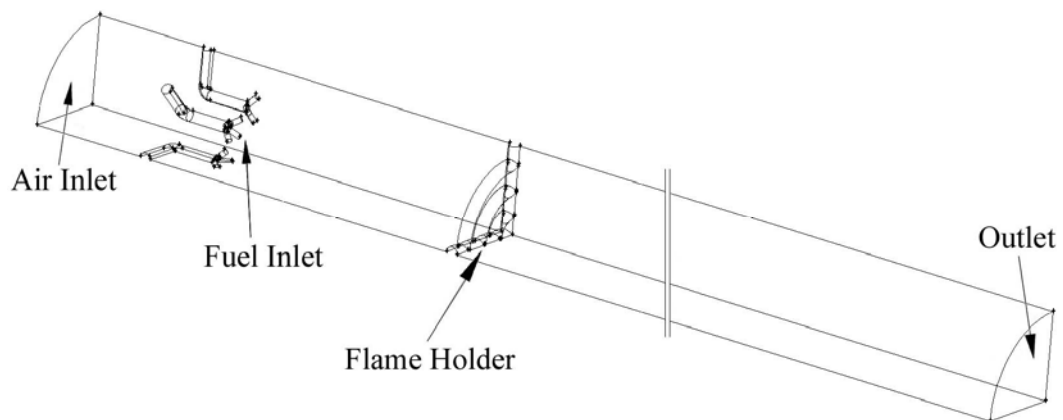


Figure 3-31. Sketch of Combustion Chamber of Case 3

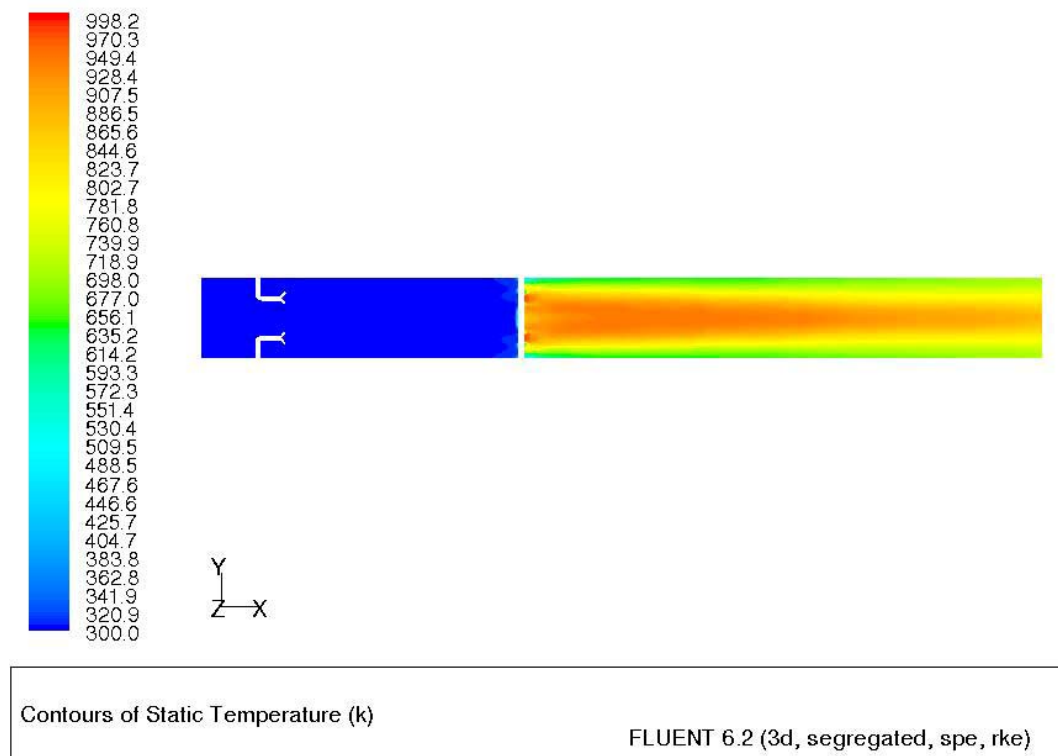


Figure 3-32. Contours of Static Temperature of Case 3

3.2.2.4. Case 4

Combustion chamber studied in this case is given in Figure 3-33. Fuel injector configuration is given in Figure 3-34. Also another flame holder configuration is studied as seen in Figure 3-33.

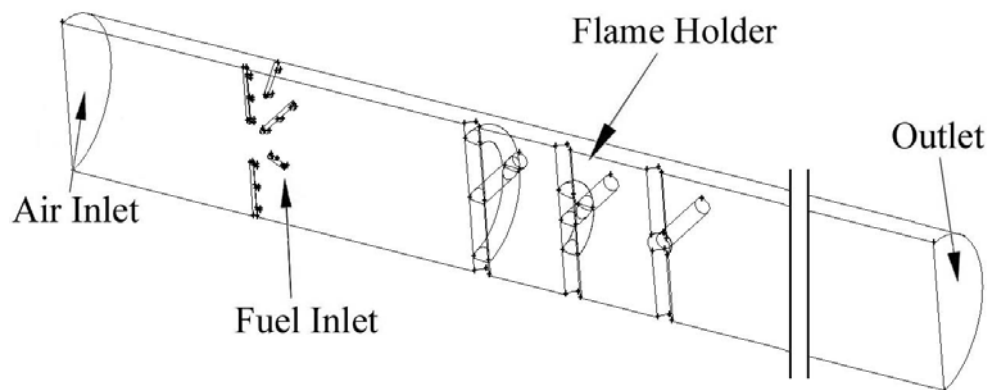


Figure 3-33. Sketch of combustion chamber of Case 4

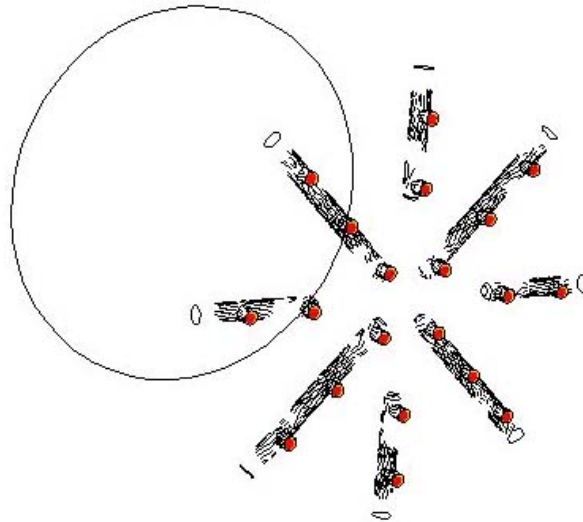


Figure 3-34. Fuel Injector Studied in Case 4

As in Case 2 and Case 3, fuel does not mix with the flow before flame holder. The maximum local temperature in the combustion chamber reaches up to 1320 K. But because of the new orientation of the flame holder, a uniform temperature profile is obtained at the outlet plane. Average temperature at the exit is 756.54 K which is close to the required temperature (747 K).

Best results are obtained in Case 4. This fuel injector and flame holder configuration is selected for the test facility vitiation. Sketch of the combustion chamber is given in Figure 3-37 and the sketch of the fuel injector is given in Figure 3-38.

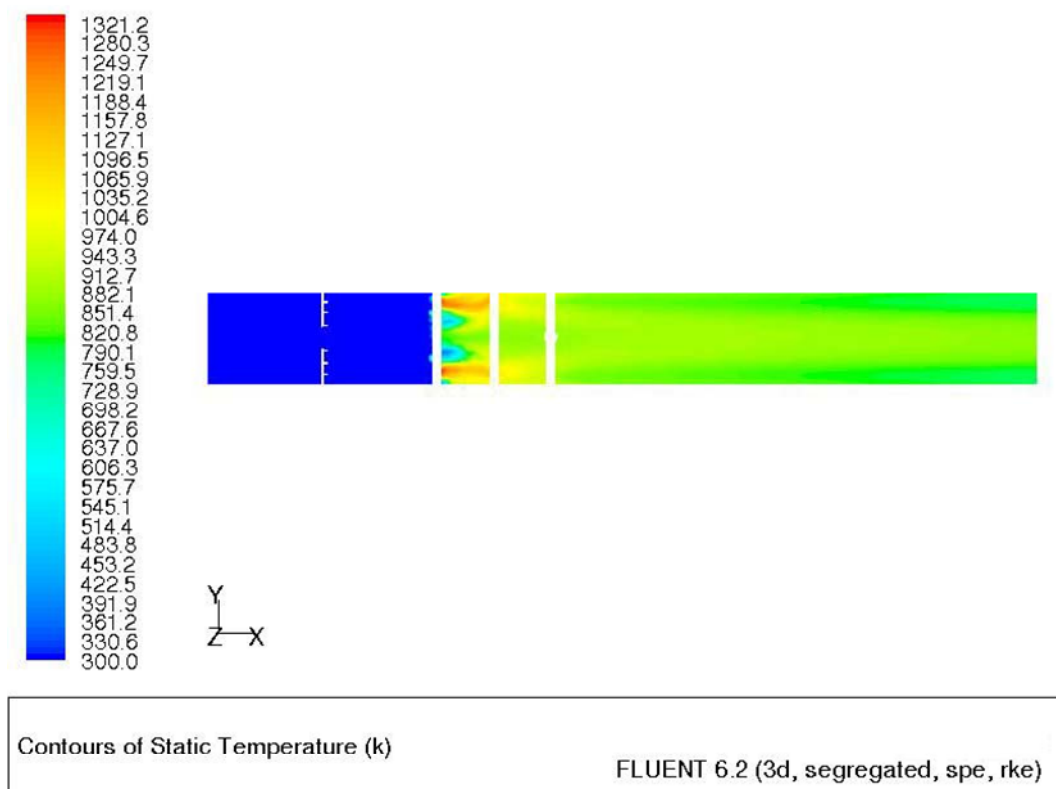


Figure 3-35. Contours of Static Temperature of Case 4

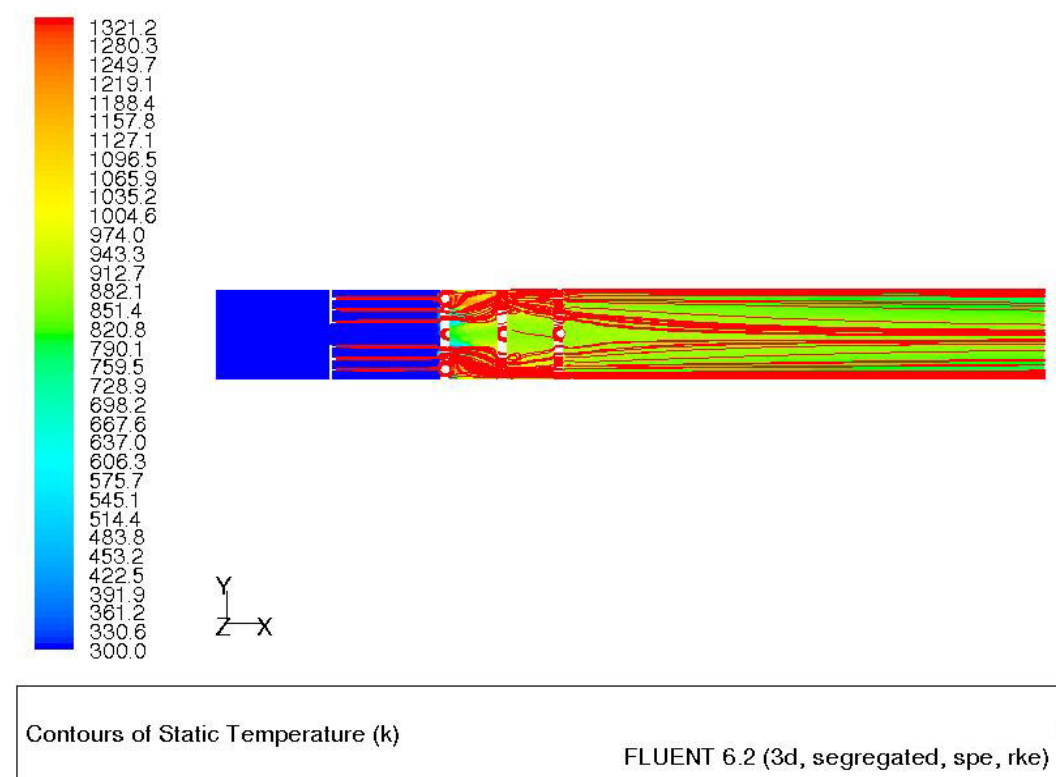


Figure 3-36. Contours of Static Temperature and Fuel Path Lines of Case 4

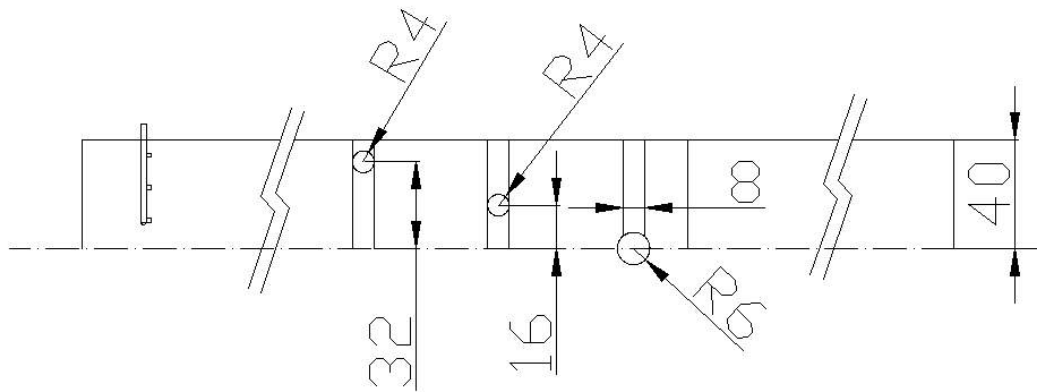


Figure 3-37. Final Configuration of the Vitiator

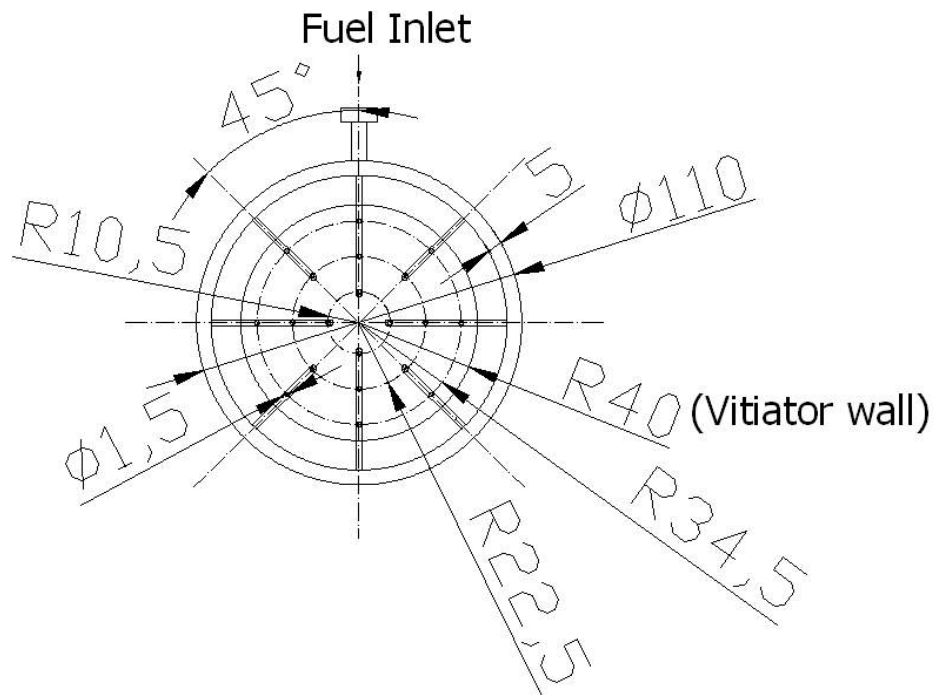


Figure 3-38. Fuel Injector Configuration

CHAPTER 4

TEST STAND DESIGN

Thrust stand is the part on which the ramjet combustors are tested. This part can be stated as the hearth of the facility because after the installation of the facility, all the test activities will take on that part.

Its purpose is to allow the measurements of thrust and must be efficiently integrated in the whole facility. This stand must allow the missile and piping displacement generated by the thrust.

The ramjet engine will be fixed on the sliding part. This part is designed in order to slide with the less friction as possible. In that way, the more precise will be the thrust measurement by the load cell.

The design of the test stand and the piping connection are linked in so far as the vitiation positioning is essential and must be as closer as possible to the missile inlets.

4.1. TEST STAND DESIGN

4.1.1. REQUIREMENTS

- The missile should slide freely with minimum friction along its main axis:
One of the parameters to be tested in the facility is nozzle thrust. Load cells will be employed to measure the thrust. In order to get accurate values, a design with minimum friction should be achieved.

- The effect of piping should be minimized: Since the air is supplied to the engine to simulate ramjet inlets, a piping system is mandatory. In order to measure thrust, flexible pipes have to be used. These pipes have to be selected and oriented in such a way that, their contribution to the nozzle is minimal.
- Air heated at the vitiator should be delivered to the combustor with minimum cooling: If the vitiator is placed far from the ramjet combustion chamber, the heated air will cool down. Also air at high temperatures may have negative effects on flexible hoses, so it would be a good solution to place the vitiator after the flexible hoses, as close to the ramjet engine as possible.

4.1.2. COMPONENTS OF THE THRUST STAND

4.1.2.1. STAND SLIDING MECHANISM

An optimum solution is investigated to achieve a sliding mechanism with minimum friction possible. Three alternatives are considered:

4.1.2.1.1. Wheel Rolling on Rails

The first alternative that is considered is to use a wheel which will slide on a rail. The wheel should be designed to fit the rail as seen in Figure 4-1.

This alternative will be a good solution in terms of friction reduction but on the other hand, the wheel can go off the rails in case of a thrust misalignment, which is possible during development testing. To overcome this problem, a second wheel can be used as shown in Figure 4-2, but this solution complicates the thrust stand design.

4.1.2.1.2. Antifriction Bearings Rolling on Rails

To use antifriction bearing instead of wheels is another possibility. Antifriction bearings are efficient against friction but on the other hand, they are not reliable.

Again, to overcome a thrust misalignment, a set of antifriction bearing as shown in Figure 4-2 has to be used.

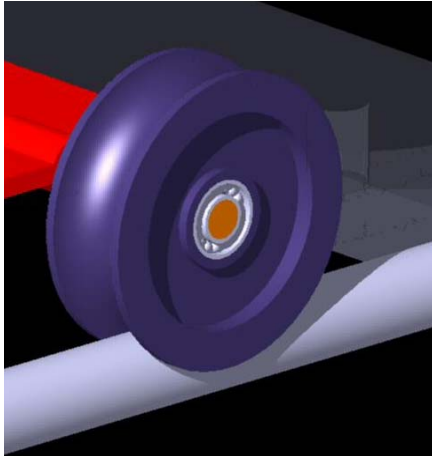


Figure 4-1. Wheel Configuration

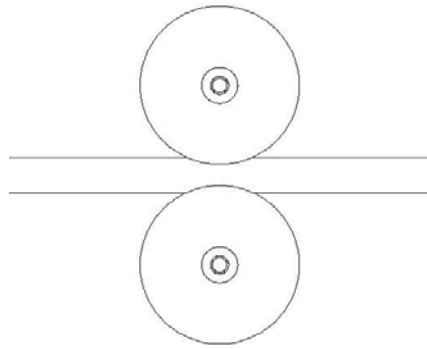


Figure 4-2. Double Wheel Configuration

4.1.2.1.3. Stand Sliding on Cylindrical Rods

An other alternative is to use a stand sliding on cylindrical rods as shown in Figure 4-3. Comparing the wheel and antifriction bearings, this alternative is poor in terms of friction reduction, but on the other hand it is simple and can resist to misaligned thrust. Friction is reduced by applying grease on the cylindrical rod and the sliding pad.

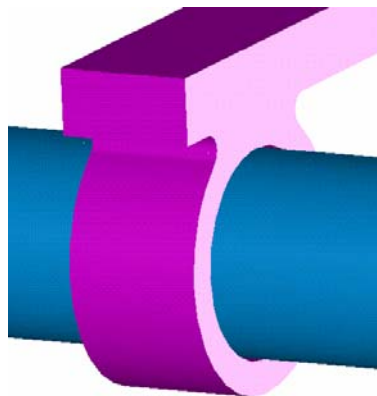


Figure 4-3. Cylindrical Rod and Sliding Pad Configuration

4.1.2.2. SLIDING TABLE

This is the table placed on the sliding pad. It carries the ramjet engine to be tested, v blocks, and the other equipments.

4.1.2.3. V BLOCKS

V blocks are the parts that fix the ramjet engine and the gas generator to the sliding table. V blocks have two parts. The lower part is fixed to the sliding table by bolts. Lower part contains 4 vertical threaded bars. The upper part has four holes which match to the bars of the lower part. Ramjet engine is placed on the lower part, then the upper part is put on the engine and the nuts are fastened as shown in Figure 4-4.

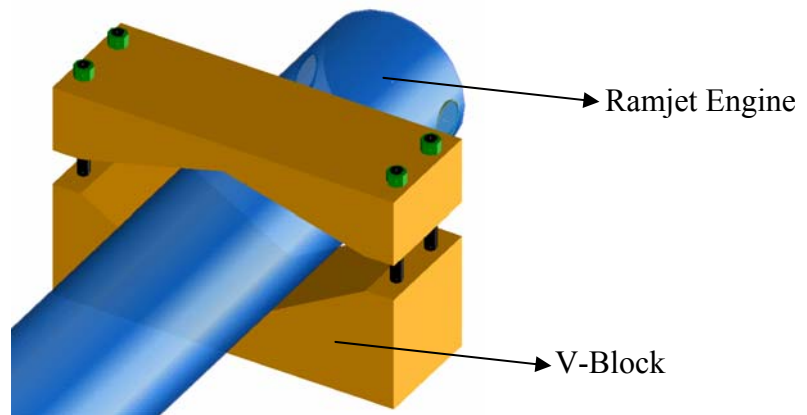


Figure 4-4. V-Blocks Configuration

The advantage of selecting v-blocks is that, it can fix the engines with different diameters. So, these blocks can be used for several different engines.

4.1.2.4. VITIATOR TABLE

After the heated air leaves the vitiator, it flows through pipes to the ramjet engine. Even if the pipes are well insulated, there will be a temperature loss during this process. To overcome this, vitiator has to be placed close to the ramjet engine. Additionally, flexible hoses generally can not stand the temperatures that are generated by the air heater. The best place for the vitiator appears to be on the

thrust stand. This position will also provide the quickest response for the temperature variation during a flight-envelope temperature simulation. Vitiator table is the part that fix the vitiator to the sliding table, as shown in Figure 4-5.

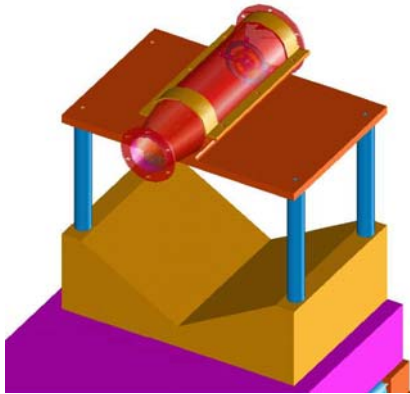


Figure 4-5. Vitiator Table

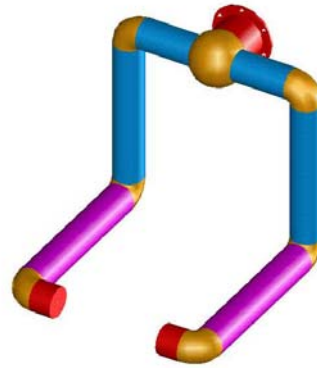


Figure 4-6. Piping Systems

4.1.2.5. PIPES

Pipe configuration is used to duct the air heated in the vitiator. The orientation of the pipes should be designed to supply the air to the ramjet engine at correct Mach number. While testing different engines, the pipe configuration should be partially or completely changed to achieve the desired air properties at the ramjet entrance. A typical pipe configuration is given in Figure 4-6. Details of piping are given in section 4.2.

4.1.2.6. FLEXIBLE PIPES

Conventional rocket motor propellant grains contains the oxygen needed for combustion, so during static testing, the only connection of the rocket motor is the connection with the sliding table. There is no ducting to the engine. Whereas in air breathing engines, air has to be supplied to the combustion chamber. This requirement brings the need for piping system. With rigid pipes connected to the ramjet engine, thrust can not be measured. So flexible pipes has to be used.

To obtain the effect of piping on thrust measurement, cold flow tests has to be utilized. By discharging the air tank without using vitiator and ramjet motor, the resistive forces can be obtained. During facility operation, these resistive forces should be added to the measured thrust value to obtain the correct thrust value.

4.1.3. 3D CAD MODELING OF THE TEST CENTER

The test stand is designed on Ideas CAD software. 3D model of the test center is given in Figure 4-7.

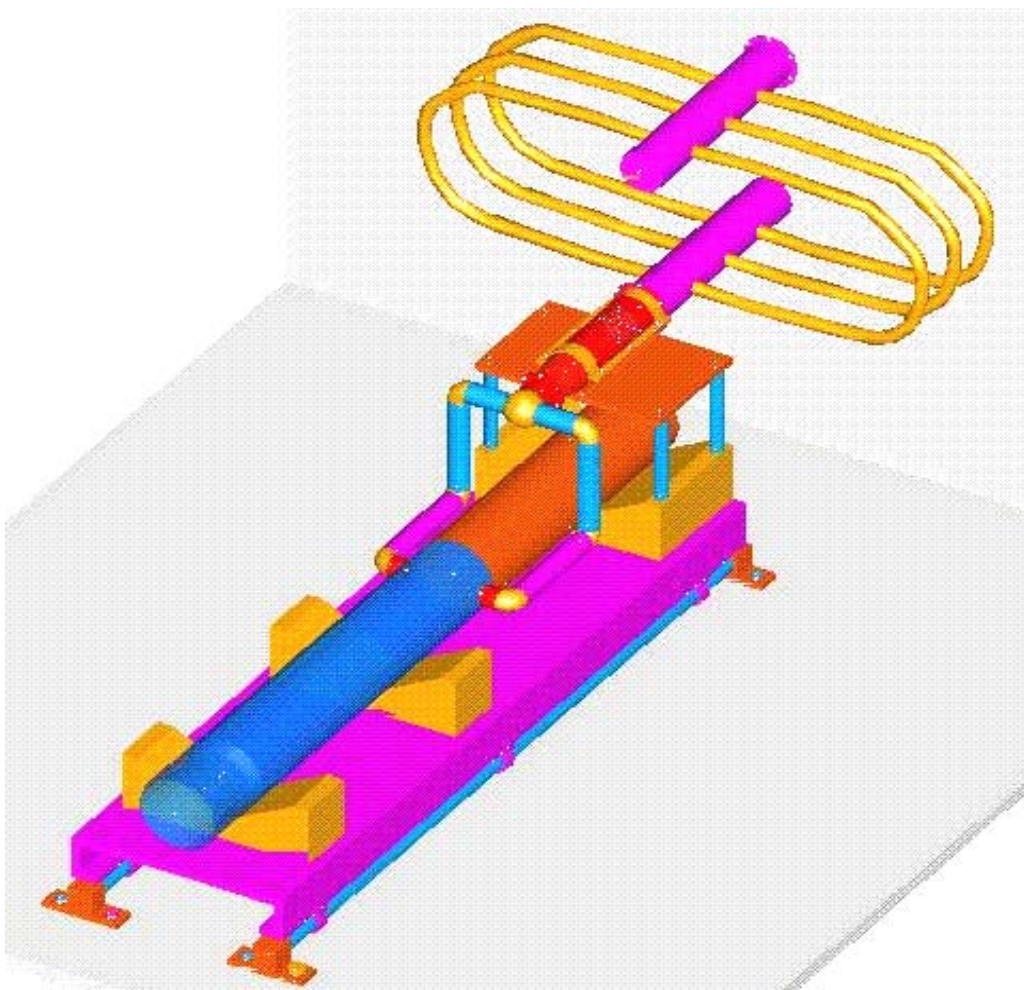


Figure 4-7. 3D Model of the Test Center

4.2. PIPING SYSTEM DESIGN

4.2.1. HEAD LOSS IN A PIPE

The pressure change (ΔP) along a pipe in turbulent flow depend on the following quantities:

- 1. D , Pipe diameter
- 2. L , Length of pipe over which the pressure is to be determined
- 3. μ , coefficient of viscosity
- 4. V , mean time averaged velocity over the cross section (equivalent to q / A)
- 5. ρ , density
- 6. e , the average variation in pipe radius (a measure of pipe roughness)

Average roughnesses of some commercial pipes are given in Table 4-1 [21] .

Table 4-1. Average Roughness of Commercial Pipes

Material	e	
	ft	mm
Glass	0.000001	0.0003
Drawn tubing	0.000005	0.0015
Steel	0.00015	0.046
Asphalted cast iron	0.0004	0.12
Galvanized iron	0.0005	0.15
Cast iron	0.00085	0.26
Wood stave	0.0006-0.003	0.18-0.9
Concrete	0.001-0.01	0.3-3.0
Riveted steel	0.003-0.03	0.9-9.0

There are different semi empirical correlation formulas to evaluate friction factor, f . One recent formula valid for certain large ranges of e/D and Reynolds number is:

$$f = \frac{0.25}{\left[\ln(e/3.7D) + (5.74/R_{ey}^{0.9}) \right]^2} \quad (\text{eqn. 1}) [21]$$

This formula is valid for the ranges:

$$5 \times 10^3 \leq R_{ey} \leq 10^8$$

$$10^{-6} \leq \left(\frac{e}{D} \right) \leq 10^{-2} \quad (\text{eqn. 2}) [21]$$

4.2.2. MINOR LOSSES IN PIPE SYSTEMS

The head loss of devices such as pipe bends, valves etc., has to be considered. This must always be done using experimental results. Head loss is given as:

$$h_l = K \frac{V^2}{2} \quad (\text{eqn. 3})$$

where the coefficient K is given for commercial fittings. No difference is made between laminar and turbulent flow.

In Table 4-2, K factors for a number of important fittings for pipes having certain nominal diameters are listed [21]. Nominal diameter does not correspond exactly to the inside diameter of the pipe. In Table 4-3, nominal diameters of some standard pipes are listed with their inside diameters [21].

Table 4-2. K Factors for Fittings

	Nominal diameter, in									
	$\frac{1}{2}$	$\frac{3}{4}$	1	$1\frac{1}{2}$	2	3	4	5	6	8
Gate valve (open)	0.22	0.20	0.18	0.16	0.15	0.14	0.14	0.13	0.12	0.11
Globe valve (open)	9.20	8.50	7.80	7.10	6.50	6.10	5.80	5.40	5.10	4.80
Standard elbow (screwed) 90°	0.80	0.75	0.69	0.63	0.57	0.54	0.51	0.48	0.45	0.42
Standard elbow (screwed) 45°	0.43	0.40	0.37	0.34	0.30	0.29	0.27	0.26	0.24	0.22
Standard tee (flow through)	0.54	0.50	0.46	0.42	0.38	0.36	0.34	0.32	0.30	0.28
Standard tee (flow branched)	1.62	1.50	1.38	1.26	1.14	1.08	1.02	0.96	0.90	0.84

Table 4-3. Nominal Pipe Sizes for Standard Pipes

Nominal pipe Diameter, in	Inside diameter, in	Nominal pipe Diameter, in	Inside diameter, in
$\frac{1}{2}$	0.364	3	3.068
$\frac{3}{4}$	0.824	4	4.026
1	1.049	5	5.047
$1\frac{1}{2}$	1.610	6	6.065
2	2.067	8	7.981

4.2.3. PRESSURE DROP AT AN ELBOW

Sketch of an elbow is given in Figure 4-8.

Assumptions:

- Flow is incompressible in the elbow
- $y_1 = y_2$
- $A_1 = A_2$

Bernoulli equation between 1 & 2:

$$\left(\frac{V_1^2}{2} + \frac{P_1}{\rho} + gy_1 \right) = \left(\frac{V_2^2}{2} + \frac{P_2}{\rho} + gy_2 \right) + h_l \quad (\text{eqn. 4})$$

Continuity Equation:

$$\rho_1 V_1 A_1 = \rho_2 V_2 A_2 \quad \Rightarrow \quad V_1 = V_2 \quad (\text{eqn. 5})$$

Combining equations :

$$\frac{P_1}{\rho} = \frac{P_2}{\rho} + K \frac{V^2}{2}$$

$$\Delta P = K \frac{\rho V^2}{2}$$

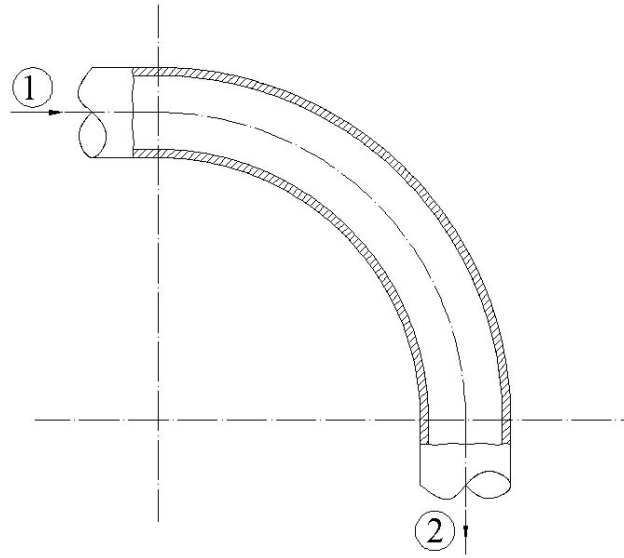


Figure 4-8. Sketch of an Elbow

4.2.4. PRESSURE DROP IN A PIPE

One-dimensional flow with friction calculations are performed by using sonic flow reference calculations, where flow properties are denoted by *. Sketch of a pipe is given in Figure 4-9.

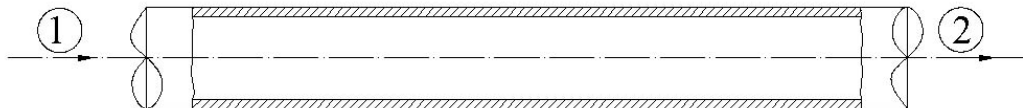


Figure 4-9. Sketch of a Pipe

$$\frac{T}{T^*} = \frac{\gamma + 1}{2 + (\gamma - 1)M^2} \quad (\text{eqn.6.})$$

$$\frac{P}{P^*} = \frac{1}{M} \left[\frac{\gamma + 1}{2 - (\gamma - 1)M^2} \right]^{1/2} \quad (\text{eqn.7.})$$

$$\frac{\rho}{\rho^*} = \frac{1}{M} \left[\frac{2 + (\gamma - 1)M^2}{\gamma + 1} \right]^{1/2} \quad (\text{eqn. 8})$$

$$\frac{4fL^*}{D} = \frac{1 - M}{\gamma M^2} + \frac{\gamma + 1}{2} \ln \left[\frac{(\gamma + 1)M^2}{2 + (\gamma - 1)M^2} \right] \quad (\text{eqn. 9})$$

Given the flow properties at station 1 and the length of the pipe, station 2 properties can be calculated as follows:

1. Calculate f from (eqn.1)
2. Calculate $\frac{4fL^*}{D}$ from (eqn. 9)
3. Calculate L_2^* from $L_2^* = L_1^* - L$
4. Calculate M_2 from (eqn. 9)
5. Calculate T_2 from $T_2 = \frac{T_2}{T^*} \frac{T^*}{T_1} T_1$ using (eqn.6)
6. Calculate P_2 from $P_2 = \frac{P_2}{P^*} \frac{P^*}{P_1} P_1$ using (eqn.7)
7. Calculate ρ_2 from $\rho_2 = \frac{\rho_2}{\rho^*} \frac{\rho^*}{\rho_1} \rho_1$ using (eqn.8)

Sample calculations for the piping system are given APPENDIX E. Piping configuration after the vitiator is given in Figure 4-10. Piping configuration before the vitiator is given in Figure 4-11.

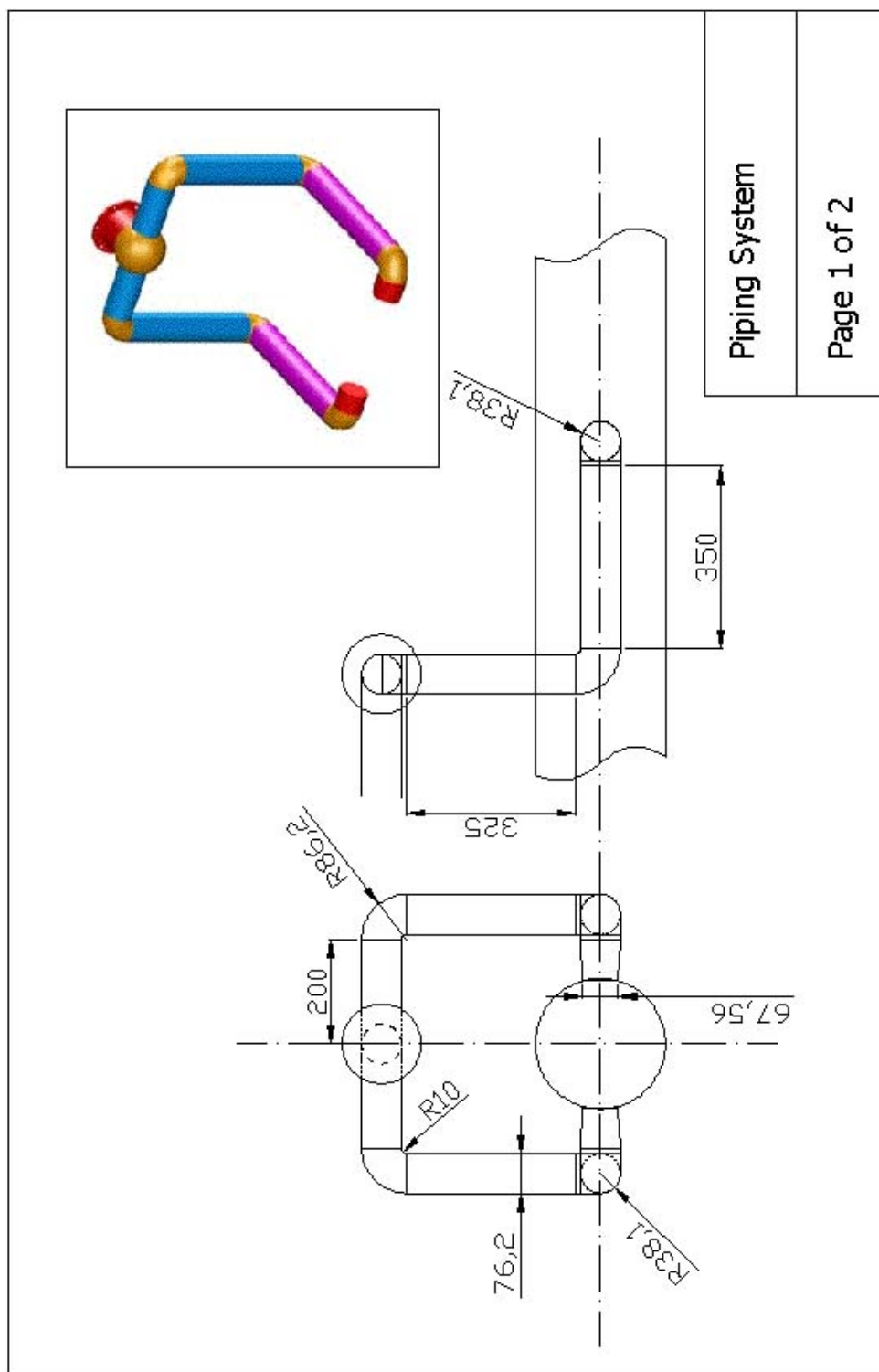
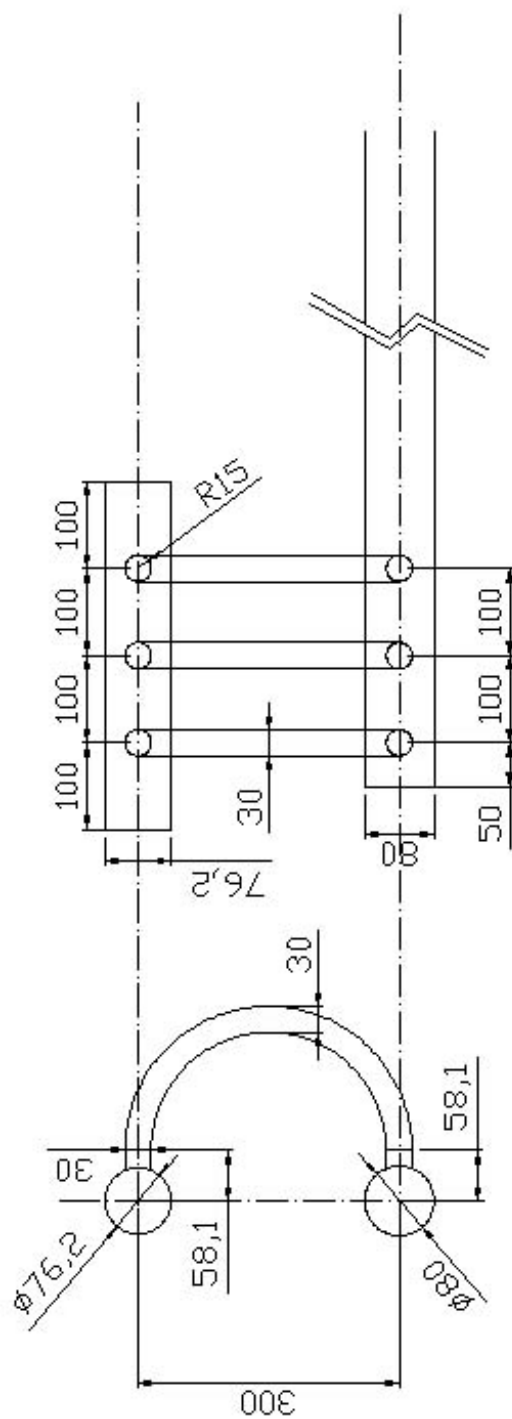


Figure 4-10. Piping Configuration Following the Vitiator



4.2.5. MODELLING OF PIPING SYSTEM BY FLUENT

3D model of the piping system with the vitiator is generated. Inputs for FLUENT are based on the sample calculations given in APPENDIX E. Inlet and outlet pressures to the piping system are input to the code and the pressure values are calculated. The temperature profile of the piping system obtained by FLUENT is given in Figure 4-12. The average temperature at the outlet (combustor inlet) is calculated as 762.45 K which is close to the required temperature (747 K). From the calculation in APPENDIX E, a 7.5 K temperature drop is obtained in the piping. Temperature at the combustor exit is 770.72 which gives a temperature drop of 8.27 K. FLUENT Model agree with the calculations given in APPENDIX E.

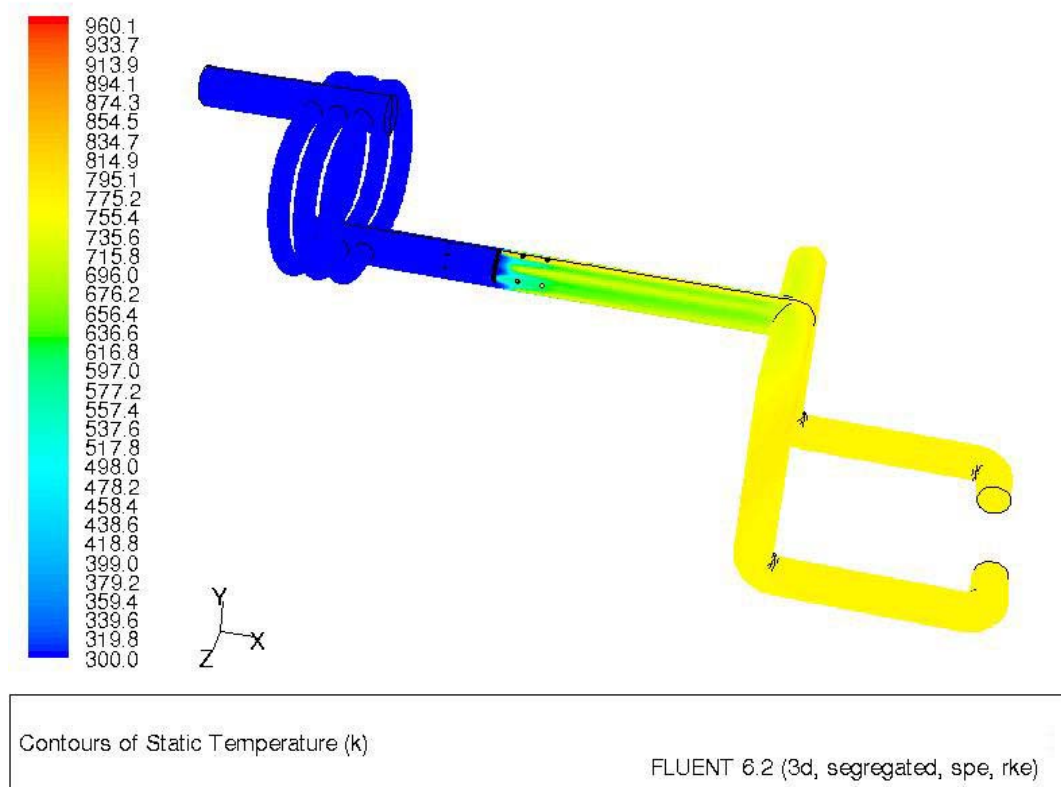


Figure 4-12. Temperature Contours on the Fluent Model of the Piping System

4.3. RAMJET COMBUSTOR DESIGN

In this section flame holding mechanism for ramjet combustion chamber is studied. Ramjet combustion chamber analysis is based on the test data supplied by [6]. Data supplied by [6] is as follows:

Geometric Data of Ramjet Motor:

$$A_2 = 0.010325 \text{ m}^2 \quad (\text{Combustor air inlet area})$$

$$A_4 = 0.022698 \text{ m}^2 \quad (\text{Combustion chamber cross section area})$$

$$A_5 = 0.013668 \text{ m}^2 \quad (\text{Nozzle throat area})$$

Measured Test Data:

$$\dot{m}_{air} = 6.692 \text{ kg/s} \quad (\text{Air mass flow rate})$$

$$\dot{m}_{fuel} = 0.311 \text{ kg/s} \quad (\text{Fuel (kerosene) mass flow rate})$$

$$F_{LC} = 8400 \text{ N} \quad (\text{Load cell thrust})$$

4.3.1. Case 1

In this case, a combustion chamber similar to Case 2 presented in 3.1.1.2.2 is selected. The sketch of the combustion chamber is given in Figure 4-13. Contours of static temperatures obtained are given in Figure 4-14 and contours of Mach Number are given in Figure 4-15.

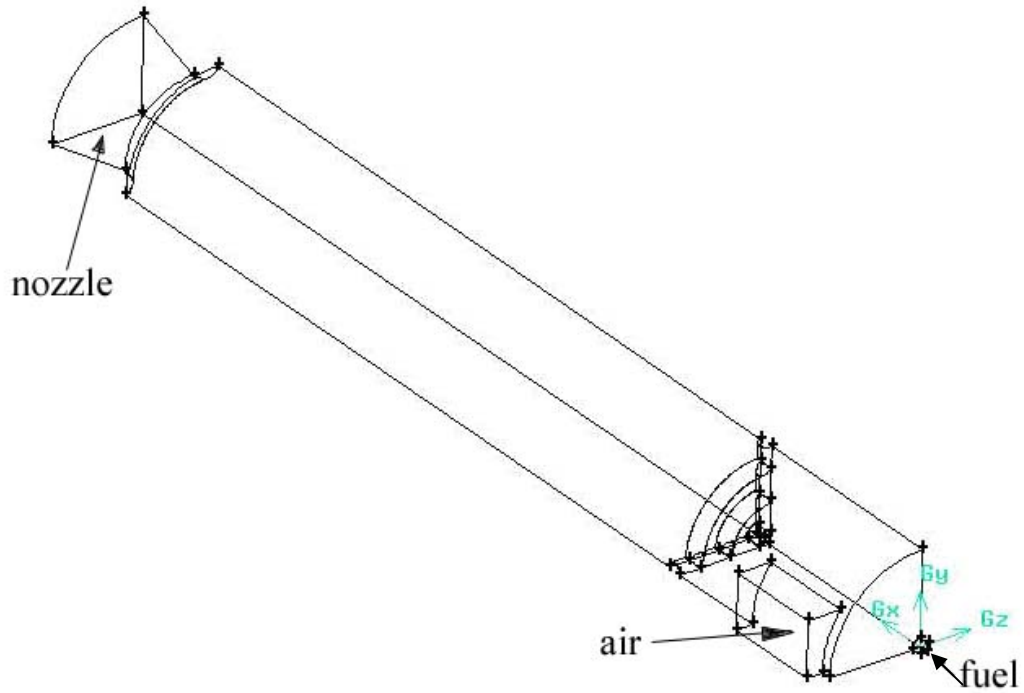


Figure 4-13. Sketch of Case 1

One dimensional thrust equation is [22]:

$$T = \dot{m}_6 u_6 + (P_6 - P_a) A_6$$

where 6 denotes the nozzle exit plane properties and P_a is the ambient pressure.

$$P_6 = 18990.7 \text{ Pa}$$

$$V_6 = 1187.0 \text{ m/s}$$

$$\dot{m}_6 = 7.0 \text{ kg/s}$$

The thrust is calculated as : $T = 8713.48 \text{ N}$

Table 4-4. Comparison of FLUENT Results with Experimental Results

	Experiment	FLUENT
P_4	568800 Pa	580863.9 Pa
M_4	0.35	0.40
Thrust	8400 N	8713.48 N

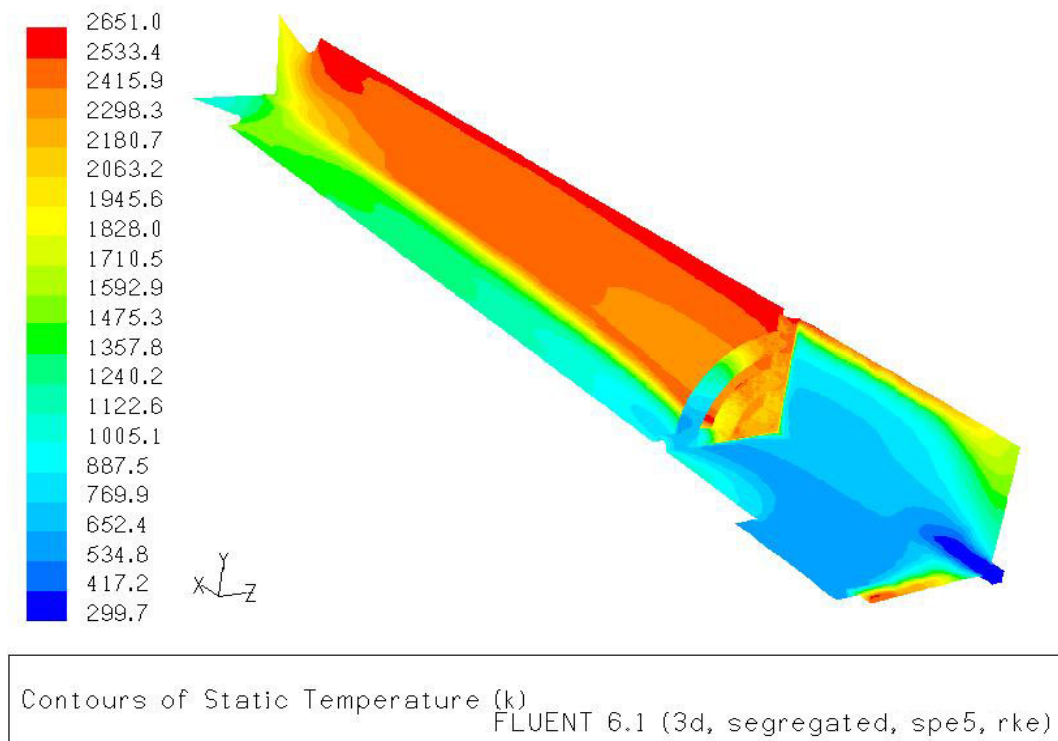
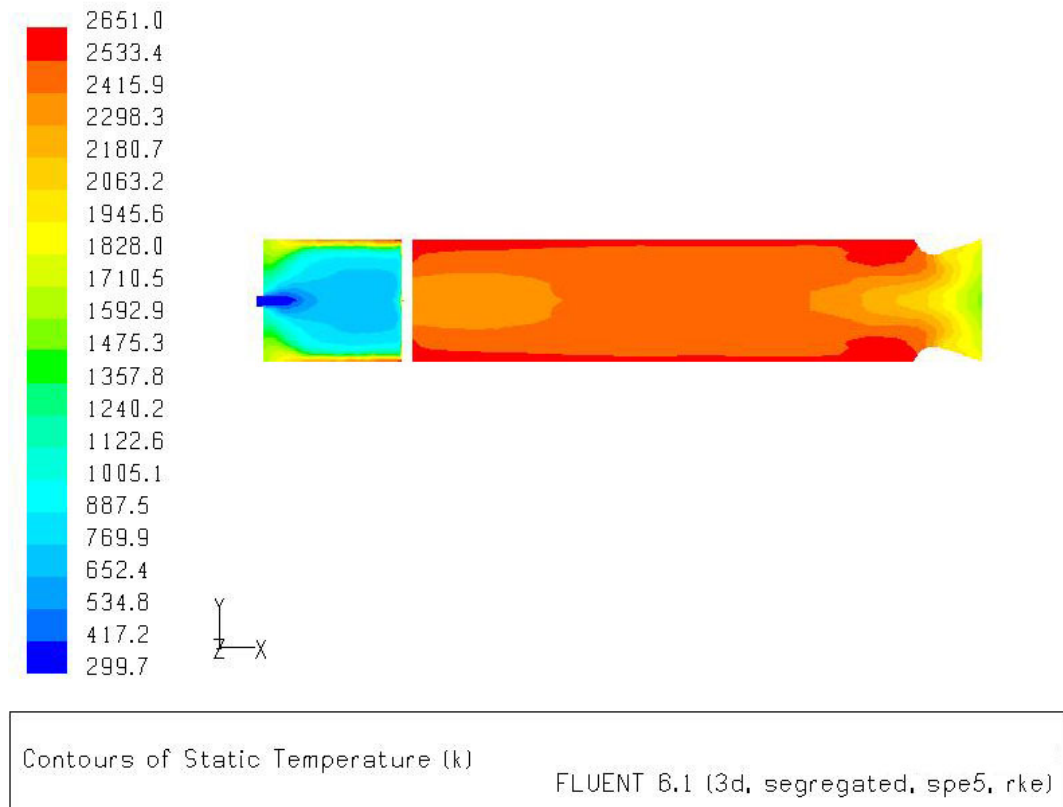


Figure 4-14. Contours of Static Temperature of Case 1.

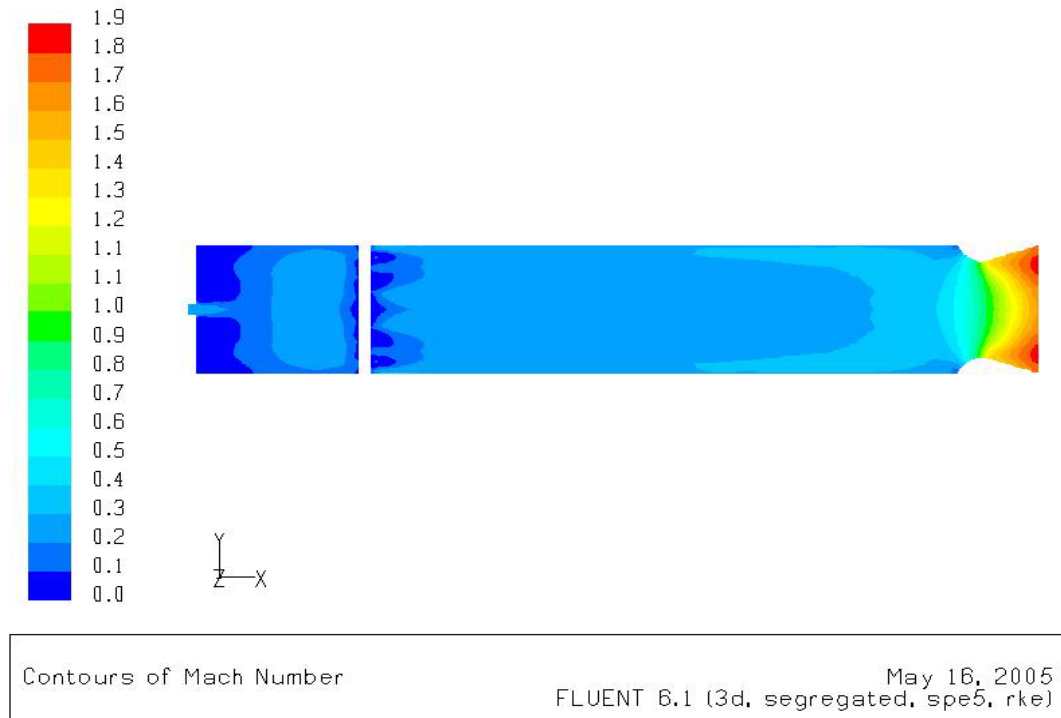


Figure 4-15. Contours of Mach Number of Case 1.

Results

- Since the flow speed is higher than the flame speed, combustion starts after the bluff body where the circulation occurs.
- Pressure at the aft section of the combustion chamber is slightly higher than the measured value.
- Mach number at the aft section of the combustion chamber is slightly higher than the value stated in [6].
- Thrust calculated is higher than the measured value.

Comments

The results obtained are close to the measured value. The difference in the pressure and the Mach number seems to be caused by the flame holder mechanism. The flow is forced to flow through a narrow area which helps the flow to accelerate.

Higher pressure and Mach number effected the thrust calculation which is calculated higher than the measured value. To overcome this problem, an alternative flame holder mechanism is studied.

4.3.2. Case 2

In this case, an alternative flame holder is mounted on the same combustion chamber presented in 4.3.1. A better nozzle contour is utilized in this case. The sketch of the combustion chamber is given in Figure 4-16.

contours of Mach Number are given in Figure 4-17 and contours of static temperatures obtained are given in Figure 4-18.

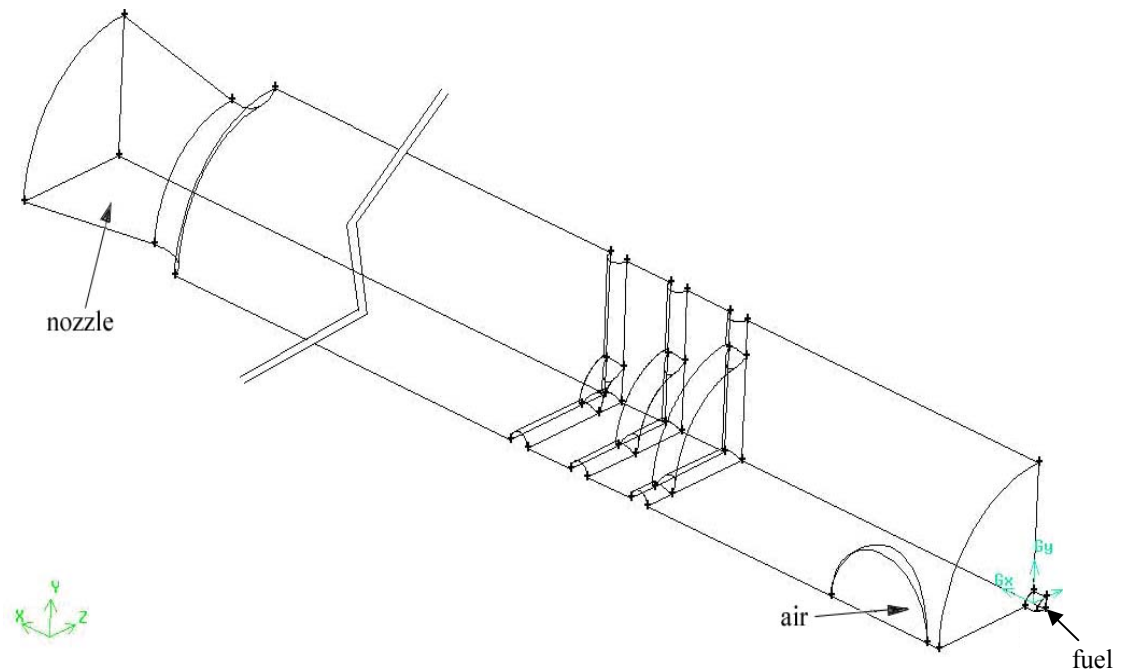


Figure 4-16. Sketch of Case 2

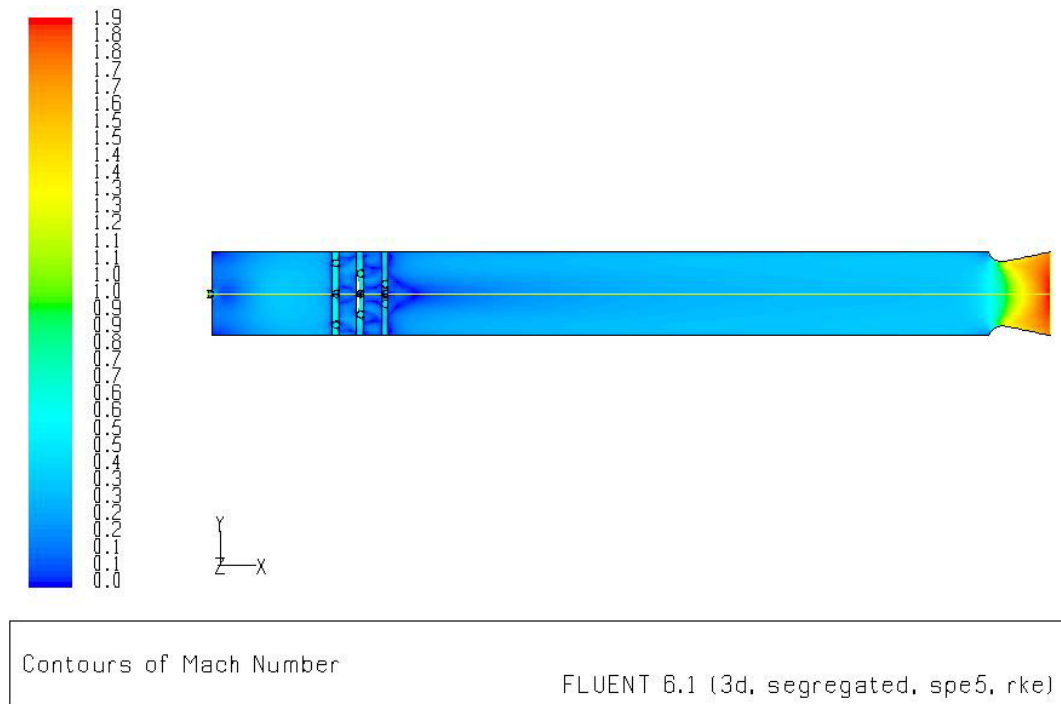


Figure 4-17. Contours of Mach Number of Case 1.

Properties at the nozzle outlet are as follows:

$$P_6 = 101325 \text{ Pa}$$

$$V_6 = 1241.4 \text{ m/s}$$

$$\dot{m}_6 = 7.0 \text{ kg/s}$$

The thrust is calculated as : $T = 8693.8 \text{ N}$

Table 4-5. Comparison of FLUENT Results with Experimental Results

	Experiment	FLUENT
P_4	568800 Pa	569580.1 Pa
M_4	0.35	0.37
Thrust	8400 N	8693.8 N

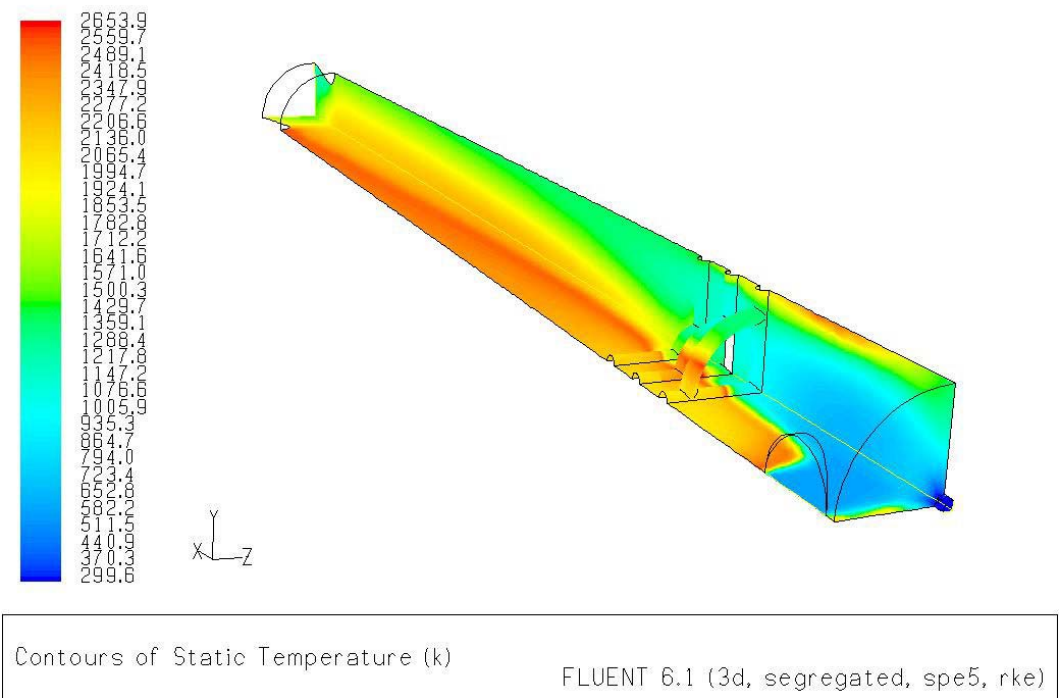
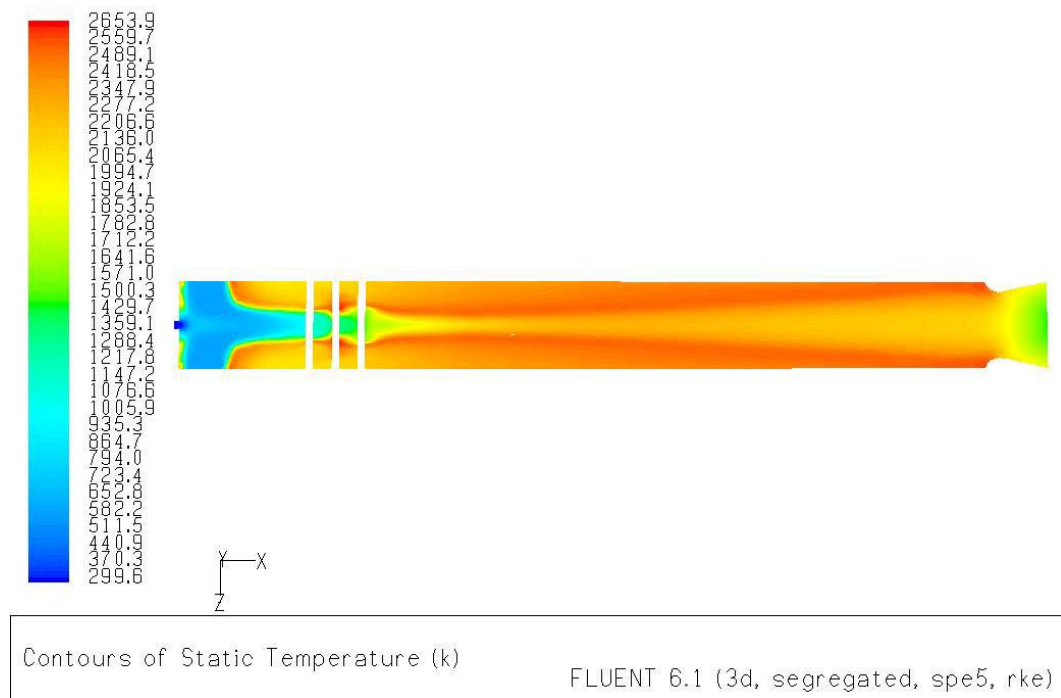


Figure 4-18. Contours of Static Temperature of Case 2.

Results

- Pressure at the aft section of the combustion chamber is close to the measured value.
- Mach number at the aft section of the combustion chamber is close to the value stated in [6].
- Thrust calculated is higher the measured value.

Comments

The results obtained are better than the ones obtained in case 1. Pressure and the Mach number values are now close to the expected values. Thrust is again higher than the measured one. The reason is that, the new nozzle utilized in this case offered a better expansion.

CHAPTER 5

CONCLUSION AND DISCUSSION

5.1. SUMMARY OF THE WORK

In this work, design calculations of a sample connected pipe ramjet test facility are completed. Three main systems of the facility are detailed; air storage system, air heater system and the test stand.

In the air storage system design part (Chapter 2), designs of pressure vessel and flow regulation systems are detailed. Design of air tank is based on ASME Codes. The volume of the air storage system is 27.8 m^3 and the design pressure is 50 bar. The stored air allows test duration of 200 seconds at an average mass flow rate of 3 kg/s.

Aerodynamic heating of the air in the missile inlet is simulated by the air heater system. Combustion analysis of the air heater is performed by Fluent CFD Code. First, combustion model of Fluent Code is validated by an experimental study. Then in the air heater system design part (Chapter 3), several different vitiator configurations are studied. Two dimensional combustion chambers are modeled by Fluent. The most efficient flame holding configuration is selected. Then three dimensional model of this configuration is modeled and optimized. A final combustor configuration is obtained. Designed air heater system is capable of supplying air at temperature range 400-1000 K and mass flow rate 1.5-8 kg/s at Mach numbers between 0.1-0.5 and pressure between 2-8 bar.

Design of thrust stand, piping system and the ramjet combustor is examined in test stand design section (Chapter 4). Three dimensional CAD model of the test center is generated. Pressure and temperature losses in the pipe line are calculated in the piping system design part. In the ramjet combustor design part, ramjet combustion chamber is modeled by Fluent and the results are compared by an experimental study.

Four Fortran codes are generated; discharge code, pipe code, valve code and combustion code. Discharge code calculates the pressure and temperature variation of the air tank during discharge. Mass flow rate – time data is input to the code. In the pipe code, pressure and temperature losses in the pipe line is calculated and the required properties in the vitiator and valve outlet are calculated. Valve code read the pressure and temperature data from the discharge and pipe outputs and calculates the valve coefficients. Finally combustion code calculates the mass flow rate value to obtain the required temperature and the oxygen mass flow rate to replenish the lost oxygen during vitiator combustion.

5.2. SUGGESTIONS FOR FUTURE WORK

For future development of the present design, the following topics can be proposed:

- If temperature requirement for the missile combustor is above 1500K, an insulation or cooling system should be designed for the vitiator and the piping system.
- Ramjet combustor model and valve models may be added to the FLUENT piping system solution presented in section 4.2.5.
- Test duration is limited by the temperature drop of the air tank. Higher test durations can be achieved by heating the air tanks. On the other hand, the heater has to respond quickly to the rapid temperature drop, so it may not be economical. A water recirculation system between the air tanks and vitiator can help heating the tanks while cooling the vitiator.
- A detailed study on flex hose configuration may be necessary to minimize their negative effect on the thrust measurement.

- To upgrade the facility, an ejector system may be added to the system which will improve the simulation accuracy.

5.3. CONCLUSION

The summary of properties of the designed connected pipe test facility is as follows:

Nozzle Exit/ Combustor Inlet Mach number	0.1 - 0.5
Test Fuel	Methane
Heater Type	Vitator
Pressure Range (bar)	2 – 8
Temperature Range (K)	400 - 1000
Airflow Rate Range(kg/s)	1.5 – 8.0
Air Storage (m ³)	27.8
Test Duration (s)	200

REFERENCES

- [1] DUNSWORTH L.C., REED G.J., “*Ramjet Engine Testing and Simulation Techniques*”, J. Spacecraft, Vol.16, No.6, 1978
- [2] Bruno CORITON, “*Design of a liquid fuel ramjet and a ducted rocket engine*”, Internship ENSMA-ROKETSAN, 2002.
- [3] Nurhan AYAZ-“*Conceptual Design Of An Integral Rocket-Ramjet Air-Launched Missile*”, METU Aerospace Dept Master Thesis, 2000.
- [4] DAVENAS A., “*Solid Rocket Propulsion Technology*” Pergamon Press, 1993.
- [5] Leisch,S. and Netzer, D.W., “*Solid Fuel Ramjets*”, Tactical Missile Propulsion, AIAA Progress Series, Vol 170, 1996, Chapter 13, pp. 469-493.
- [6] AGARD-AR-323-“*Experimental and analytical methods for the determination of connected-pipe ramjet and ducted rocket internal performance*”, NATO 1994.
- [7] ARNOLD ENGINEERING DEVELOPMENT CENTER,
“<http://www.arnold.af.mil>”, last accessed on 8 April 2005
- [8] NASA LANGLEY RESEARCH CENTER, “<http://www.larc.nasa.gov>”,
last accessed on 8 April 2005
- [9] MITSUBISHI HEAVY INDUSTRIES, LTD.
“<http://www.sdia.or.jp/mhikobe-/products/etc/siken/high/jet/jisseki1.html>”,
last accessed on 8 April 2005
- [10] INSTITUTE OF SPACE TECHNOLOGY AND AERONAUTICS,
“<http://www.nal.go.jp>”, last accessed on 8 April 2005
- [11] ATLANTIC RESEARCH CORPORATION,
“<http://www.atlantic-research.com>” , last accessed on 8 April 2005

- [12] THE FRENCH AERONAUTICS AND SPACE RESEARCH CENTER
“<http://www.onera.fr>”, last accessed on 8 April 2005
- [13] GRUBER M., DONBAR J., JACKSON K., “*Newly Developed Direct-Connect High-Entropy Supersonic Combustion Research Facility*”, Journal of Propulsion and Power, Vol. 7, No.6, 2001
- [14] KANURY M., “*Introduction to Combustion Phenomena*”, Gordon and Breach Science Publishers, 1977.
- [15] MELLOR A., “*Design of Modern Turbine Combustors*”, Academic Press Limited, 1990
- [16] SPALDING B., “*Combustion and Mass Transfer*”, Pergamon Press, 1979
- [17] ESAPYRONICS “<http://www.esacombustion.it/esauk/manuals.asp>”, last accessed on 8 April 2005
- [18] AIR LIQUIDE GROUP : INDUSTRIAL GAS AND MEDICAL GAS DISTRIBUTION “<http://www.airliquide.com/en/business/products/gases/gasdata/>”, last accessed on 8 April 2005
- [19] FISHER.-ROSEMOUNT, “*Control Valve Handbook*”, Fisher Controls International Inc., 1998
- [20] GORDON S.-MCBRIDE B., “*NASA SP-273 Computer Program For Calculation Of Complex Equilibrium Compositions, Rocket Performance, Incident And Reflected Shocks, And Chapman-Jouguet Detonations*”, NASA 1976
- [21] SHAMES I., “*Mechanics of Fluids*”, McGraw Hill, 1982
- [22] OATES G., “*Aerothermodynamics of Gas Turbine and Rocket Propulsion, Revised and Enlarged*”, AIAA Education Series, 1988
- [23] POPE E., “*Rule of Thumb For Mechanical Engineers*”, Gulf Publishing, 1996
- [24] SHIGLEY J., “*Mechanical Engineering Design*”, McGraw Hill, 1986
- [25] MEGYESY E., “*Pressure Vessel Handbook*”, Pressure Vessel Publishing Inc., 1998
- [26] CARSON B., CHUSE R., “*The ASME Code Simplified Pressure Vessels*”, McGraw Hill, 1993

- [27] Magnussen B. F., Hjertage B. H., “*On mathematical models of turbulent combustion with special emphasis on soot formation and combustion*” 16th Symp. (Int'l.) on Combustion. The Combustion Institute, 1976.
- [28] Magnussen B. F., “*On the Structure of Turbulence and a Generalized Eddy Dissipation Concept for Chemical Reaction in Turbulent Flow*”, Nineteenth AIAA Meeting, St. Louis, 1981.
- [29] S. M. CANNON, B. S. BREWSTER, and L. D. SMOOT, “*PDF Modeling of Lean Premixed Combustion Using In Situ Tabulated Chemistry*”, Combustion And Flame 119:233–252 (1999)

APPENDIX A

AIR TANK DESIGN

A.1. STRESS ANALYSIS

Stress analysis is the determination of the relationship between the forces applied to a vessel and the corresponding stress. The aim is to analyze vessels and their component parts to arrive at an economical and safe design. The stresses are analyzed to determine the thickness of material and sizes of members. It is not necessary to find every stress but rather to know the governing stresses and how they relate to the vessel or its respective parts, attachments, and supports. The starting place for stress analysis is to determine all the design conditions for a given problem and then determine all the related external forces. Then the forces should be related to the vessel parts which must resist the corresponding stresses. [23]

A.2. MEMBRANE STRESS ANALYSIS

Pressure vessels commonly have the form of spheres, cylinders, cones, ellipsoids or composites of these. The types of heads closing the vessel, effects of supports, variation in thickness and cross section, nozzles, external attachments, and overall bending due to weight, wind, and seismic all cause varying stress distributions in the vessel. [24]

In any pressure vessel subjected to internal or external pressure, stresses are set up in the shell wall. The state of stress is triaxial and the three principal stresses are:

σ_x = Longitudinal stress

σ_ϕ = Circumferential stress

σ_r = radial stress

The radial stress is a direct stress, which is a result of the pressure acting directly on the wall, and causes a compressive stress equal to the pressure. In thin-walled vessels this stress is so small compared to the other “principal” stresses that it is generally ignored. Thus we assume for purposes of analysis that the state of stress is biaxial. This greatly simplifies the method of combining stresses in comparison to triaxial stress states. For thick-walled vessels ($R_m/t < 10$), the radial stress cannot be ignored and formulas are quite different from those used in finding “membrane stresses” in thin shells.

“Membrane stress analysis” is not completely accurate but allows certain simplifying assumptions to be made while maintaining a fair degree of accuracy. The main simplifying assumptions are that the stress is biaxial and that the stresses are uniform across the shell wall. For thin-walled vessels these assumptions have proven themselves to be reliable.

A.2.1. FAILURES IN PRESSURE VESSELS

Vessel failures can be grouped into four major categories [23]:

1. Material; Improper selection of material; defects in material.
2. Design; Incorrect design data; inaccurate or incorrect design methods; inadequate shop testing.
3. Fabrication; Poor quality controls; improper or insufficient fabrication procedures including welding; heat treatment or forming methods.
4. Service; Change of service condition by the user; inexperienced operations or maintenance personnel.

A.2.2. LOADINGS

Loadings or forces are the “causes” of stresses in pressure vessels. The stresses from the various loadings to arrive at the worst possible combination of stresses should be obtained. Then the results to an acceptable stress level have to be compared to obtain an economical and safe design.

The stresses due to pressure are the primary membrane stresses. These stresses would cause the bursting or collapse of the vessel if allowed to reach an unacceptably high level.

For steady loads, the vessel must support these loads more or less continuously during its useful life. As a result, the stresses produced from these loads must be maintained to an acceptable level.

For nonsteady loads, the vessel may experience some or all of these loadings at various times but not all at once and not more or less continuously. Therefore a temporarily higher stress is acceptable.

For general loads that apply more or less uniformly across an entire section, the corresponding stresses must be lower, since the entire vessel must support that loading. Loadings can be outlined as follows:

A. Categories of loadings

1. General loads-Applied more or less continuously across a vessel section.
 - a. Pressure loads-Internal or external pressure (design, operating, hydrotest, and hydrostatic head of liquid).
 - b. Moment loads-Due to wind, seismic, erection, transportation.
 - c. Compressive tensile loads-Due to dead weight, installed equipment, ladders, platforms, piping, and vessel contents.
 - d. Thermal loads-Hot box design of skirt-head attachment.
2. Local loads-Due to reactions from supports, internals, attached piping, attached equipment, i.e., platforms, mixers, etc.
 - a. Radial load-Inward or outward.
 - b. Shear load-Longitudinal or circumferential.

- c. Torsional load.
- d. Tangential load.
- e. Moment load-Longitudinal or circumferential.
- f. Thermal loads.

B. Types of loadings

1. Steady loads-Long-term duration, continuous.
 - a. Internal/external pressure.
 - b. Dead weight.
 - c. Loadings due to attached piping and equipment.
 - d. Thermal loads.
 - e. Wind loads.
2. Nonsteady loads-Short-term duration; variable.
 - a. Shop and field hydrotests.
 - b. Earthquake.
 - c. Erection.
 - d. Transportation.
 - e. Upset, emergency.
 - f. Thermal loads.
 - g. Start up, shut down.

A.2.3. PRESSURE VESSEL FORMULAS

Pressure vessel formulas are given in [25]

Notation:

P = internal pressure, psi	K, M = coefficients
D_i, D_o = inside / outside diameter, in.	σ_x = longitudinal stress, psi
S = allowable or calculated stress, psi	σ_ϕ = circumferential stress, psi
E = joint efficiency	t = thickness or thickness required
R_i, R_o = inside / outside radius, in.	of shell, head, or cone, in.

A.2.3.1. CYLINDRICAL SHELL

Below equations are valid for $P < 0.385SE$ and $t < R/2$

Formulas in terms of inside dimensions:

$$t = \frac{PR}{SE - 0.6P} \quad P = \frac{SE t}{R + 0.6t}$$

Formulas in terms of outside dimensions:

$$t = \frac{PR}{SE + 0.4P} \quad P = \frac{SE t}{R - 0.4t}$$

A.2.3.2. ELLIPTICAL HEAD

Below equations are valid when the ratio of the major and minor axis is 2:1

Formulas in terms of inside dimensions:

$$t = \frac{PD}{2SE - 0.2P} \quad P = \frac{2SE t}{D + 0.2t}$$

Formulas in terms of outside dimensions:

$$t = \frac{PD}{2SE + 1.8P} \quad P = \frac{2SE t}{kD - 1.8t}$$

General configuration and dimensional data for vessel shells and head is given in Figure A-1

A.2.3.3. OPENINGS

This chapter is from [26].

A.2.3.3.1. Shape of Openings

Openings in pressure vessels shall preferably be circular or elliptical. The openings made by a pipe or a circular nozzle, the axis of which is not perpendicular to the vessel wall or head, may be considered an elliptic opening for design purposes.

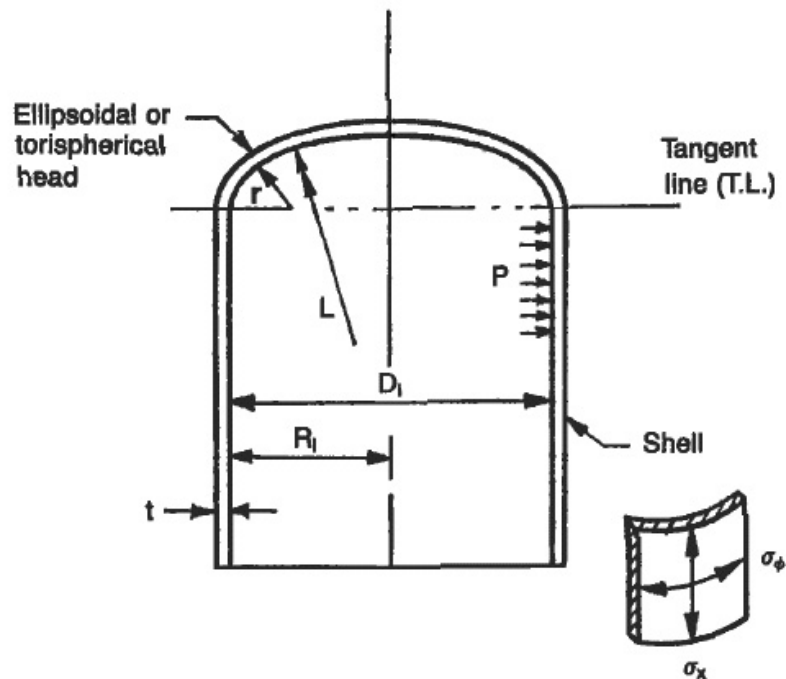


Figure A-1. General Configuration for Vessel Shells and Head

A.2.3.3.2. Reinforcement Of Openings Design For Internal Pressure

Vessels shall be reinforced around the openings, except single, welded openings not subjected to rapid pressure fluctuations do not require reinforcement if not larger than:

- 3 1/2 in. diameter in not over 3/8 in thick vessel wall;
- 2 3/8 in. diameter in not over 2 3/8 in. vessel wall. (Code UG-36

(c)(3)(a)

The design procedure described below conforms to the Code UG-36 through UG-43, which apply to openings not exceeding:

- One-half or 20 in. diameter in vessels of maximum 60 in. inside diameter.
- One-third or 40 in. diameter in vessels over 60 in. diameter.

The basic requirement is that around the opening the vessel must be reinforced with an equal amount of metal which has been cut out for the opening. The reinforcement may be an integral part of the vessel and nozzle, or may be an additional reinforcement pad. (Figure A-2)

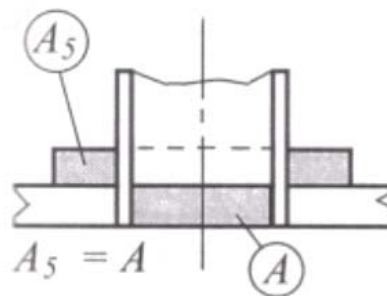


Figure A-2. Nozzle Reinforcement

This rule needs further refinements as follows:

- It is not necessary to replace the actually removed amount of metal, but only the amount which is required to resist the internal pressure (A). This required thickness of the vessel at the openings is usually less than at other points of the shell or head.
- The plate actually used and nozzle neck usually are thicker than would be required according to calculation. The excess in the vessel wall (A_1) and nozzle wall (A_2) serve as reinforcements. Likewise the inside extension of the opening (A_3) and the area of the weld metal (A_4) can also be taken into consideration as reinforcement.
- The reinforcement must be within a certain limit.
- The area of reinforcement must be proportionally increased if its stress value is lower than that of the vessel wall.

- The area required for reinforcement must be satisfied for all planes through the center of opening and normal to vessel surface.

The required cross sectional area of the reinforcement shall then be the required area for the shell or head to resist the internal pressure (A). From this area subtract the excess areas within the limit ($A_1 A_2 A_3 A_4$). If the sum of the areas available for reinforcement ($A_1+A_2+ A_3+ A_4$) is equal or greater than the area to be replaced (A), the opening is adequately reinforced. Otherwise the difference must be supplied by reinforcing pad (A_5).

a. Area of Reinforcement

For vessels under internal pressure the total cross-sectional area required for reinforcement of opening shall not be less than:

$$A = d \times t_r \quad \text{where}$$

d = The inside diameter of opening in its corroded condition.

t_r = The required thickness of shell or head computed by the applicable formulas.

b. Available Area of Reinforcement

A_1 = Area of excess thickness in the vessel wall

“($t - t_r$) d ” or “($t - t_r$)($t_n + t$)₂” use the larger value. If the stress value of the opening’s material is less than that of the material, area A_1 shall be decreased.

A_2 = Area of excess thickness in the nozzle wall

“($t_n - t_{rn}$) $5t$ ” or “($t_n - t_{rn}$) $5t_n$ ” use the smaller value.

A_3 = Area of inside extension of nozzle: ($t_n - c$) $2h$

A_4 = Area of welds.

If the sum of A_1, A_2, A_3 and A_4 is less than the area of reinforcement required, A the difference must be supplied by reinforcing pad.

c. Limits of Reinforcement

The metal used as reinforcement must be located within the limits.

The limit measured parallel to the vessel wall “ $X = d$ ” or “ $R_n + t_n + t$ ”. Use the larger value.

The limit measured parallel to the nozzle wall “ $Y = 2.5 t$ ” or “ $2.5 t_n$ ”. Use smaller value.

When additional reinforcing pad is used, the limit, Y to be measured from the outside surface of the reinforcing pad.

R_n = inside radius of nozzle in corroded condition

d. Strength of Reinforcement

If the strength of materials in A_1 A_2 A_3 A_4 and A_5 or the material of the reinforcing pad are lower than that of the vessel material, their area considered as reinforcement shall be proportionately decreased and the required area, A in inverse proportion increased. The strength of the deposited weld metal shall be considered as equivalent to the weaker material of the joint.

It is advisable to use for reinforcing pad material identical with the vessel material.

No credit shall be taken for additional strength of reinforcement having heigher stress value than that of the vessel wall.

APPENDIX B

AIR TANK DESIGN CALCULATIONS

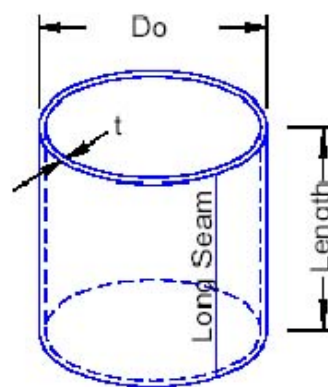
B.1. DESIGN OF VESSEL SHELL

Dimensions

1100.0	Do - Outside Diameter (mm)
10.0	t - Nominal Wall Thickness (mm)
1080.0	Di - Inside Diameter (mm)
1000.0	Length
0.0	Corr, Corrosion allowance

Material and Conditions:

828.0	UTS, Steel (quenched/tempered alloy)
3.0	Safety Factor
276.0	S, Allowable Stress Level (MPa)
1	EI - Longitudinal Efficiency (circ. stress)
1	Ec - Circ. Connecting Efficiency (longitudinal stress)
0.0%	UTP, Undertolerance allowance (%)
0.000	UTI, Undertolerance allowance (m)
5	P, Interior Pressure (MPa)
0	Pa, Exterior Pressure



Variables:

UT = t*UTP+UTI	= 10*0+0	
	undertolerance	UT = 0.0
nt = t-Corr	= 10-0	
	nominal thick	nt = 10.0
Ri = Do/2-nt	= 1100/2-10	
	effective inside radius	Ri = 540.0
LDo = Le/Do	= 1000/1100	LDo = 0.9
DoT = Do/nt	= 1100/10	DoT = 110.0

Interior Pressure

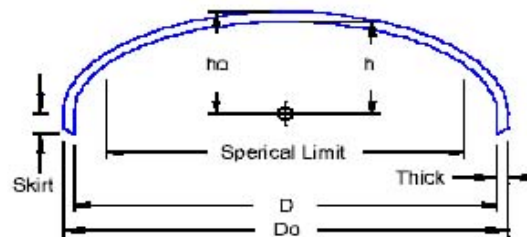
ta = P*Ri/(S*EI-0.6*P)	= 5e6*0.540/(276e6*1-0.6*5e6)	ta = 9.890
------------------------	-------------------------------	------------

$$\begin{aligned}
 t_b &= P \cdot R_i / (2 \cdot S \cdot E_c + 0.4 \cdot P) = 5e6 \cdot 0.540 / (2 \cdot 276e6 \cdot 1 + 0.4 \cdot 5e6) & t_b &= 4.874 \\
 t_{min} &= \text{Max}(t_a, t_b, t_{minUG16b}) & t_{min} &= \boxed{10.0} \text{ mm} \\
 P_{MaxA} &= (S \cdot E_l \cdot t) / (R_i + 0.6 \cdot t) = (276e6 \cdot 1 \cdot 0.010) / (0.540 + 0.6 \cdot 0.010) & P_{MaxA} &= 5.1 \\
 P_{MaxB} &= (2 \cdot S \cdot E_c \cdot t) / (R_i - 0.4 \cdot t) = (2 \cdot 276e6 \cdot 1 \cdot 0.010) / (0.540 - 0.4 \cdot 0.010) & P_{MaxB} &= 10.299 \\
 P_{Max} &= \text{Min}(P_{MaxA}, P_{MaxB}) & P_{Max} &= \boxed{5.1} \text{ MPa}
 \end{aligned}$$

B.2. DESIGN OF VESSEL HEAD

Dimensions

1100.0	Do - Outside Diameter (mm)
261.0	h (mm)
14.0	tf, Thickness after forming (mm)
0	Corr, Corrosion allowance
50.0	Skirt, straight skirt length (mm)



Material and Conditions:

828.0	UTS, Steel (quenched/tempered alloy)
4.0	Safety Factor
207.0	S, Allowable Stress Level (MPa)
1.0	Efficiency
7916.0	Density (kg/m ³)

5.0	P, Interior Pressure (MPa)
0.0	Pa, Exterior Pressure

Variables:

$$\begin{aligned}
 D &= D_o - 2 \cdot t = 1100 - 2 \cdot 14 & D &= 1072.0 \\
 h_o &= h + t = 261 + 14 & h_o &= 275.0 \\
 D/2h &= D / (2 \cdot h) = 1072 / (2 \cdot 261) & D/2h &= 2.054 \\
 D_o/2h_o &= D_o / (2 \cdot h_o) = 1100 / (2 \cdot 275) & D_o/2h_o &= 2.000 \\
 T &= t_f - \text{corr} = 14 - 0 & t &= 14.0
 \end{aligned}$$

Interior Pressure

$$\begin{aligned}
 T_{minI} &= (P \cdot D \cdot K) / (2 \cdot S \cdot E - 0.2 \cdot P) \\
 &= (5e6 \cdot 1.072 \cdot 1.064) / (2 \cdot 207e6 \cdot 1 - 0.2 \cdot 5e6)
 \end{aligned}$$

$$T_{Minl} \text{ (min thickness)} = 13.8 \text{ mm}$$

$$P_{max} = (2 \cdot S \cdot E \cdot t) / (K \cdot D + 0.2 \cdot t)$$

$$= (2 \cdot 207 \cdot 1 \cdot 0.014) / (1.064 \cdot 1.072 + 0.2 \cdot 0.014)$$

$$P_{Max} = 5.1 \text{ MPa}$$

B.3. QUICK DISCHARGE NOZZLE

Head:

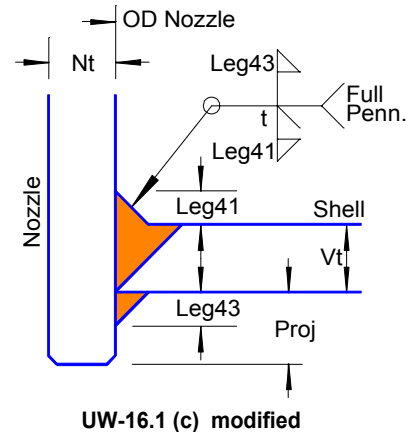
207.0	<- Sv, allowable stress level
14.0	<- t, wall thick, uncorroded
13.8	<- tr, required wall thickness int. press.
0.0	<- trE, required wall thickness ext. press.
1.0	<- E1, efficiency of shell at nozzle
0.0	<- corr, corrosion allowance

Nozzle:

101.6	<- Do, outside diameter (3,5" standart pipe)
71.6	<- d, inside diameter
37.5	<- h, exterior Projection
15.0	<- tn, wall thick, uncorroded
1.0	<- E nozzle
SS (302)	<- Nozzle material (Cold Rolled)
117.9	<- Sn, allowable stress level (Sn)
5.0	<- P, internal design pressure

Reinforcing Flange Pad:

15.0	<- Leg41, size of weld fillet
15.0	<- Leg43, size of weld fillet
1.0	<- F



Pipe Dimensions : XX-STG	inch	mm
Outside diameter	4	101.6
Nominal Pipe Size	3.5	88.9
Nom. Pipe Wall Thickness	0.636	16.1544
Min. Pipe Wall Thickness	0.557	14.1478
Max Allowable pressure	4701	32.41225

Variables:

$$R_n = D_o / 2 - t_n$$

$$R_n = 35.8$$

$$t_{rn} = (P \cdot R_n) / (S_n \cdot E - 0.6 \cdot P) \leq t_n - UT$$

$$t_{rn} = 1.5579$$

$$f_r = \min(S_n / S_v, 1)$$

$$f_r = 0.5696$$

Geometry Constraints:

$$t_n \cdot 1.25 \leq 0.7 \cdot (\text{Leg41} + \text{Leg43})$$

$$18.75 \leq 21 \text{ Okey}$$

$$0.7 \cdot \text{Leg41} \geq 0.7 \cdot t_n$$

$$0.0189 \geq 0.014 \text{ Okey}$$

$$0.7 \cdot \text{Leg43} \geq 0.7 \cdot t_n$$

$$0.014 \geq 0.014 \text{ Okey}$$

Area Replacement:

$$A = d \cdot t_r \cdot F$$

$$\text{mm}^2$$

$$988.71$$

$$A1 = \max((E1 \cdot t \cdot F \cdot tr) \cdot d); (2 \cdot (E1 \cdot t \cdot F \cdot tr) \cdot (t + tn))$$

$$A2 = \min((2 \cdot (2.5 \cdot tn) \cdot (tn - trn)); (2 \cdot (2.5 \cdot t) \cdot (tn - trn)))$$

$$A3 = 2 \cdot h \cdot tn \cdot fr$$

$$A41 = Leg41^2 \cdot fr$$

$$A43 = Leg43^2 \cdot fr$$

A1 =	13.69
A2 =	535.93
A3 =	640.76
A41 =	128.15
A43 =	128.15
Actual	1446.69
Actual-	457.98

Acceptable

B.4. AIR SUPPLY PIPE

Head:

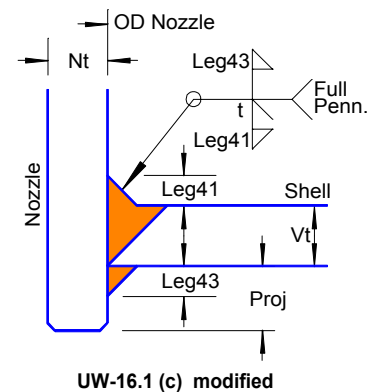
207.0	<- Sv, allowable stress level
14.0	<- t, wall thick, uncorroded
13.8	<- tr, required wall thickness int. press.
0.0	<- trE, required wall thickness ext. press.
1.0	<- E1, efficiency of shell at nozzle
0.0	<- corr, corrosion allowance

Nozzle:

60.3	<- Do, outside diameter
49.3	<- d, inside diameter
20.0	<- h, exterior Projection
5.5	<- tn, wall thick, uncorroded
SS (302)	<- Nozzle material (Cold Rolled)
117.9	<- Sn, allowable stress level (Sn)
5.0	<- P, internal design pressure

Reinforcing Flange Pad:

15.0	<- Leg41, size of weld fillet
15.0	<- Leg43, size of weld fillet
1.0	<- F



Pipe Dimensions : XX-STG	inch	mm
Outside diameter	2.375	60.32
Nominal Pipe Size	2	50.80
Nom. Pipe Wall Thickness	0.218	5.54
Min. Pipe Wall Thickness	0.191	4.85
Max Allowable pressure	2578	17.77

Variables:

$$Rn = Do/2 - tn$$

$$trn = (P \cdot Rn) / (Sn \cdot E - 0.6 \cdot P) \leq tn - UT$$

$$fr = \min(Sn/Sv, 1)$$

$$Rn = \mathbf{24.63}$$

$$trn = \mathbf{1.071}$$

$$fr = \mathbf{0.57}$$

Geometry Constraints:

$$tn \cdot 1.25 \leq 0.7 \cdot (Leg41 + Leg43)$$

$$0.7 \cdot Leg41 \geq 0.7 \cdot tn$$

$$6.9215 \leq 21 \quad \text{Okey}$$

$$0.0189 \geq 0.014 \quad \text{Okey}$$

$$0.7 \cdot Leg43 \geq 0.7 \cdot tn$$

131

$$0.014 \geq 0.014 \quad \text{Okey}$$

Area Replacement:

$$A = d \cdot t_r \cdot F$$

$$A1 = \max((E1 \cdot t - F \cdot t_r) \cdot d); (2 \cdot (E1 \cdot t - F \cdot t_r) \cdot (t + t_n))$$

$$A2 = \min((2 \cdot (2.5 \cdot t_n) \cdot (t_n - t_{rn})); (2 \cdot (2.5 \cdot t) \cdot (t_n - t_{rn})))$$

$$A3 = 2 \cdot h \cdot t_n \cdot f_r$$

$$A41 = \text{Leg41}^2 \cdot f_r$$

$$A43 = \text{Leg43}^2 \cdot f_r$$

mm²**680.09**

$$A1 = \mathbf{9.41}$$

$$A2 = \mathbf{70.42}$$

$$A3 = \mathbf{126.15}$$

$$A41 = \mathbf{128.15}$$

$$A43 = \mathbf{128.15}$$

$$\text{Actual} = \mathbf{462.29} \quad \text{Reinforcing}$$

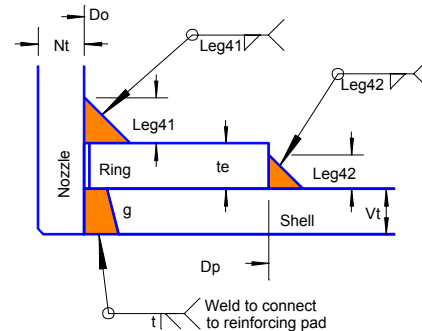
$$\text{Actual-Required} = \mathbf{217.80} \quad \text{Pad Required}$$

Reinforcing:**SA 516 70** <- Reinforcing plate material**137.9** <- Sp, allowable stress level**120.0** <- Dp, outside diameter**20.0** <- te, reinforcement thick**15.0** <- Leg41, size of weld fillet**15.0** <- Leg42, size of weld fillet**10.0** <- LegG, depth of groove

$$A41 = \text{Leg41}^2 \cdot f_r$$

$$A42 = \text{Leg42}^2 \cdot f_r$$

$$A5 = (D_p - d - 2t_n) \cdot t_e \cdot f_r$$



UW-16.1 (h) - modified

$$A41 = 128.15$$

$$A42 = 128.15$$

$$A5 = 679.77$$

A Required (internal) =	680.1
A1 =	9.4
A2 =	70.4
A41 =	128.2
A42 =	128.2
A5 =	679.8
Actual Area =	1015.9
Actual-Required =	335.8

Internal Weld Load: (UG-41)

$$W_{\max 1} = (A - A1 + 2 \cdot T_n \cdot F_r1 \cdot (E1 \cdot t - F \cdot t_r)) \cdot S_v$$

Max value for weld

$$W_{\max 1} = \mathbf{139079.62} \text{ N}$$

$$W_{1-1} = \min((A2 + A5 + A41 + A42) \cdot S_v, W_{\max 1})$$

$$W_{1-1} = \mathbf{139079.62} \text{ N}$$

$$W_{2-2} = \min((A2 + A3 + A41 + A43 + 2 \cdot T_n \cdot t \cdot f_{r1}) \cdot S_v, W_{\max 1})$$

$$W_{2-2} = \mathbf{59383.62} \text{ N}$$

$$W_{3-3} = \min((A2 + A3 + A5 + A41 + A42 + A43 + 2 \cdot T_n \cdot t \cdot f_{r1}) \cdot S_v, W_{\max 1})$$

$$W_{3-3} = \mathbf{139079.62} \text{ N}$$

Component Strength (UG-45(c), UW-15(c))

$$A2 \text{ shear} = \pi() / 2 * (Do - t_n) * t_n * S_n * 0.7$$

$$A2s = 39328.47$$

$$g \text{ tension} = \pi() / 2 * Do * LegG * \text{Min}(S_v, S_n) * 0.74$$

$$gt = 82673.06$$

$$A41 \text{ shear} = \pi() / 2 * Do * Leg41 * \text{Min}(S_n, S_p) * 0.49$$

$$A41s = 82114.46$$

$$A42 \text{ shear} = \pi() / 2 * DP * Leg42 * \text{Min}(S_v, S_p) * 0.49$$

$$A42s = 191045.71$$

Failure mode along strength path

$$S_{1-1} = A42s + A2s \geq W1-1$$

$$S_{1-1} = \mathbf{230374.19} \text{ Acceptable}$$

$$S_{2-2} = A41s + gt \geq W2-2$$

$$S_{2-2} = \mathbf{164787.52} \text{ Acceptable}$$

$$S_{3-3} = gt + A42s \geq W3-3$$

$$S_{3-3} = \mathbf{273718.77} \text{ Acceptable}$$

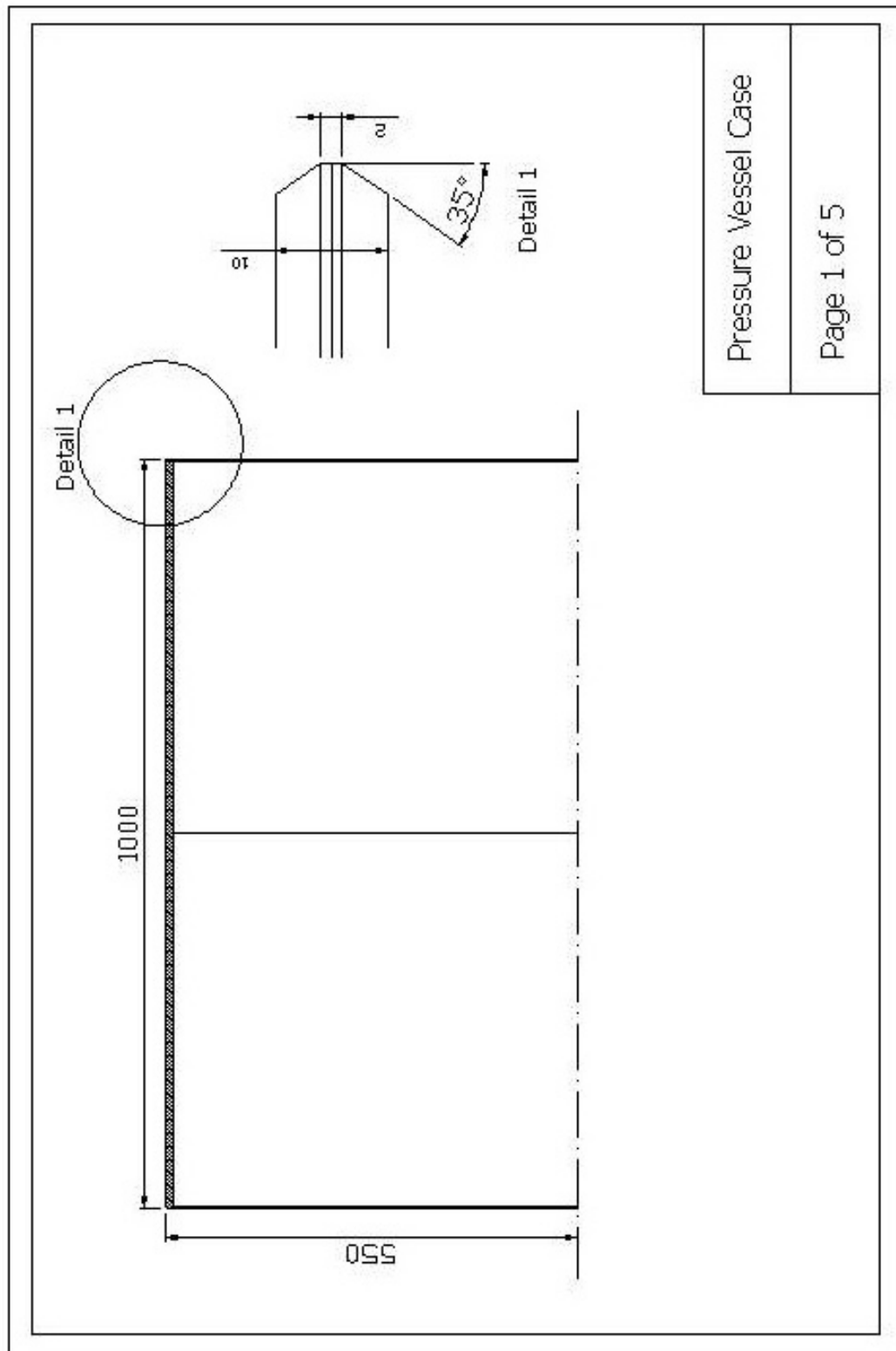


Figure B-1. Technical Drawing of Case

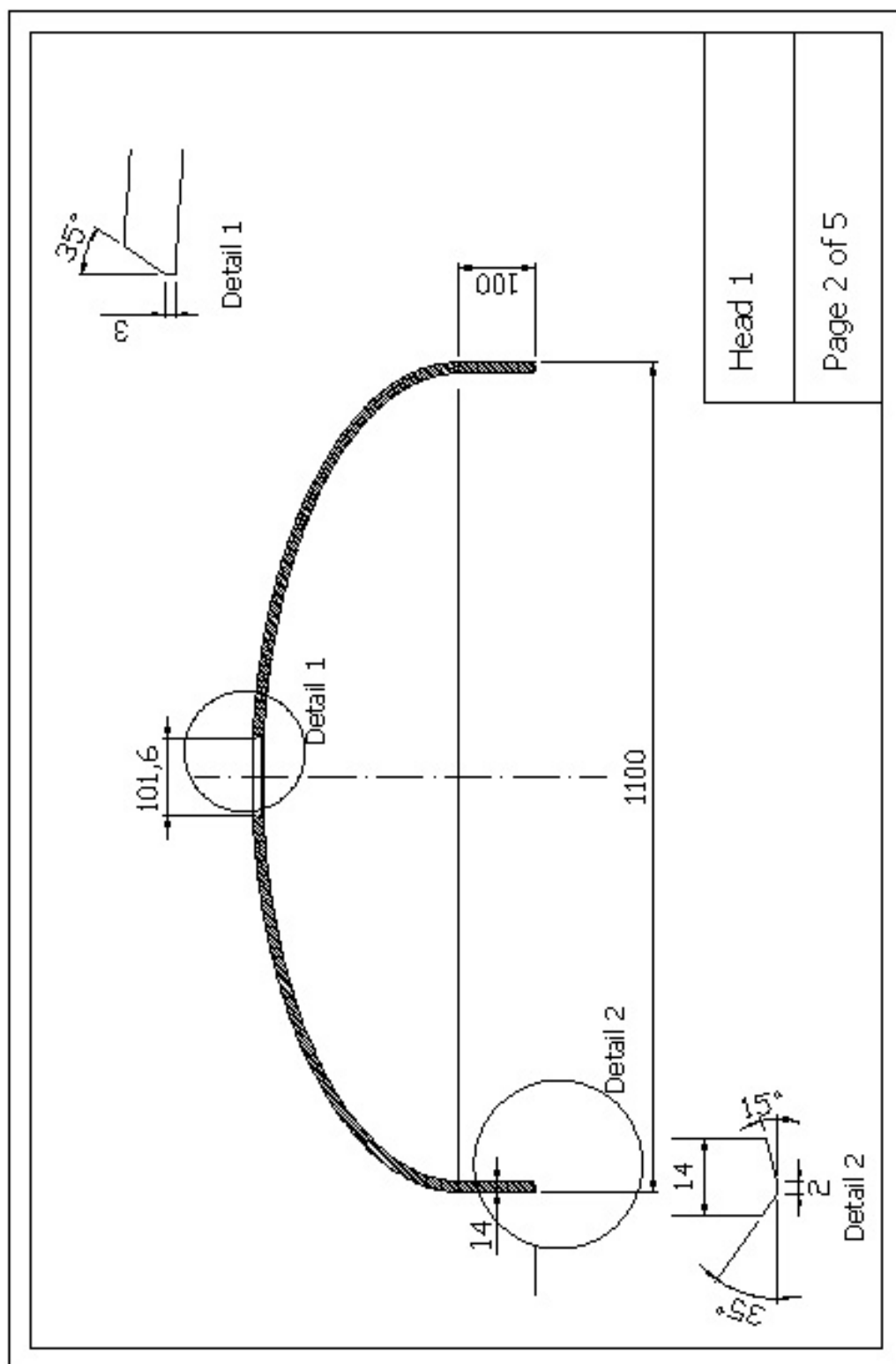


Figure B-2. Technical Drawing of Head 1

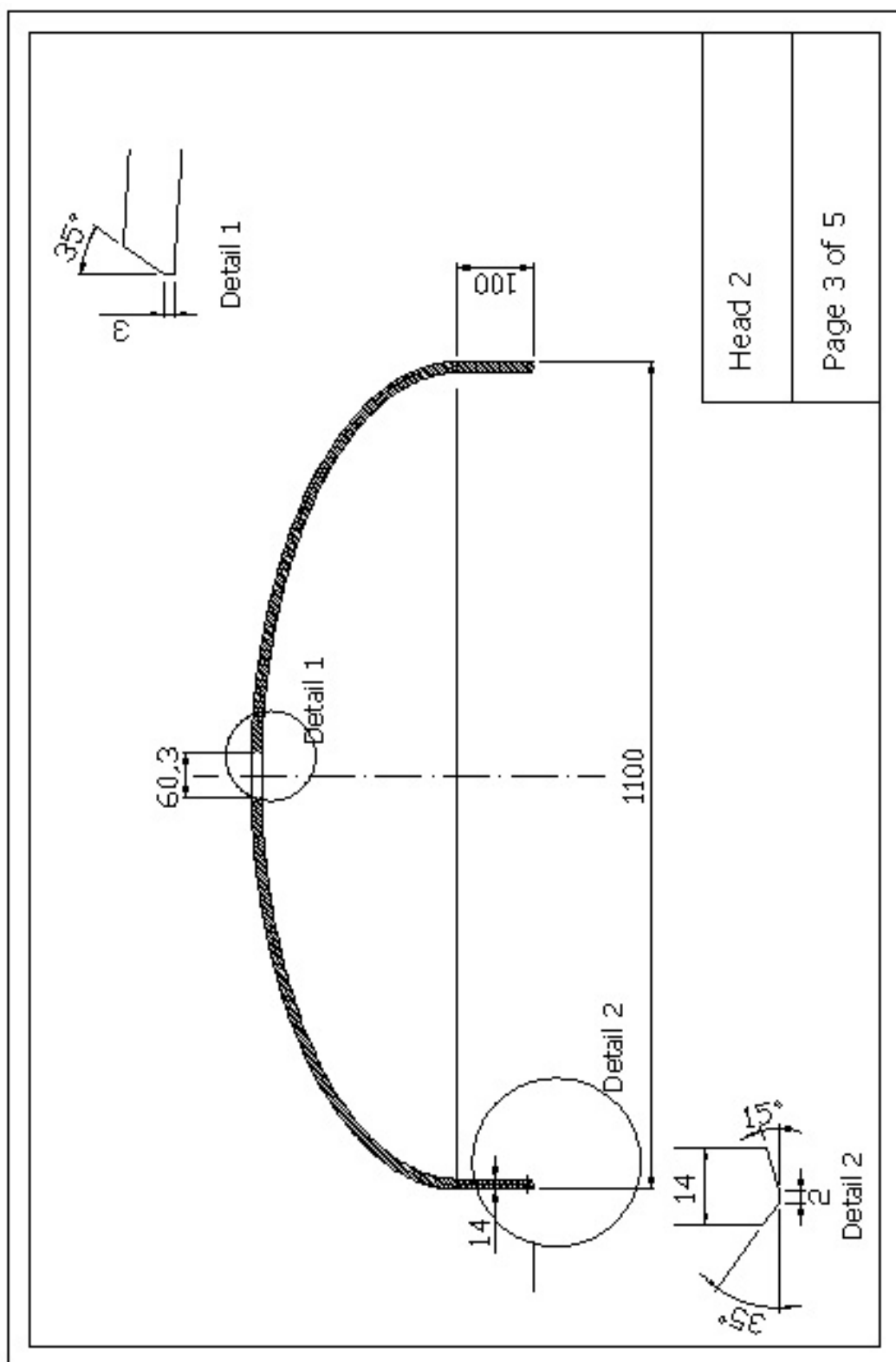


Figure B-3. Technical Drawing of Head 2

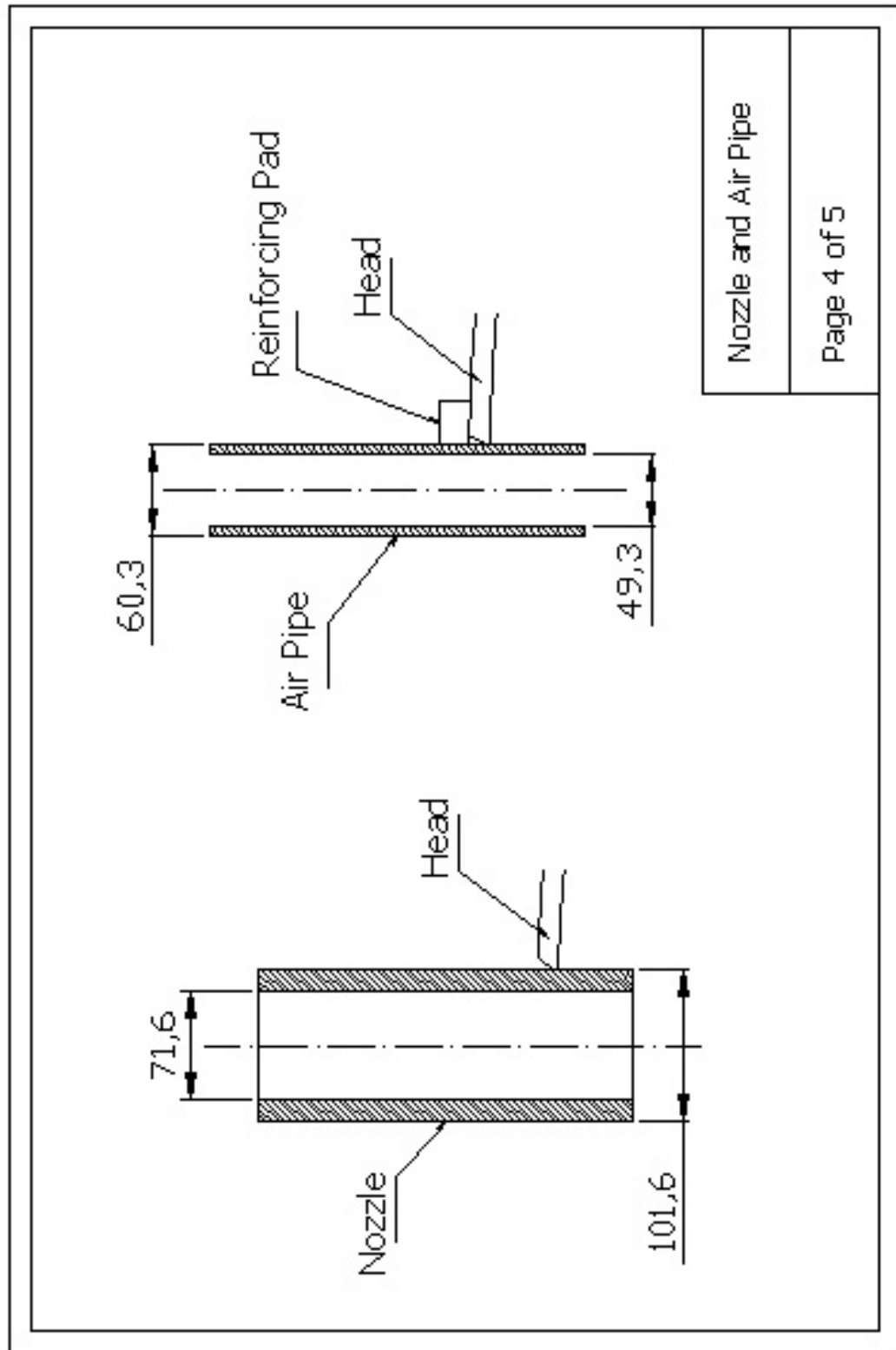


Figure B-4. Technical Drawing of Nozzle and Air Pipe

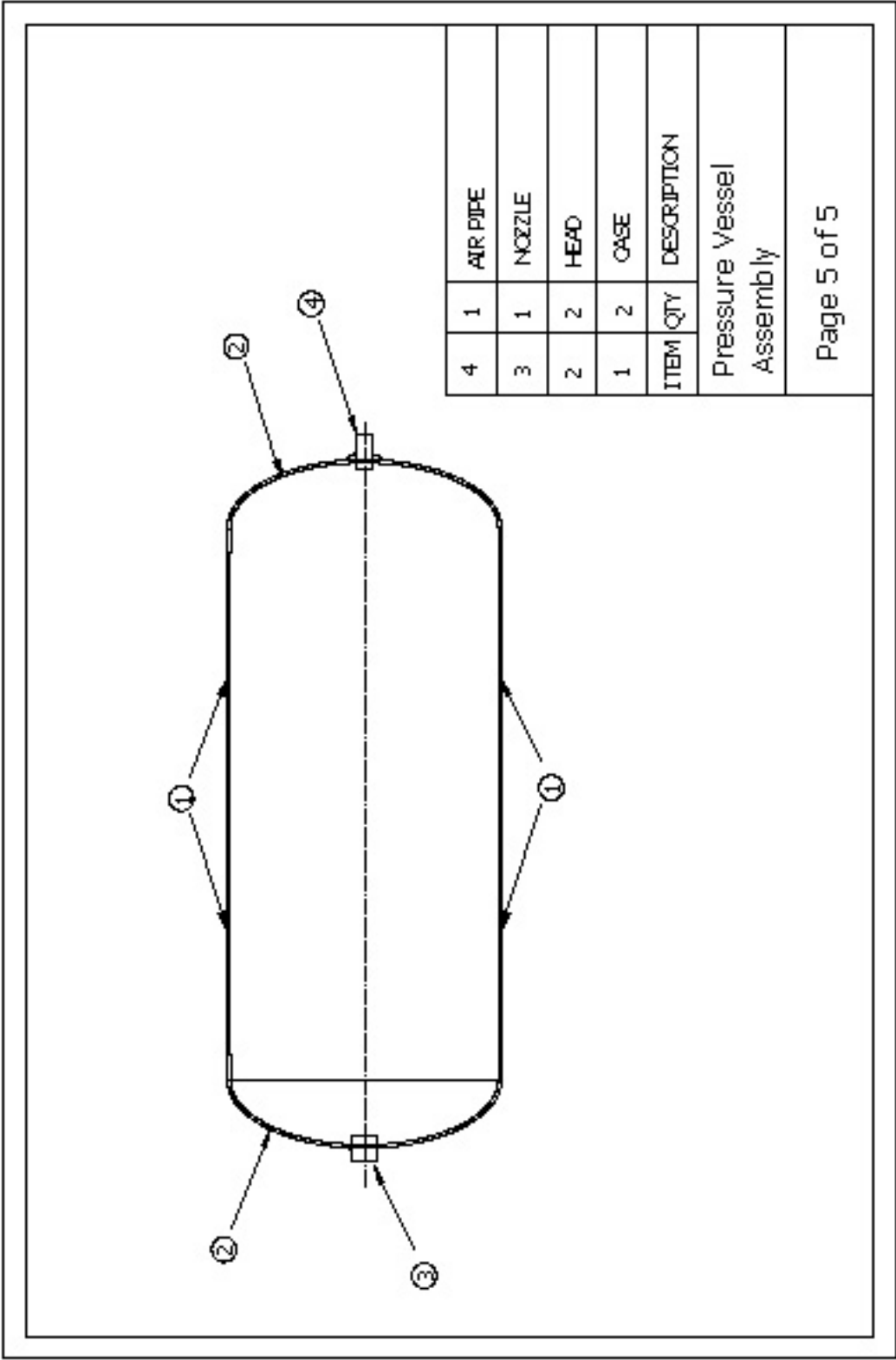


Figure B-5. Assembly Drawing of Pressure Vessel

APPENDIX C

COMBUSTION MODELLING BY FLUENT

C.1. COMBUSTION MODELLING BY FLUENT

FLUENT provides five approaches to modeling gas phase reacting flows:

- Generalized finite-rate model
- Non-premixed combustion model
- Premixed combustion model
- Partially premixed combustion model
- Composition PDF Transport model

C.1.1. GENERALIZED FINITE-RATE MODEL

This approach is based on the solution of transport equations for species mass fractions, with the chemical reaction mechanism defined by the user. The reaction rates that appear as source terms in the species transport equations are computed from Arrhenius rate expressions, from the eddy dissipation model of Magnussen and Hjertager [27] or from the EDC model [28]. Models of this type are suitable for a wide range of applications including premixed, partially premixed, and non-premixed turbulent combustion.

C.1.1.1. MODELING SPECIES TRANSPORT AND FINITE-RATE CHEMISTRY

FLUENT can model the mixing and transport of chemical species by solving conservation equations describing convection, diffusion, and reaction sources for each component species. Multiple simultaneous chemical reactions can be modeled, with reactions occurring in the bulk phase (volumetric reactions) and/or on wall or particle surfaces, and in the porous region.

C.1.2. PREMIXED COMBUSTION MODEL

This model has been specifically developed for turbulent combustion systems that are of the purely premixed type. In these problems perfectly mixed reactants and burned products are separated by a flame front. The "reaction progress variable" is solved to predict the position of this front. The influence of turbulence is accounted for by means of a turbulent flame speed.

In premixed flames, the fuel and oxidizer are intimately mixed before they enter the combustion device. Reaction then takes place in a combustion zone that separates unburnt reactants and burnt combustion products. Partially premixed flames exhibit the properties of both premixed and diffusion flames. They occur when an additional oxidizer or fuel stream enters a premixed system, or when a diffusion flame becomes lifted off the burner so that some premixing takes place prior to combustion.

C.1.2.1. LIMITATIONS

The following limitations apply to the premixed combustion model:

- You must use the segregated solver. The premixed combustion model is not available with either of the coupled solvers.
- The premixed combustion model is valid only for turbulent, subsonic flows.
- The premixed combustion model can not be used to simulate reacting discrete-phase particles, since these would result in a partially premixed system. Only inert particles can be used with the premixed combustion model.

C.1.3. CHOOSING A REACTION MODEL

The first step in solving any problem involving species transport and reacting flow is to determine which model is appropriate. Consider the following guidelines:

- For cases involving the mixing, transport, or reaction of chemical species, or reactions on the surface of a wall or particle (e.g., chemical vapor deposition), generalized finite-rate model is used.

- For reacting systems involving turbulent diffusion flames that are near chemical equilibrium where the fuel and oxidizer enter the domain in two or three distinct streams, non-premixed combustion model is used.
- For cases with a single, perfectly premixed reactant stream, use the premixed combustion model.

For cases involving premixed flames with varying equivalence ratio in the domain, use the partially premixed combustion model. For turbulent flames where finite-rate chemistry is important, use the laminar flamelet model

C.1.4. FLUENT MODELLING USED FOR MODELLING AIR HEATER MODEL

In combustion analysis, Finite rate chemistry model is used. Species transport model is selected for species handling and volumetric reactions are considered. **Eddy-Dissipation** (for turbulent flows, computes the mixing rate) is chosen for the “Turbulence – Chemistry Interaction” model. For mixture properties, “methane-air” mixture which is already available in FLUENT database is used.

Physical properties for the species in the mixture like molecular weight, viscosity, thermal conductivity etc., default values from the FLUENT database is used.

A turbulent model has to be specified. The realizable k- ϵ model is used.

Boundary conditions :

Operating Pressure: Input the pressure that combustion takes place

Inlet (for premixed flow):

- mass flow rate of the mixture is defined
- mass fractions of fuel and oxygen are defined
- turbulence parameters are defined

Outlet: only turbulence parameters are defined

For non premixed flows, the same parameters are input at boundary conditions. Fuel mass fraction at the fuel inlet is 1.

Mass fractions of fuel and oxygen are calculated from the mass flow rates. An example is available in section C.2.

C.2. FLUENT COMBUSTION MODEL VERIFICATION

Combustion model of FLUENT is verified by an experimental study stated in [29]. Experimental data used in analysis is as follows:

The model assumed an axisymmetric geometry. The mass flow rate for the bluff-body combustor model was specified by using the measured values reported for the air (3960 standard liters per minute [slpm]) and the CH₄ fuel (244 slpm). This corresponded to a CH₄–air equivalence ratio of 0.59. A turbulence grid was placed at the entrance of the combustor section, upstream of the bluff body. The corresponding uniform velocity and free stream turbulence at the inlet to the combustor, just downstream of the turbulence grid, were 15 m/s and 24%, respectively. An inlet temperature of 300 K and a combustor pressure of 1 atm were also specified in the model. A combustor wall temperature of 500 K was used in the simulations.

$$Q_{air} = 3960 \text{ slpm}$$

$$T_{inlet} = 300 \text{ K}$$

$$Q_{CH_4} = 244 \text{ slpm}$$

$$P = 1 \text{ atm}$$

$$\phi = 0.59$$

$$T_{wall} = 500 \text{ K}$$

Schematic and turbulent flame structure of bluff body stabilized lean premixed combustor is given in Figure C-1 .

Grid generated for analysis is given in Figure C-2.

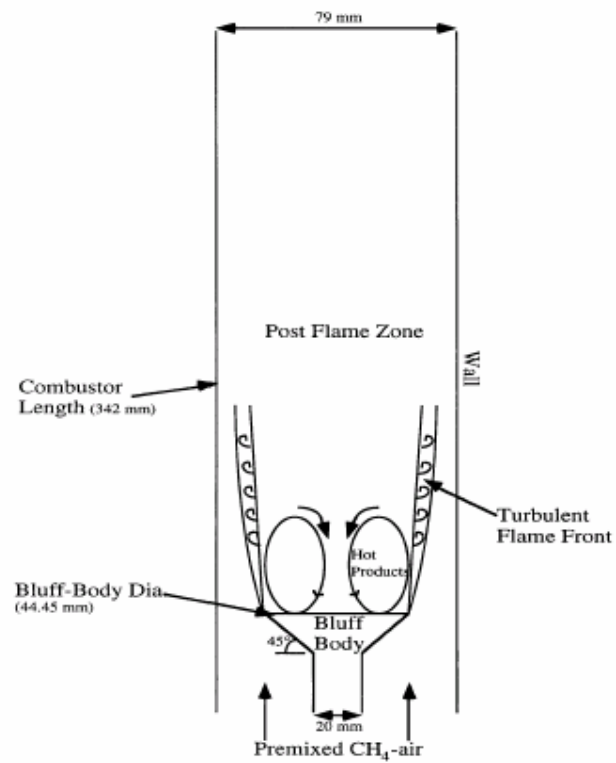
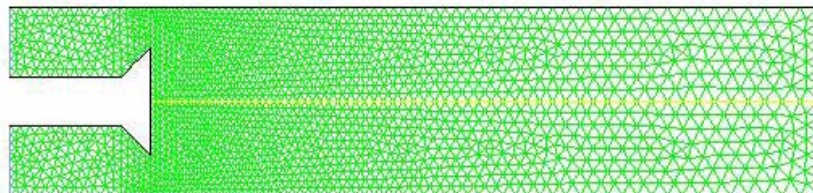


Figure C-1. Schematic of the Combustor

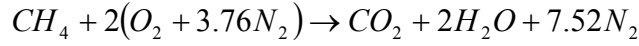


Grid

Jan 15, 2005
FLUENT 6.1 (axi, segregated, rke)

Figure C-2. Grid Used in FLUENT Analysis

C.2.1. INPUT ANALYSIS FOR FLUENT



$$Q_{scmh} = Q_{acmh} \frac{Pascal}{101325} \frac{294.24}{Kelvin}$$

$$Q_{air} = 3960 \text{ slpm} = 237.6 \text{ scmh} = 242.234 \text{ m}^3/h$$

$$\rho_{air@1atm} = 3.2 \text{ kg/m}^3$$

$$Q_{CH_4} = 244 \text{ slpm} = 14.64 \text{ scmh} = 14.925 \text{ m}^3/h$$

$$\rho_{CH_4@1atm} = 1.819 \text{ kg/m}^3$$

$$\dot{m}_{CH_4} = 14.925 \times 1.819 = 25.15 \text{ kg/h} = 0.00754 \text{ kg/s}$$

$$\dot{m}_{air} = 242.234 \times 3.2 = 775.15 \text{ kg/h} = 0.2153 \text{ kg/s}$$

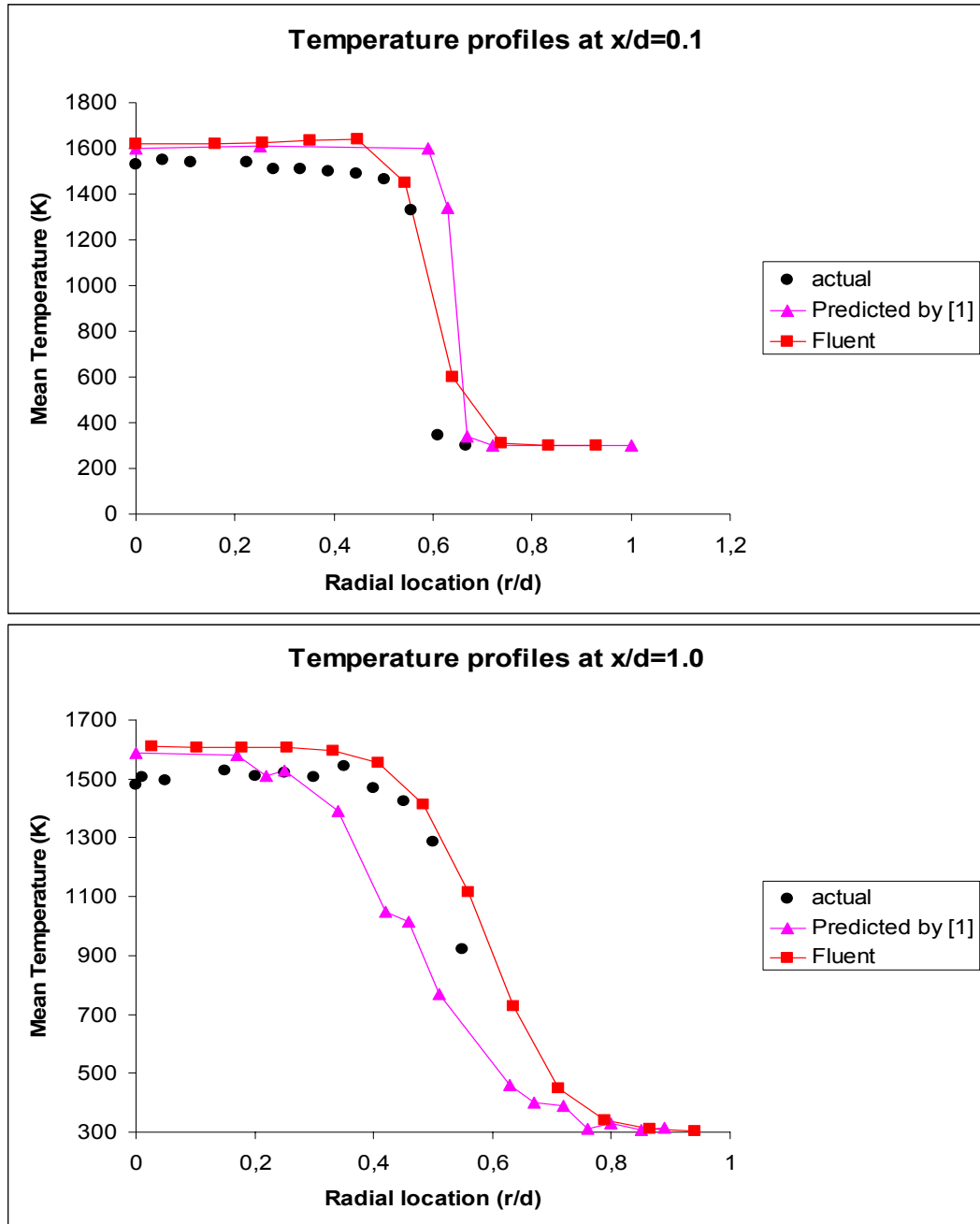
$$\dot{m}_{O_2} = 0.2153 \times 0.232 = 0.0499 \text{ kg/s}$$

$$\dot{m}_{N_2} = 0.2153 \times 0.768 = 0.1654 \text{ kg/s}$$

$$\dot{m}_{total} = 0.00754 + 0.2153 = 0.22284 \text{ kg/s}$$

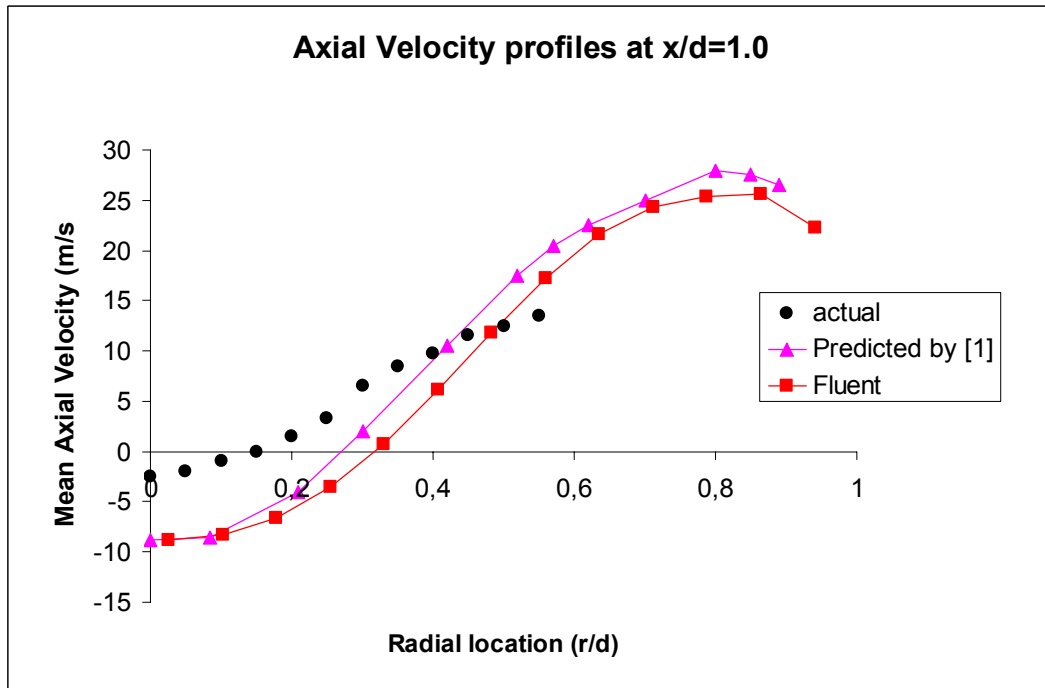
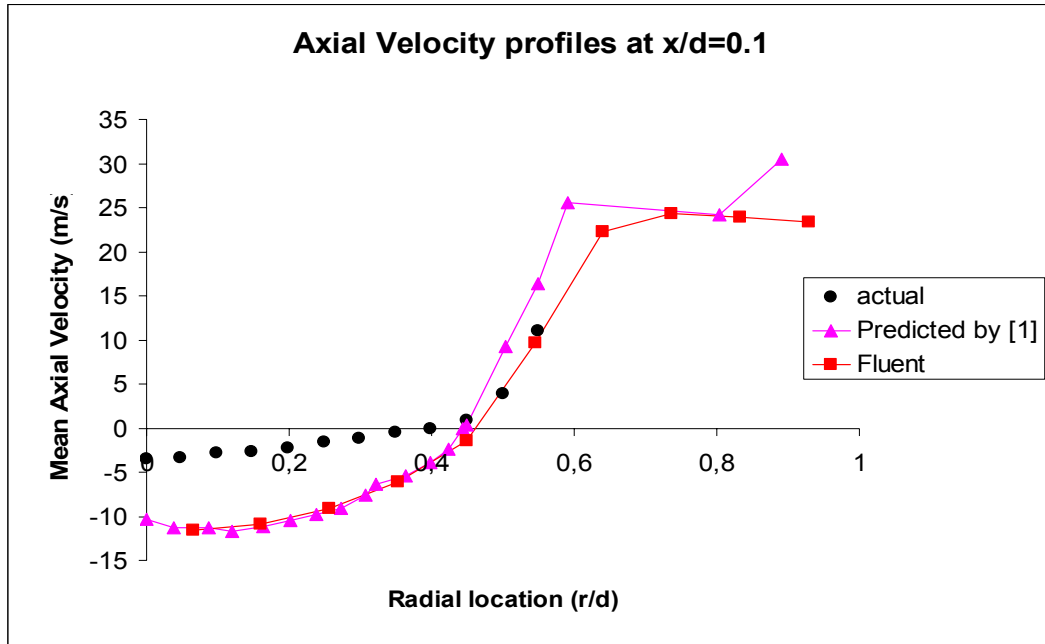
$$\left. \begin{aligned} \%CH_4 &= \frac{0.00754}{0.22284} = \%3.38 \\ \%O_2 &= \frac{0.0499}{0.22284} = \%22.39 \\ \%N_2 &= \frac{0.1654}{0.22284} = \%74.23 \end{aligned} \right\} \text{ Used as boundary condition in FLUENT}$$

C.2.2. RESULTS



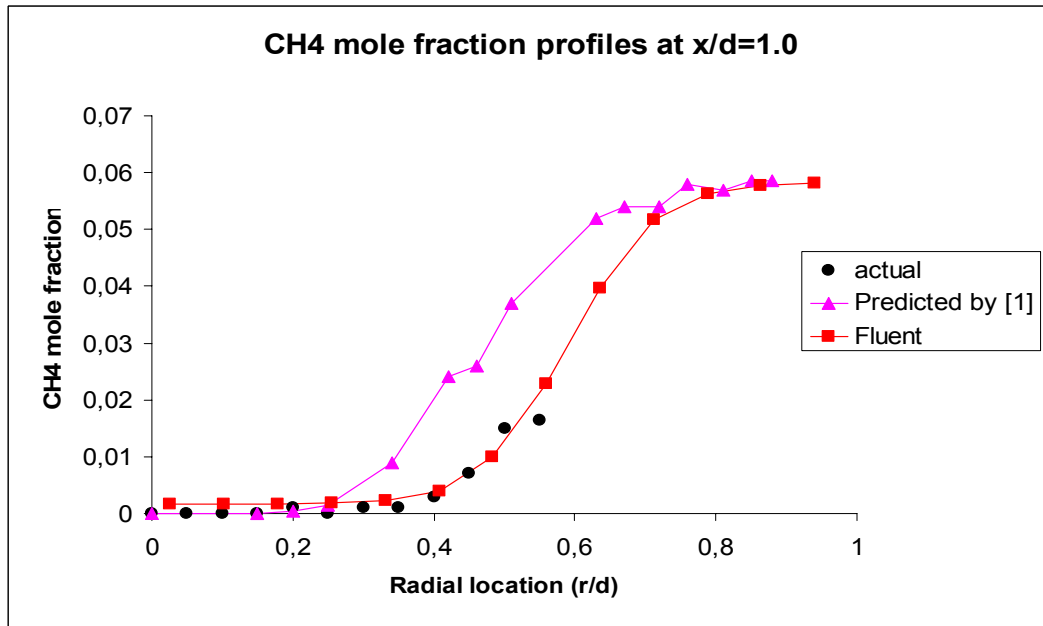
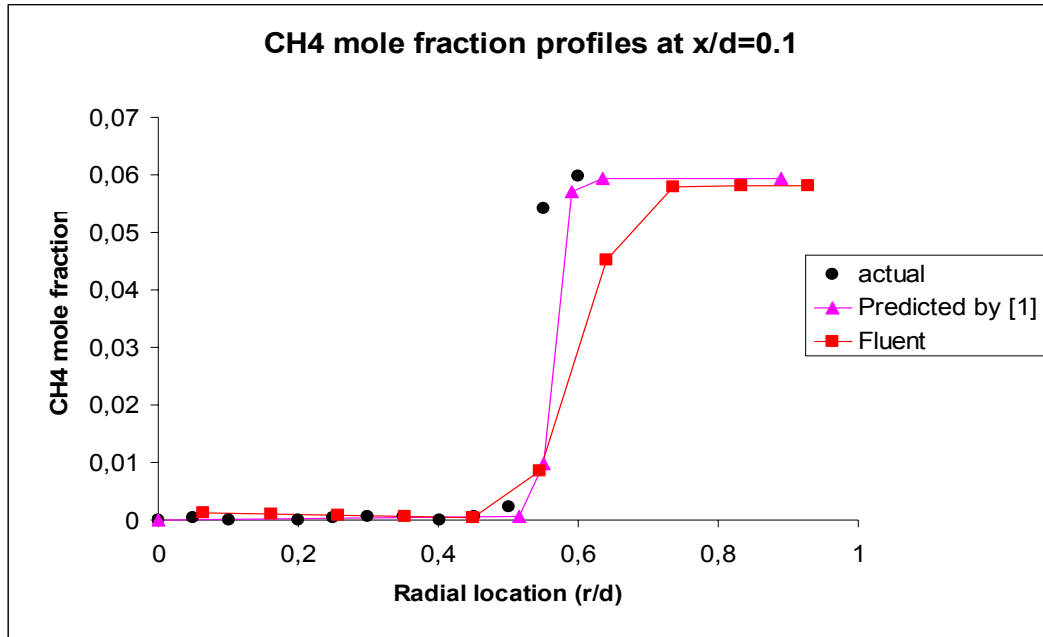
@ $x/d=0.1$ Fluent prediction and the prediction stated in [29] are close to each other. Also both methods solutions are close to the actual case.

@ $x/d=1.0$ again Fluent and [29] predictions are close to each other but Fluent predictions are better.



@ $x/d=0.1$ for $r/d < 0.5$ Fluent prediction and the prediction stated in [29] are close to each other but deviated from the actual case. For $r/d > 0.5$ Fluent predicts better than the [29].

@ $x/d=1.0$ again Fluent and [29] predictions are close to each other but both predictions can not get the actual result.



@ $x/d=0.1$ prediction stated in [29] predicts better than Fluent.

@ $x/d=1.0$ again Fluent predicts better than [29].

C.2.3. CONCLUSION

Fluent prediction of the experiment stated in [29] is quite good. Some of the results obtained by Fluent is better than the results obtained in [29].

APPENDIX D

TEST CENTER DESIGN CODES

D.1. DESIGN CODES

FORTRAN codes are generated to evaluate pressure and temperature losses in the pipe lines, to evaluate the temperature and pressure change during tank discharge, to calculate fuel and oxygen mass flow rate for vitiator and to calculate required valve coefficients.

A visual interface is generated to combine the codes. When the “mainvisual.exe” is executed, main frame shown in Figure D-1 is opened.

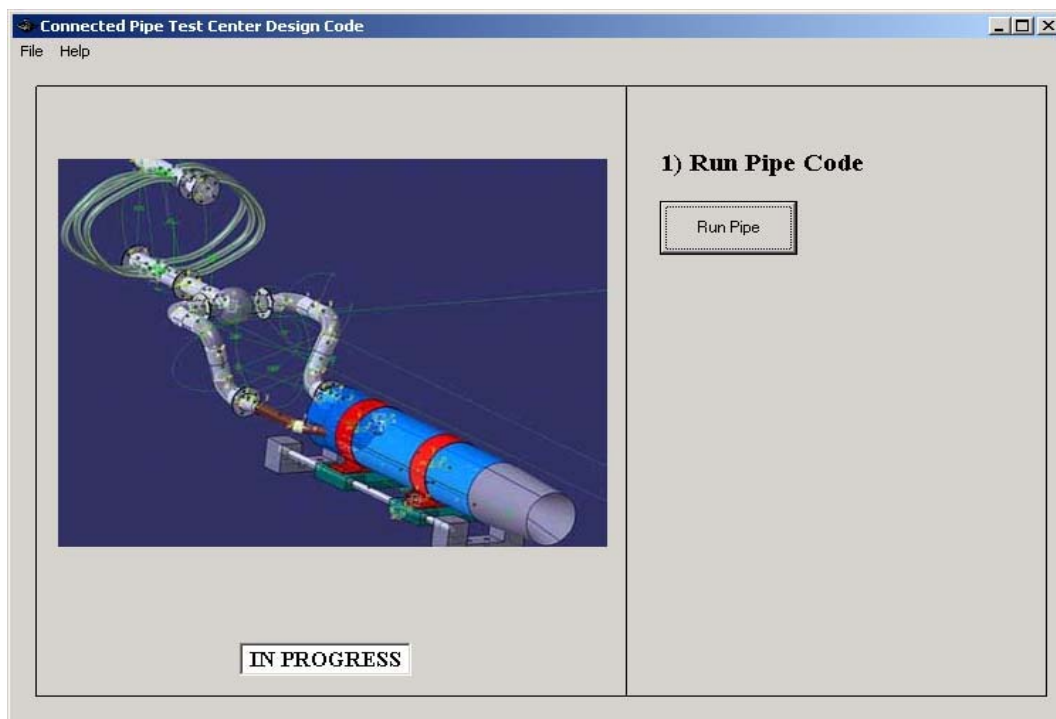


Figure D-1. Main Window of the Program

The program has four main codes: Pipe code, discharge code, O₂ replenishment code and valve code. All the codes has to be executed in an order. In the main window shown in Figure D-1, only “Pipe Code” button is active. Second button is not activated before pressing the “Run Pipe” button.

D.2. PIPE CODE

When the “Run Pipe” button is pressed on the main window, window shown on Figure D-2 appears. Number of data points states total number of pipe and elbows (shown in different colors on the left bottom picture). Starting from the combustor inlet to vitiator outlet, state the component and its length and diameter. For the flex hose, number of hose and its length has to be written to the inputs frame. The code needs temperature, pressure and mass flow rate data at the combustor inlet. The name of the files are “temp.txt”, “pressure.txt” and “mfr.txt”, respectively. Press “Run” button to execute the code. A MS-Dos window will appear until the end of execution process. When this window disappears, press “Done” button.

Enter Data	Length (mm)	Nom. Diameter (in)
Elbow	0	3
Pipe	350	3
Elbow	0	3
Pipe	325	3
Elbow	0	3
Pipe	175	3
Elbow	0	3
Pipe	0	3
Elbow	0	3
Pipe	0	3
Elbow	0	3
Pipe	0	3

INPUTS

Test duration: 200 (s)

Time step: 0.1 (s)

Comb. Inlet area: 3673.4296 (cm²)

Number of flex hoses: 6

Length of flex hoses: 100 (cm)

OUTPUT FILE

presin.txt tempin.txt

Figure D-2. Pipe Code Window

D.3. DISCHARGE CODE

After the pipe code window is closed, window shown in Figure D-. If the Pipe Code window is closed before execution of the code, “Not Complete” warning will given beside the “Run Pipe” button instead of “OK!”. Press “Run Discharge” button to continue with the Discharge Code.

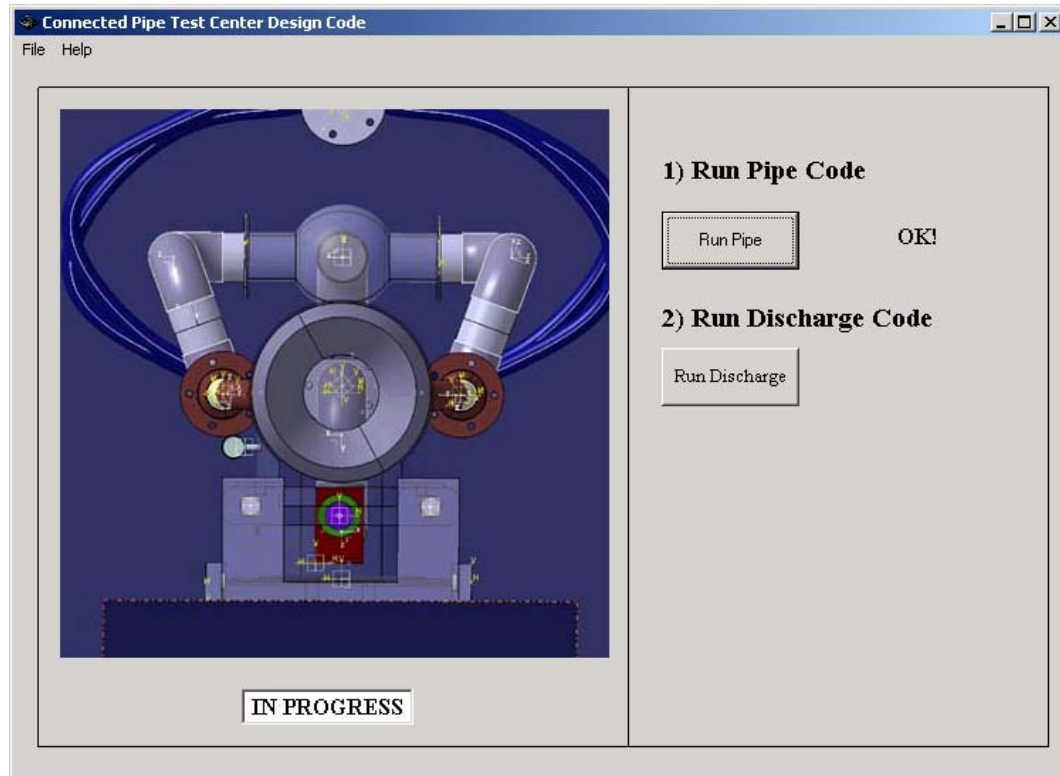


Figure D-3. Main Window Following the Pipe Code Window

Temperature and pressure history during discharge is obtained by discharge code. This code use the same mass flow rate with the pipe code (mfr.txt). The calculation process is as follows:

Assumption: Tank is insulated

Quasi-steady state solution of discharging tank has been completed.

$$Q - W = m_e \left(h_e + \frac{V_e^2}{2} + gz_e \right) - m_i \left(h_i + \frac{V_i^2}{2} + gz_i \right) + (m_2 e_2 - m_1 e_1)_{cv}$$

$$Q = 0, W = 0, m_i = 0, \Delta ke = 0, \Delta pe = 0$$

$$m_e h_e = m_2 u_2 - m_1 u_1$$

$$m_e h_1 = m_2 u_2 - m_1 u_1$$

$$u_2 = \frac{m_1 u_1 + \dot{m} \Delta t h_1}{m_2} \quad \text{where} \quad m_e = \dot{m} \Delta t \quad \text{and} \quad m_2 = m_1 - \dot{m} \Delta t$$

From u_2 , T_2 is obtained.

$$P_2 \text{ is obtained by: } \rho_2 = \frac{m_2}{V} \text{ and } P_2 = Z \cdot \rho_2 \cdot R \cdot T_2$$

Repeating above procedure at Δt intervals pressure-time history of the tank is obtained.

DISCHARGE

TANK DISCHARGE CALCULATIONS

INPUTS

Time Step	0.1	(s)
Initial temp of the tank	298	(K)
Initial tank pressure	5	(MPa)
Volume of tank	27.8	(m ³)
Mass flow out of the tank	2.77	(kg/s)
Final pressure in the tank	2	(MPa)
Test center operation time	300	(s)

OUTPUTS

Initial mass in the tank	1701,271	(kg)
Final mass in the tank after discharge	1098,014	(kg)
Time to discharge	217,8041	(s)
Final tank temperature	249,9879	(K)

Run

Show Results

Done

Output File

discharge.txt

Figure D-4. Discharge Code Window

Inputs required are stated in the INPUTS frame. After completing the inputs, press the “Run” button. When the execution is complete, press the “Show Results” button to see the results in the output frame. Press “Done” to close the window.

D.4. O₂ REPLENISHMENT CODE

Once the discharge code window is closed, main window shown in Figure D- is opened. Third step appears at this stage. If the Discharge Code window is closed before execution of the code, “Not Complete” warning will given beside the “Run Discharge” button instead of “OK!”. Press “Run O₂ Replenishment” button to continue with the O₂ Replenishment Code.

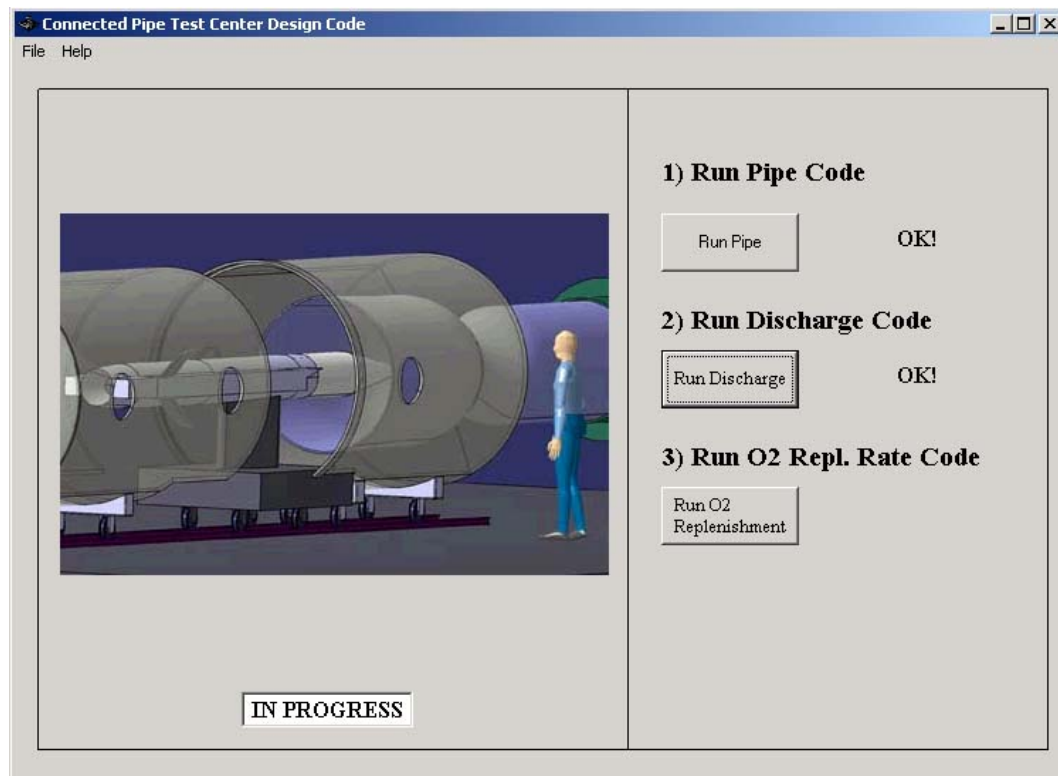


Figure D-5. Main Window Following the Discharge Code Window

Combustion analysis in the vitiator is performed using the thermochemical code Cet93. NASA Cet93 Code is used for calculations involving chemical equilibrium. The method applied is based on a minimization of Gibbs free energy.

Two programs are written to work coupled with Cet93. One of them generates the inputs for Cet93. The other calls the Cet93 code for each iteration. Program uses two output file of pipe code and the mass flow rate data. For each time step, temperature and pressure values are read from files and iterations for oxygen and fuel mass flow rate. Methane-air combustion is performed. O₂ Replenishment Code Window is shown in Figure D-.

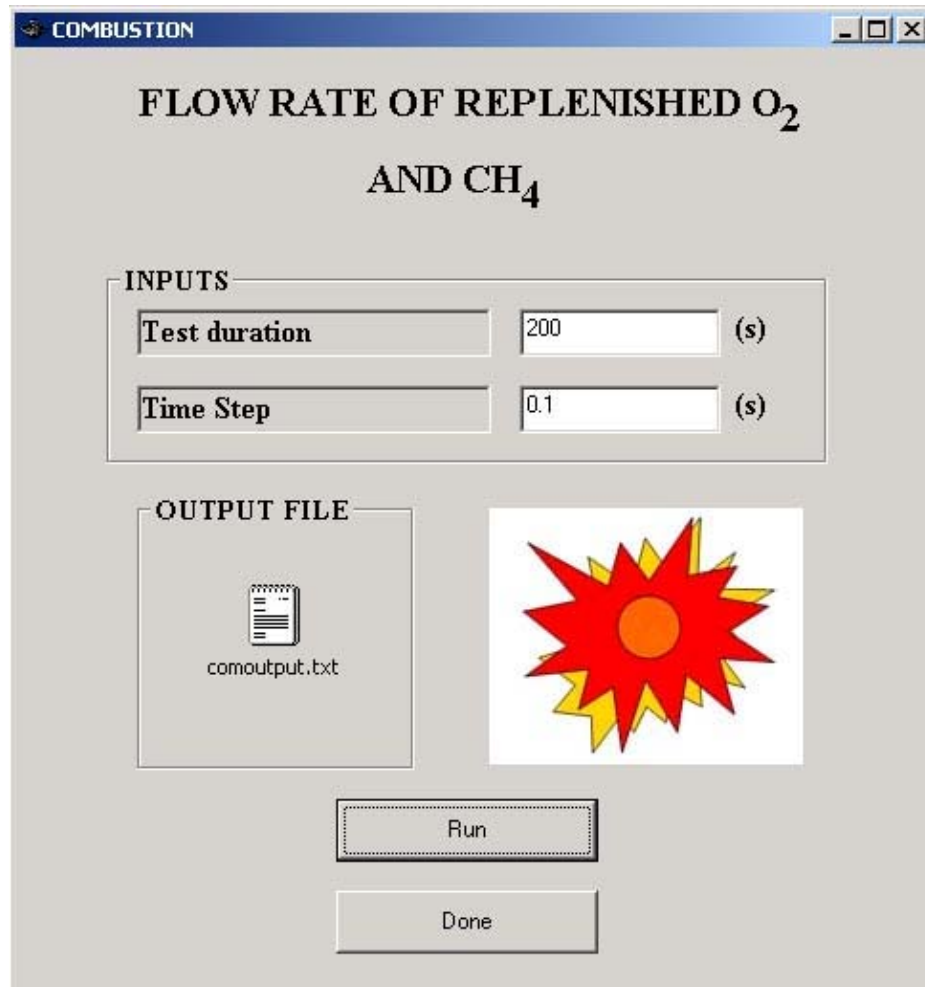


Figure D-6. O₂ Replenishment Code Window

D.5. VALVE CODE

Once the O₂ Replenishment Code Window is closed, main window shown in Figure D-8 is opened. Fourth step appears at this stage. If the O₂ Replenishment Code Window is closed before execution of the code, "Not Complete" warning will

given beside the “Run O₂ Replenishment” button instead of “OK!”. Press “Run Valve” button to continue with the Valve Code. Frame shown in Figure D-8 appears.

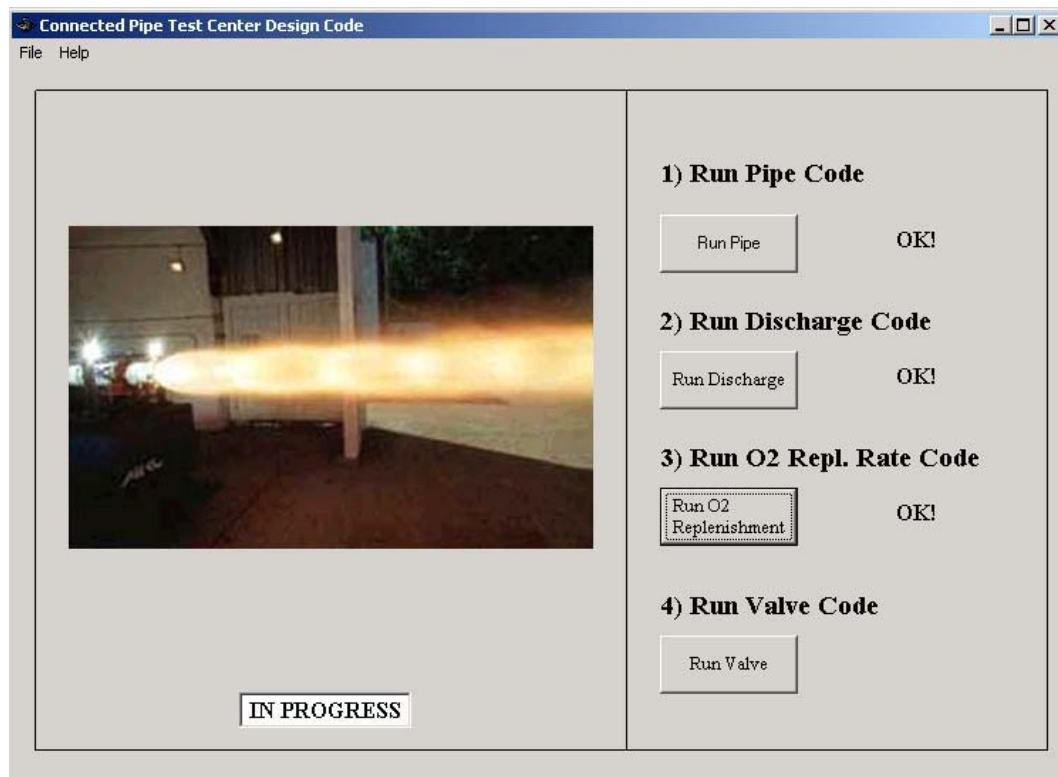


Figure D-7. Main Window Following the O₂ Replenishment Code Window

Solution procedure of the code is as explained in section 2.3. Pressure and temperature data calculated by pipe code and discharge codes are used as input and output temperatures of the valve system. Output file “cv.txt” includes the cv values for the two valves for each time step. If a valid solution can not be obtained, “NOT POSSIBLE” is written instead of “VALID SOLUTION”. Press “Done” to end the program.


VALVE COEFFICIENT CALCULATION

INPUTS

Test duration	200	(s)
Time step	0.1	(s)
Pressure drop on first valve	1.7	(MPa)

OUTPUTS

VALID SOLUTION

First Valve			Second Valve	
Max. Cv	33,23199		Max. Cv	33,6203
Min. Cv	9,464092		Min. Cv	9,941981

Output File

cv.txt

Run

Show Results

Done

Figure D-8. Valve Code Window

Finally Figure D-9 appears. If all the notices beside the buttons are “OK!” (all codes are run), text box returns to “COMPLETE” from “IN PROGRESS”. Output files of all codes are given in the “Output Files” frame at the bottom of the window. On the file menu, select “Restart” to restart the solution procedure. Press exit to close the program.

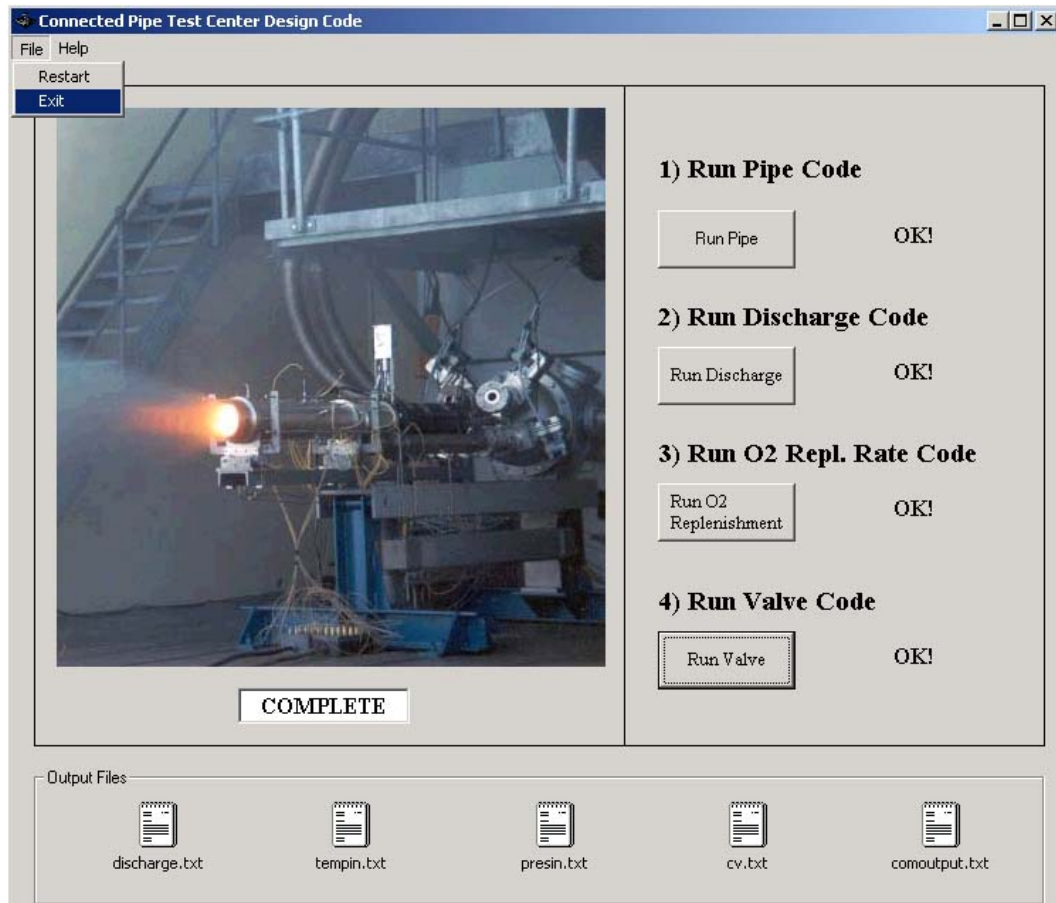


Figure D-9. Final Window of the Code

APPENDIX E

SAMPLE CALCULATIONS FOR PIPING SYSTEM

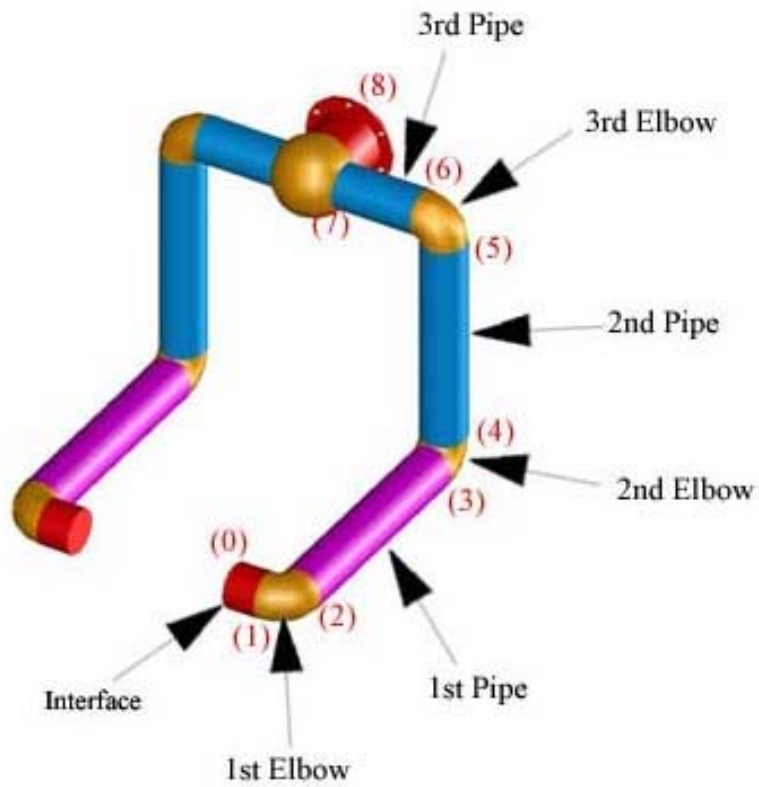


Figure E-1. Pipe Configuration of the Test Center

E.1. SAMPLE CALCULATIONS

E.1.1. COMBUSTOR INLET TO 1ST ELBOW INTERFACE

Combustor air inlet area (A_0): $A_0 = 3673.42 \text{ mm}^2$ 68.4 mm

Nominal Pipe size: 3 inch $\Rightarrow D_p = 3.068 \text{ inch} = 77.93 \text{ mm}$

Mass flow rate at A₀: $\dot{m}_1 = 2.56 \text{ kg/s}$

Temperature at A₀: $T_0 = 747 \text{ K}$

Pressure at A₀: $P_0 = 510000 \text{ Pa}$

$$T_r = \frac{747}{132.65} = 5.65 \quad P_r = \frac{0.51}{3.771} = 0.135 \quad Z = 1.002$$

$$\rho_0 = \frac{P_0}{ZRT_0} = \frac{510000}{1.002 \times 287.1 \times 750} = 2.364 \text{ kg/m}^3$$

$$c_0 = \sqrt{\gamma RT_0} = \sqrt{1.4 \times 287.1 \times 750} = 549.05 \text{ m/s}$$

$$V_0 = \frac{\dot{m}_0}{\rho_0 A_0} = \frac{2.56}{2.363 \times 0.003673} = 294.95 \text{ m/s}$$

$$M_0 = \frac{V_0}{c_0} = \frac{294.95}{549.05} = 0.537$$

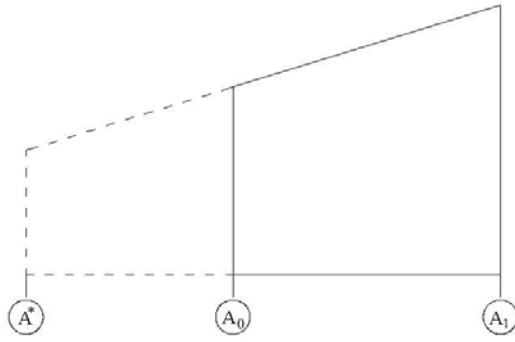
$$P_{T0} = P_0 \left(1 + \frac{\gamma - 1}{2} M_0^2 \right)^{\frac{\gamma}{\gamma - 1}} = 536092 \text{ Pa}$$

$$T_{T0} = T_0 \left(1 + \frac{\gamma - 1}{2} M_0^2 \right) = 760.37 \text{ K}$$

$$\left(\frac{A}{A^*} \right) = \frac{1}{M^2} \left[\frac{2}{\gamma + 1} \left(1 + \frac{\gamma - 1}{2} M^2 \right) \right]^{\frac{\gamma + 1}{\gamma - 1}}$$

$$\left(\frac{A_1}{A^*} \right) = \frac{1}{M_1^2} \left[\frac{2}{\gamma + 1} \left(1 + \frac{\gamma - 1}{2} M_1^2 \right) \right]^{\frac{\gamma + 1}{\gamma - 1}} = 1.626$$

$$A_1 = \frac{\pi D_p^2}{4} = 4769.44 \text{ mm}^2$$



$$A_1 = \left(\frac{A_1}{A^*} \right) \left(\frac{A^*}{A_0} \right) A_0 \quad \Rightarrow$$

$$\left(\frac{A_1}{A^*} \right) = \frac{A_1}{A_0} \left(\frac{A_0}{A^*} \right) = \frac{4769.44}{3673.42} (1.626) = 2.908$$

$$\left(\frac{A_1}{A^*} \right) = \frac{1}{M_1^2} \left[\frac{2}{\gamma + 1} \left(1 + \frac{\gamma - 1}{2} M_1^2 \right) \right]^{\frac{\gamma + 1}{\gamma - 1}} = 2.908 \quad \Rightarrow \quad M_1 = 0.204$$

$$P_1 = \frac{P_{T0}}{\left(1 + \frac{\gamma - 1}{2} M_1^2 \right)^{\frac{\gamma}{\gamma - 1}}} = 520960 \text{ bar}$$

$$T_1 = \frac{T_{T0}}{\left(1 + \frac{\gamma - 1}{2} M_1^2 \right)} = 754.40 \text{ K}$$

E.1.2. 1ST ELBOW

$$\rho_1 = \frac{P_1}{RT_1} = 2.406 \text{ kg/m}^3$$

$$V_1 = M_1 \sqrt{\gamma R T_1} = 0.204 \sqrt{1.38 \times 287 \times 754.4} = 111.53 \text{ m/s} \quad K = 0.54$$

$$\Delta P = \rho_1 K \frac{V_1^2}{2} = 8031 \text{ Pa}$$

$$P_2 = P_1 + \Delta P_1 = 52096 + 8031 = 529051.2 \text{ Pa}$$

$$T_2 = T_1 = 754.4 \text{ K}$$

$$M_2 = M_1 = 0.204$$

E.1.3. 1ST PIPE

$$\mu = 0.0001695 \frac{\text{kg}}{\text{m s}} \quad L_{\text{pipe1}} = 350 \text{ mm}$$

$$\rho_2 = \frac{P_2}{RT_2} = 2.44 \text{ kg/m}^3$$

$$\frac{e}{D_p} = \frac{0.000045}{0.07793} = 0.000577462$$

$$\text{Re} = \frac{\rho_2 V_2 D_p}{\mu} = 125298.8$$

$$f = \frac{0.25}{\left[\ln\left(\frac{e}{3.7 D_p}\right) + \left(\frac{5.74}{\text{Re}^{0.9}}\right) \right]^2} = 0.0032541$$

$$\frac{4 f L_2^*}{D_p} = \frac{1 - M_2^2}{\gamma M_2^2} + \frac{\gamma + 1}{2} \ln\left(\frac{(\gamma + 1)M_2^2}{2 + (\gamma - 1)M_2^2}\right) \quad L_2^* = 61471.11 \text{ mm}$$

$$L_3^* = L_2^* + L_{\text{pipe1}} = 61471.11 + 350 = 61821.11 \text{ mm}$$

$$\frac{4 f L_3^*}{D_p} = \frac{1 - M_3^2}{\gamma M_3^2} + \frac{\gamma + 1}{2} \ln\left(\frac{(\gamma + 1)M_3^2}{2 + (\gamma - 1)M_3^2}\right) \quad M_3 = 0.203$$

$$\frac{T_2}{T^*} = \frac{\gamma + 1}{2 + (\gamma - 1)M_2^2} = 1.18$$

$$\frac{T_3}{T^*} = \frac{\gamma + 1}{2 + (\gamma - 1)M_3^2} = 1.18$$

$$T_3 = \frac{T_3}{T^*} \frac{T^*}{T_2} T_2 = 754.4 \text{ K}$$

$$\frac{P_2}{P^*} = \frac{1}{M_2^2} \left(\frac{\gamma + 1}{2 - (\gamma - 1)M_2^2} \right) = 5.878$$

$$\frac{P_3}{P^*} = \frac{1}{M_3^2} \left(\frac{\gamma + 1}{2 - (\gamma - 1)M_3^2} \right) = 5.89$$

$$P_3 = \frac{P_3}{P^*} \frac{P^*}{P_2} P_2 = 530103.2 \text{ Pa}$$

E.1.4. 2ND ELBOW

$$\rho_3 = \frac{P_3}{RT_3} = 2.448266 \text{ kg/m}^3$$

$$V_3 = M_3 \sqrt{\gamma R T_3} = 111.3136 \text{ m/s} \quad K = 0.54$$

$$\Delta P = \rho_3 K \frac{V_3^2}{2} = 8191 \text{ Pa}$$

$$P_4 = P_3 + \Delta P = 537241.8 \text{ Pa}$$

$$T_4 = T_3 = 754.4316 \text{ K}$$

$$M_4 = M_2 = 0.203$$

E.1.5. 2ND PIPE

$$L_{pipe2} = 320 \text{ mm}$$

$$\rho_4 = \frac{P_4}{RT_4} = 2.48 \text{ kg/m}^3$$

$$\frac{e}{D_p} = \frac{0.000045}{0.07793} = 0.000577462$$

$$\text{Re} = \frac{\rho_2 V_2 D_p}{\mu} = 126980.1$$

$$f = \frac{0.25}{\left[\ln\left(\frac{e}{3.7 D_p}\right) + \left(\frac{5.74}{\text{Re}^{0.9}}\right) \right]^2} = 0.0032541$$

$$\frac{4 f L_4^*}{D_p} = \frac{1 - M_4^2}{\gamma M_4^2} + \frac{\gamma + 1}{2} \ln\left(\frac{(\gamma + 1) M_4^2}{2 + (\gamma - 1) M_4^2}\right) \quad L_4^* = 61821.14 \text{ mm}$$

$$L_5^* = L_4^* + L_{pipe2} = 61821.14 + 325 = 62146.14 \text{ mm}$$

$$\frac{4 f L_5^*}{D_p} = \frac{1 - M_5^2}{\gamma M_5^2} + \frac{\gamma + 1}{2} \ln\left(\frac{(\gamma + 1) M_5^2}{2 + (\gamma - 1) M_5^2}\right) \quad M_5 = 0.203$$

$$\frac{T_4}{T^*} = 1.18$$

$$\frac{T_5}{T^*} = 1.18$$

$$T_5 = \frac{T_5}{T^*} \frac{T^*}{T_4} T_4 = 754.4 \text{ K}$$

$$\frac{P_4}{P^*} = 5.89 \quad \frac{P_5}{P^*} = 5.9$$

$$P_5 = \frac{P_5}{P^*} \frac{P^*}{P_4} P_4 = 538305.3 \text{ Pa}$$

E.1.6. 3RD ELBOW

$$\rho_5 = \frac{P_5}{RT_5} = 2.486069 \text{ kg/m}^3$$

$$V_5 = M_5 \sqrt{\gamma RT_5} = 111.0919 \text{ m/s} \quad K = 0.54$$

$$\Delta P = \rho_5 K \frac{V_5^2}{2} = 8284 \text{ Pa}$$

$$P_6 = P_5 + \Delta P = 546589.3 \text{ Pa}$$

$$T_6 = T_5 = 754.45 \text{ K}$$

$$M_6 = M_5 = 0.203$$

E.1.7. 3RD PIPE

$$L_{pipe3} = 175 \text{ mm}$$

$$\rho_6 = \frac{P_6}{RT_6} = 2.524327 \text{ kg/m}^3$$

$$\frac{e}{D_p} = \frac{0.000045}{0.07793} = 0.000577462$$

$$\text{Re} = \frac{\rho_2 V_2 D_p}{\mu} = 128928.1$$

$$f = \frac{0.25}{\left[\ln \left(\frac{e}{3.7 D_p} \right) + \left(\frac{5.74}{\text{Re}^{0.9}} \right) \right]^2} = 0.0032541$$

$$\frac{4 f L_6^*}{D_p} = \frac{1 - M_6^2}{\gamma M_6^2} + \frac{\gamma + 1}{2} \ln \left(\frac{(\gamma + 1) M_6^2}{2 + (\gamma - 1) M_6^2} \right)$$

$$L_6^* = 62171.17 \text{ mm}$$

$$L_7^* = L_5^* + L_{pipe3} = 62346.17 \text{ mm}$$

$$\frac{4 f L_7^*}{D_p} = \frac{1 - M_7}{\gamma M_7^2} + \frac{\gamma + 1}{2} \ln \left(\frac{(\gamma + 1) M_7}{2 + (\gamma - 1) M_7} \right) \quad M_7 = 0.203$$

$$\frac{T_6}{T^*} = 1.18 \quad \frac{T_7}{T^*} = 1.18$$

$$T_7 = \frac{T_7}{T^*} \frac{T^*}{T_6} T_6 = 754.4 \text{ K}$$

$$\frac{P_6}{P^*} = 5.9 \quad \frac{P_7}{P^*} = 5.9$$

$$P_7 = \frac{P_5}{P^*} \frac{P^*}{P_4} P_4 = 547128.2 \text{ Pa}$$

E.1.8. 4TH ELBOW

$$\rho_7 = \frac{P_7}{RT_7} = 2.52 \text{ kg/m}^3$$

$$V_7 = M_7 \sqrt{\gamma R T_7} = 110.9 \text{ m/s} \quad K = 0.54$$

$$\Delta P = \rho_7 K \frac{V_7^2}{2} = 8403 \text{ Pa}$$

$$P_8 = P_7 + \Delta P = 555531.2 \text{ Pa}$$

$$T_8 = T_7 = 754.4 \text{ K}$$

$$M_8 = M_7 = 0.203 \text{ K}$$

Summary of the results are tabulated in Table E-1.

Table E-1. Summary of Results

	P (Pa)	T (K)	M
0	510000	747	0.537
1	520960	754.4	0.204
2	529050	754.4	0.204
3	530103.2	754.43	0.203
4	537241.8	754.43	0.203
5	538305.3	754.45	0.203
6	546589.3	754.45	0.20
7	547128.2	754.46	0.203
8	555531.2	754.46	0.203